UNIVERSITÄT ZU LÜBECK

From the Lübecker Institut für Experimentelle Dermatologie
of the University of Lübeck
Director: Prof. Dr. Ralf Ludwig

Identification of novel autoantigens in Stiff-Person Syndrome and associated hyperexcitability disorders

Dissertation for the Fulfilment of Requirements
for the Doctoral Degree
of the University of Lübeck

from the Department of Natural Sciences

Submitted by
Iswariya Venkataraman
from Chennai, India

Lübeck, 2017

First referee: Prof. Dr. Ralf Ludwig

Second referee: Prof. Dr. Rudolf Manz

Chairman of board: Prof. Dr. Henrik Oster

Date of oral examination: 27.04.2018

Approved for printing: 02.05.2018, Lübeck

Table of Contents

Contents

Contents

Abstract

Patients with stiff-person-syndrome (SPS), progressive encephalitis with rigidity and myoclonus (PERM), and certain other neurological movement related disorders develop autoantibodies frequently directed against glutamic acid decarboxylase (GAD). However, to this date, the pathogenic significance of anti-GAD autoantibodies remains unproven. Patients might harbor additional autoantibodies against indeterminate pre-synaptic antigens that may induce or support the disorders. Therefore, this study focused on screening for unrevealed autoantigens in SPS, PERM, cerebellitis, and associated neurological movement disorders.

In indirect immunofluorescence, 53/100 patients' sera, as verified by anti-GAD ELISA, were positive for anti-GAD65/67 autoantibodies. These sera produced a typical GAD pattern on the wild-type mouse, rat, pig, and monkey tissue substrates making observation of any additional reactions difficult. Therefore, a GAD65 knock-out (ko) mice cerebellum cryosection was included to identify unknown AAb patterns. Neither a common pattern for anti-GAD67 autoantibodies nor any novel AAb patterns were observed on the GAD65ko substrate in the patients' sera.

An alternative immunoprecipitation approach using patients' sera together with the pig cerebellum tissue corroborated the presence of GAD65/GAD67 antigens in the immunoprecipitates of 52 patients' sera, but not in the sera from 50 healthy controls. Additionally, patients' sera with as well as without anti-GAD autoantibodies, immunoprecipitated other proteins associated with synaptic vesicular trafficking such as N-ethylmaleimide-sensitive factor (NSF) and dynamin 1 (DNM1), as identified by mass spectrometry. An extended immunoblot analysis with monospecific antibodies confirmed the pull-down of SNARE proteins such as NSF (n = 29) and syntaxin 1B (n = 59) in the patients' sera. Additionally, most patients' sera that immunoprecipitated NSF also pulled down DNM1. Subsequently, the synaptic proteins were enriched from the cerebellum tissue and immunoblotted with sera from patients (n = 100) versus controls (n = 135). NSF and DNM1 were confirmed as new autoantigens with 30 and 23 patients' sera, respectively, showing immunoreactivity that was absent in the majority of controls (n = 3 and n = 1). Twenty-nine patients' sera also reacted with recombinant human NSF in the immunoblot analysis, but with a lower intensity compared with NSF from pig cerebellum. Separation of both NSF by isoelectric focusing revealed different isoelectric points indicating differing post-translational modifications as the underlying reason.

In conclusion, patients with SPS, PERM, and associated neurological movement disorders harbor autoantibodies against additional synaptic vesicle-associated proteins, primarily NSF.

Abstract

Further emphasis should be laid on implementing appropriate test systems for the detection of these autoantibodies.

Zusammenfassung

Patienten mit Stiff-Person-Syndrom (SPS), progredienter Enzephalomyelitis mit Rigidität und Myoklonie (PERM), zerebellärer Ataxie und anderen neurologisch bedingten Bewegungsstörungen weisen häufig Autoantikörper (AAK) gegen Glutamatdecarboxylase (GAD) auf. Bis heute ist jedoch unklar, ob die Anti-GAD-AAK in die Pathogenese der Erkrankungen involviert sind. Die Patienten könnten weitere AAK gegen bisher nicht-identifizierte präsynaptische Antigene aufweisen, welche die Symptome verursachen.

In dieser Arbeit wurden Seren von Patienten mit SPS, PERM und weiteren neurologischen Bewegungsstörungen auf AAK gegen unbekannte Autoantigene untersucht. Es wurden indirekte Immunfluoreszenz-Tests (IIFT) mit Gefrierschnitten des Kleinhirns von wildtypischen Mäusen, Ratten und Schweinen sowie von GAD65-Knock-out (Ko)-Mäusen durchgeführt. 53 von 100 Patientenseren, die im Anti-GAD-ELISA positiv für Anti-GAD65/67-AAK getestet wurden, zeigten im IIFT auf den Wildtyp-Substraten, nicht auf dem GAD65-Ko-Substrat, das Anti-GAD-typische Fluoreszenzmuster. Immunpräzipitationen mit den Patientenseren und 50 Blutspender-Seren aus Kleinhirngewebe (Schwein) bestätigten die Anwesenheit von Anti-GAD65/67-AAK in 52 Patientenproben, die Kontrollproben waren negativ. Zusätzlich konnten sowohl mit den Anti-GAD65/67-positiven als auch –negativen Patientenseren weitere Proteine aus dem Gewebe immunpräzipitiert werden, die durch Massenspektrometrie als N-ethylmaleimide-sensitive factor (NSF, Komponente des SNARE-Komplexes) und Dynamin 1 (DNM1) identifiziert wurden. Beide Proteine sind mit dem synaptischen Vesikeltransport assoziiert. Bei einer Westernblot-Analyse der Patienten-Immunpräzipitate mit monospezifischen Antikörpern wurde neben dem NSF (n = 29/100) auch das SNARE-Protein Syntaxin 1B (n = 59/100) nachgewiesen. Fast alle Seren, mit denen NSF gefällt wurde, immunpräzipitierten auch DNM1. Die Proteine wurden daraufhin aus Kleinhirngewebe angereichert und in Westernblots mit 100 Patientenproben und 135 Kontroll-Seren von 70 Blutspendern und 65 Patienten mit anderen neurologischen Erkrankungen inkubiert. NSF (n = 30/100) und DNM1 (n = 23/100) wurden in ca. 25-30% der Patientenseren als Zielantigene für AAK bestätigt. Im Vergleich zeigten nur sehr wenige Kontrollseren eine positive Immunreaktion gegen die Proteine (NSF: 3/135 DNM1: 1/135). 29 der 100 Patientenseren zeigten auch eine Immunreaktion gegen rekombinant hergestelltes NSF im Immunblot. Die Intensität der Reaktion war jedoch gegenüber dem nativen NSF geringer. Bei der isoelektrischen Fokussierung der nativen und rekombinanten NSF-Proteine ergaben sich verschiedene isoelektrische Punkte,

was für unterschiedliche posttranslationale Modifikationen spricht, die auch zu den abweichenden Immunreaktivitäten führen können.

Die Ergebnisse zeigen, dass Patienten mit SPS, PERM und verwandten neurologischen Erkrankungen zusätzliche AAK gegen verschiedene mit Vesikeln assoziierte, synaptische Proteine bilden können. Die Entwicklung von Testsystemen zum Nachweis dieser AAK sollte angestrebt werden.

1. Introduction

1.1. Autoimmunity and Autoantibodies

The immune system aids in maintaining and regulating an optimum functional homeostasis of the body. One of the primary functions of the immune system is to distinguish between self- and non-self-antigens and to produce an effective immune response against non-self-components (Poletaev and Boura, 2011). When the body is attacked by a pathogen, toxic or allergic substance, the immune system generates antibodies or immunoglobulins (Ig) to protect the host against harmful infections. These Y shaped glycoproteins can neutralize toxins, clump and cross-link different antigens, and result in phagocytosis or complement-mediated lysis and destruction of the foreign bodies. Such an immune response contributed by antibodies, which reside in body fluids, is called humoral immunity (Chaplin, 2010). The immune system largely averts self-antigens from creating an immune response. However, at times, antibodies undergo a loss of tolerance against self-proteins resulting in the production of autoantibodies (AAbs) directed against these self-antigens (Lleo et al., 2010). Such an aberrant immune response directed against healthy cells and tissues sets off “autoimmune diseases” (Lleo et al., 2010). These immune complexes might get accumulated in blood vessels and joints and mediate unnecessary inflammation and destruction of the healthy tissues. Despite previous notions about the destructive capacity of autoimmunity ("*horror autotoxicus*"), mild reactivity against self-antigens is a pre-requisite for maintaining a normal homeostasis (Lleo et al., 2010; Mackay, 2010). These natural AAbs attack various pathogens and defend the body against infections and reduce inflammation by eliminating oxidized lipids and proteins and apoptotic cells (Lleo et al., 2010). However, natural AAbs tend to have a low intrinsic affinity towards autoantigens, but at certain times they turn pathogenic, as directed by the antigen to undergo clonal selection including somatic hypermutation and class switching. Different mechanisms by which self-proteins could be modified to activate an immune response include post-translational modifications (PTMs), mutations, denaturation, native disorder or misfolding, and covalent modifications (Atassi et al., 2008). For example, aberrant missense point mutations or PTMs such as glycosylation and phosphorylation cause a variety of altered proteins in tumorigenesis. Alterations in the protein structure or their expression levels can affect antigen processing and binding and thereby activate a T-cell response necessary to initiate the humoral AAb production (Zaenker et al., 2016). The onset of autoimmune diseases, although enigmatic, could be caused by genetic, hormonal, environmental, and immune related factors. Molecular divergence in the nature of specific group of cells in terms of antigen production, secretion, and presentation

might occur long before the actual clinical symptoms, causing quantitative differences in the AAb production within the body fluids such as the serum or the cerebrospinal fluid (Poletaev and Boura, 2011). Detection of these AAbs in the serum or in the cerebrospinal fluid (CSF) aids in the early diagnosis of autoimmune diseases in patients and therefore, has become a powerful diagnostic tool to clinicians globally (Lleo et al., 2010). The clinical manifestations of autoimmune disorders, in most cases, is not caused directly by the AAbs; rather their measurement could be valuable biomarkers for the diagnosis and prediction of autoimmune disorders much earlier in life (Scofield, 2004).

1.1.1. Autoantibodies associated with central nervous system disorders

One of the most rapidly developing fields in clinical neurology is the identification of AAbs associated with the central nervous system (CNS). Neuronal AAbs were first discovered in patients with paraneoplastic cerebellar degeneration, encephalitis, or neuronopathy associated with underlying cancers. These AAbs targeted cytoplasmic proteins including Yo, Hu, Ri, Ma2 etc. and due to difficulty in accessing their targets *in vivo*, these AAbs are considered non-pathogenic, but possible markers for T-cell mediated responses against the underlying tumor and subsequently also against the neurons, which express similar antigens as the tumor. On the contrary, AAbs that target cell-surface or integral membrane proteins are regarded pathogenic due to a direct access to their target antigens such as N-methyl-D-aspartate receptor (NMDAR), leucine-rich glioma-inactivated protein 1 (LGI1), Contactin-associated protein-like 2 (CASPR2), aquaporin-4 (AQP4), α-amino-3-hydroxy-5-methyl-4-isoxazolepropionic acid receptor (AMPAR), γ-aminobutyric acid (GABA)-B receptor, glycine receptor etc. Disorders associated with AAbs targeting cell-surface proteins demonstrate rapid onset and progression, respond well to immunomodulatory drugs, are not regularly associated with underlying malignancies and these AAbs are important markers of the disease manifestations. Another group of AAb-related brain disorders intermediate to AAbs targeting paraneoplastic and cell-surface antigens include those binding to glutamic acid decarboxylase (GAD) and amphiphysin. AAbs against GAD are observed in various hyperexcitability disorders such as Stiff-Person-Syndrome (SPS), cerebellar ataxia, hyperekplexia, limbic encephalitis etc. (Irani et al., 2014; Lancaster and Dalmau, 2012; McKeon, 2013).

1.2. Stiff-Person-Syndrome (SPS)

SPS is a neurological movement disorder characterized by extreme rigidity, painful spasms, and hyperreflexia (Rakocevic and Floeter, 2012). Additionally, it is a rare disorder with an occurrence of one in a million, with two thirds of patients being women (Vives-Pi and Sabater, 2010). The classical symptoms of SPS include: (1) stiffness of the proximal and truncal limb muscles occurring due to the continuous contractions of the agonist and antagonist muscles leading to hyperlordosis, (2) episodic spasms in addition to the stiffness triggered by unexpected or abrupt noises, emotional distress, or visual stimuli, and (3) increased anxiety and duty-related paranoias (Alexopoulos and Dalakas, 2010; Dalakas, 2013; Rakocevic and Floeter, 2012; Vincent, 2008). The symptoms peak around a mean age of 35 years with a lag period of approximately 6.2 years until diagnosis (Alexopoulos and Dalakas, 2010). The disease is deemed to originate in the truncal muscles and gradually progresses to the lumbar and/or proximal limb muscles of the affected patients (Ali et al., 2011). Patients portray a stiff robotic gait resembling '*tin soldiers*', making it difficult to walk or bend, necessitating the use of walkers or wheelchairs and in some cases due to extreme stiffness, the patients are completely incapacitated (Alexopoulos and Dalakas, 2010; Dalakas, 2009; Dalakas et al., 2000).

1.2.1. Discovery of SPS

In 1956, Moersch and Woltman from the Mayo clinic reported 14 male patients experiencing extreme rigidity bearing strong similarity to tin soldiers and coined the term "Stiff Man Syndrome" (Bruckner, 1957). However, in 1958 Asher reported a female patient with similar symptoms and hence the name was changed to SPS. Additionally, there was another case reported in a seven-year-old Chinese boy in 1960. By 1967, SPS diagnostic criteria included distinctive muscular rigidity patterns that could have tangible favorable outcomes following administration of neuromuscular blocking agents as monitored by electromyography. In the following years, the criteria was further modified to include stiffness progression, periodic painful stiffness of axial muscles, stimulus elicited aching spasms, abnormal sensory and cognitive function, elevated lumbar lordosis and a beneficial effect following benzodiazepine administration (Ali et al., 2011). In 1988, SPS was identified as an autoimmune disorder with AAbs against GAD detected both in the serum and the CSF of a SPS patient with type 1 diabetes mellitus (T1DM). Subsequently, the detection of anti-GAD AAbs became a definite diagnostic biomarker for identification of SPS (Solimena and De Camilli, 1991; Solimena et al., 1990).

1.2.2. Variants of SPS and associated comorbidities

There are different types of SPS including (1) Stiff-limb-syndrome (SLS) (Barker et al., 1998; Hajjioui et al., 2010; Saiz et al., 1998), (2) jerking stiff man syndrome: due to the major involvement of the brainstem and SPS is accompanied with myoclonus (Alberca et al., 1982; Brown and Marsden, 1999; Meinck and Thompson, 2002) (3) progressive encephalomyelitis with rigidity and myoclonus (Hutchinson et al., 2008; Martinez-Martinez et al., 2014; McKeon et al., 2013; Stern et al., 2014). Occasionally, SPS is coupled with dystonia and epilepsy (Nemni et al., 1994; Vulliemoz et al., 2007) and neurophthalmologic disorders like autoimmune retinopathy (Steffen et al., 1999). SPS tends to often co-exist with other autoimmune disorders including T1DM, which is observed in ≈ 35% of SPS patients. T1DM is known to occur months to years prior to onset of SPS or in some cases right after stiffness befalls (Todd, 1995). Other diseases including Graves' disease, thyroiditis (10%), vitiligo, pernicious anemia (5%) and coeliac disease are often associated with SPS (Dalakas, 2013).

A similar phenotype as observed in SPS is also seen in patients infected with the tetanus toxin from Clostridium tetani. Patients experience involuntary activity of the voluntary muscles particularly rigidity and spasms of the abdominal and laryngeal muscles often leading to death due to respiratory failure. The toxin specifically targets the inhibitory nerve terminals, by blocking the release of neurotransmitters that act on lower motor neurons, which control the voluntary muscles. Through retrograde axonal transport, the toxins arrive at the spinal cord or brainstem and are consumed by the inhibitory neuronal circuits, where they specifically initiate the proteolysis of a synaptic protein called synaptobrevin or vesicle associated membrane protein (VAMP). VAMP plays a vital role in promoting exocytosis of synaptic vesicles containing neurotransmitters. Cleavage of VAMP prevents the release of inhibitory neurotransmitters like GABA and glycine resulting in the functional inhibition of lower motor neurons and hyperactivity of the voluntary muscles (Hassel, 2013).

1.2.3. Diagnosis of SPS

SPS continuous to remain a challenge for early diagnosis since it requires a great deal of exclusion from various other neurological disorders, psychogenic diseases, myelopathies, other pyramidal and extrapyramidal disorders etc. Diagnosis of SPS primarily includes detection of high-titer anti-GAD AAbs in the sera and the CSF of patients, which is further supported by magnetic resonance imaging of the brain and the spinal cord and electrophysiological findings concerning the electromyography studies which depict the characteristic involuntary firing of

motor units, despite voluntary relaxation (Alexopoulos and Dalakas, 2010; Dalakas, 2009; Dalakas, 2013; Folli et al., 1993; Levy et al., 1999; Levy et al., 2005; Murinson et al., 2004).

SPS is established as either paraneoplastic or idiopathic and is linked with several AAbs directed against antigens largely associated with the inhibitory neurons of the CNS. These AAbs are believed to limit the function of the inhibitory neurotransmitter GABA and destabilize the entire GABAergic system by upsetting the delicate balance between excitatory and inhibitory neurotransmission (Ali et al., 2011; Rakocevic and Floeter, 2012). Predominantly, AAbs against the GAD enzyme are observed in the serum and the CSF of SPS patients. Infrequently AAbs against gephyrin, glycine receptor subunit α-1 (GLRA1), GABA receptor associated protein (GABARAP), amphiphysin, GABA receptor etc. are also noted (Alexopoulos and Dalakas, 2010).

1.2.3.1. Autoantibodies against glutamic acid decarboxylase

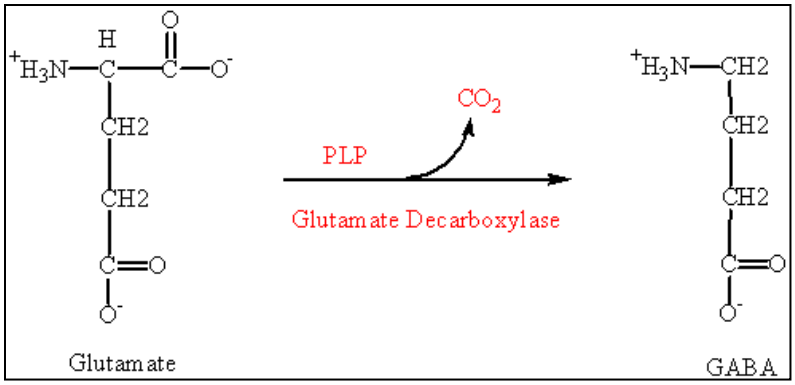

Figure 1: Decarboxylation of glutamate to GABA by GAD

(Adapted from Essential and Nonessential Amino Acids; http://homepages.rpi.edu/~bellos/)

The decarboxylation of L-glutamate to GABA is catalyzed by GAD which detaches a α-carboxyl group from glutamate to produce Y-carboxyl amino acid (GABA) using pyridoxal phosphate (vitamin B6) as the cofactor.

SPS is known to be associated with different organ-specific AAbs, with patients exhibiting a broad range of clinical symptoms, but the mostly commonly detected AAbs are the anti-GAD antibodies observed in more than 80% of the affected patients. In addition, 1% of the healthy population and 5% of patients with other neurological diseases harbor anti-GAD AAbs (Meinck et al., 2001). GAD is the rate-limiting enzyme involved the production of the inhibitory neurotransmitter GABA by using L-glutamate as the substrate and pyridoxal phosphate (PLP) as the cofactor as depicted in **Figure 1** (Alexopoulos and Dalakas, 2010). Apart from the GABAergic neurons in the CNS, GABA is also produced by the pancreatic β-cells and AAbs against GAD are also observed in patients with T1DM (Burbelo et al., 2008; Butler et al., 1993;

Solimena and De Camilli, 1991). In T1DM, anti-GAD AAb titers are 50 to 100-fold lower and probably recognize different GAD epitopes in comparison to anti-GAD AAbs detected in SPS (Baekkeskov et al., 1990; Hagopian et al., 1993). Anti-GAD AAbs detect conformational epitopes in T1DM, while linear and denatured epitopes are recognized in SPS (Baekkeskov et al., 1990; Butler et al., 1993; Ellis and Atkinson, 1996; Kim et al., 1994). Such contrasting epitope specificity and fidelity could be the reason behind the differences observed in the disease prevalence between SPS and T1DM (Ellis and Atkinson, 1996). Furthermore, anti-GAD AAbs are observed in other diseases including cerebellar ataxia (Bayreuther et al., 2008), therapy-resistant epilepsy, myoclonus (Lilleker et al., 2014) and Creutzfeldt-Jakob disease (Ali et al., 2011; Chang et al., 2007).

GAD65 and GAD67 are the two isoforms of GAD, encoded by two different genes and coined after their respective molecular weights. The majority of SPS patients (80%) have anti-GAD65 AAbs, while less than 50% of patients have AAbs against GAD67 (Meinck et al., 1984; Solimena and De Camilli, 1991). Discrete AAbs against GAD67 are rare and most patients bear cross-reacting AAbs against both these enzymes. The isoforms are 65% homologous and differ only slightly in the N-terminal region. However, they exhibit vast differences in their functionality including different subcellular localizations, co-factor interactions, regulatory characteristics etc. (Alexopoulos and Dalakas, 2010; Ali et al., 2011; Buddhala et al., 2009; Fenalti and Buckle, 2010). GAD67, the soluble form, is believed to be localized in the neuronal cytoplasm and regularly produces basal levels of GABA, which is used as a source of energy (via GABA shunt), confers protection to the CNS following neuronal damage, and aids in synaptogenesis during primary development (Lamigeon et al., 2001; Waagepetersen et al., 1999). On the contrary, GAD65, the membrane associated form, is produced in the cytoplasm and is concentrated around the synaptic vesicles of GABAergic neurons or microvesicles in the pancreatic β-cells (Reetz et al., 1991) and primarily produces GABA required for an effective inhibitory neurotransmission (Ali et al., 2011; Fenalti and Buckle, 2010). The enzyme primarily occurs as an auto-inactivated apoenzyme in the cells and is reactivated following the addition of a co-factor PLP, especially during a high demand for GABA such as response to stress (Martin and Rimvall, 1993; Patel et al., 2006)

1.2.3.2. Autoantibodies other than anti-GAD in SPS

AAbs against different inhibitory synaptic proteins have been investigated in SPS (Alexopoulos and Dalakas, 2010; Dalakas, 2009). However, till date, anti-GAD AAbs are considered to be the best serological biomarker for the diagnosis of SPS (Meinck et al., 2001; Solimena and De

Camilli, 1991). **Figure 2** depicts all known AAbs in SPS such as those directed against amphiphysin (Camilli et al., 1993), GABARAP (Raju et al., 2006), gephyrin (Butler et al., 2000) etc.

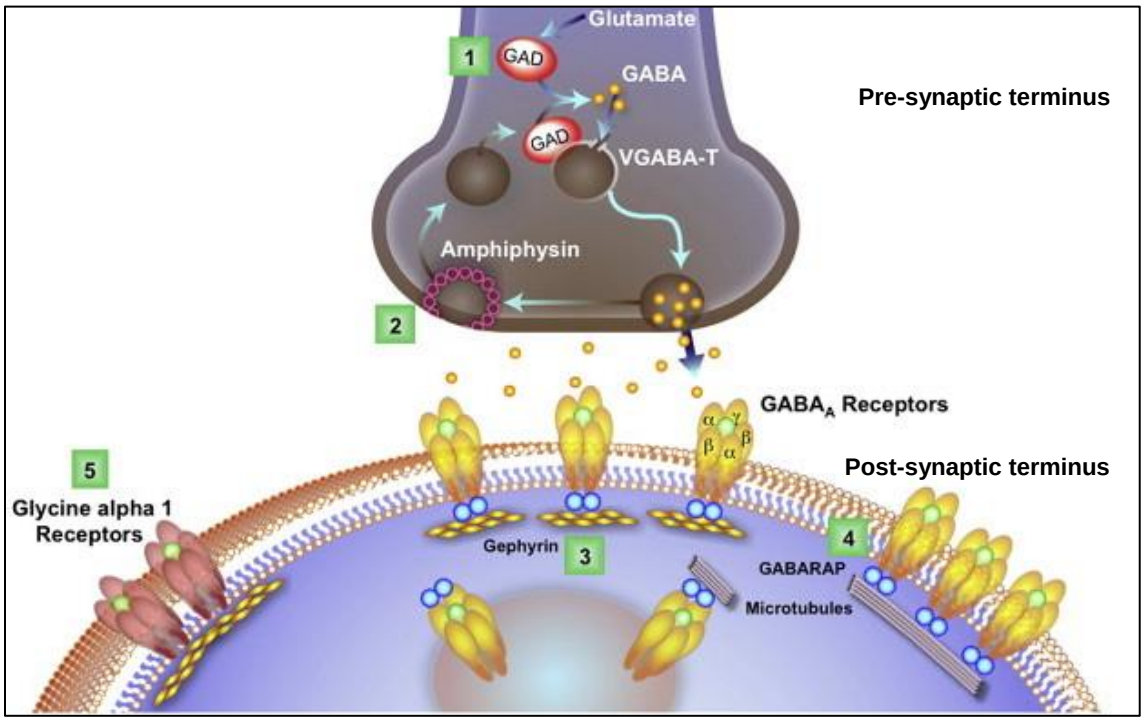

Figure 2: Representation of the pre- and post-synaptic terminus of a neuronal cell demonstrating all identified target antigens in SPS

Adapted from (Dalakas, 2013)

The target antigens present in the pre-synaptic terminus include **(1) GAD**: the enzyme involved in the synthesis of GABA and amphiphysin, **(2) Amphiphysin:** protein involved in the recycling of vesicles following exocytosis of GABA. In the post-synaptic terminus, target antigens include **(3) Gephyrin:** a tubulin-binding protein required for the clustering of GABA-A receptors and glycine receptors in the brain, **(4) GABARAP:** considered a linker protein between gephyrin and GABA-A receptors, ensures the proper recruitment of gephyrin and assembly of GABA-A receptors. **(5) GLRA1**: ligand-gated chloride channel involved in the down-regulation of neuronal excitability. The rate of occurrence of the anti-GAD, anti-GABARAP, anti-amphiphysin, anti-gephyrin, and anti-GLRA1 AAbs are 80, 70%, 5%, one case, and 10% respectively. (Other abbreviations: VGABA-T= vesicular GABA Transporter)

The two AAbs that are observed in the paraneoplastic variant of SPS include amphiphysin and gephyrin as observed in 5% of patients and one case, respectively. These patients are mostly diagnosed with breast adenocarcinoma and small-cell lung carcinoma (Camilli et al., 1993; Folli et al., 1993). Gephyrin plays an important role in the clustering of the glycine receptors and the ionotropic GABA-A receptors in the brain and the spinal cord (Butler et al., 2000). Amphiphysin is a pre-synaptic protein and plays an important role in vesicular endocytosis by recruiting

dynamin to the clathrin coated pits as well as in maintaining proper density of the GABA-A receptors (Takei et al., 1999). Impairment of the synaptic transmission by anti-amphiphysin AAbs have been researched in greater detail in comparison to the anti-GAD AAbs. Passive transfer of amphiphysin-specific IgG from a breast cancer patient into rats resulted in a leaky blood-brain barrier (Geis et al., 2010; Sommer et al., 2005). A direct pathogenic evidence for anti-amphiphysin AAbs was demonstrated in such studies, since the animals portrayed typical signs of SPS in a dose-dependent manner. Additionally, patients showed a clinical improvement following plasmapheresis, which lowered their anti-amphiphysin AAb titers (Wessig et al., 2003). On the contrary, typical SPS symptoms were not observed following active immunization with the GAD antigens or following a passive transfer of the GAD-specific IgG into animals with an intact blood-brain barrier (Sommer et al., 2005; Wessig et al., 2003). Another AAb target in SPS is GABARAP, a post-synaptic protein that aids in the proper assembly of GABA-A receptors in the brain. A study reported the presence of anti-GABARAP AAbs in ≈ 70% of patients with SPS (Raju et al., 2006). Additionally, a pathogenic significance of anti-GABARAP AAbs was proposed since these AAbs impaired proper GABA-A receptor surface expression on the axonal processes, which in turn could down-regulate appropriate GABA uptake by the GABA receptors (Raju et al., 2006). Furthermore, AAbs are also observed in the inhibitory glycinergic pathways, primarily against the GLRA1, which were reported in 10-12% of SPS patients (Alexopoulos and Dalakas, 2010; McKeon et al., 2013) and also in cases with progressive encephalomyelitis with rigidity and myoclonus (PERM).

1.2.4. Therapeutic options in patients with SPS

Treatment options that could improve the patient's life quality by providing symptomatic relief have been the primary focus in the successful management of SPS. Promising therapeutic options have been limited due to the rarity and complications associated with the disease. The primary line of treatments included benzodiazepines and baclofen, primarily diazepam because of its property as a muscle relaxant. Other GABA agonist therapy consisted of treatments with valproate, tiagabine, gabapentin etc. Dosages of all drugs were gradually increased to prevent dangerous side effects. Baclofen was administered intrathecally and provided significant improvements in the management of spasticity in patients. Following GABAergic drugs, treatment with intravenous immunoglobulins (IVIG), plasmapheresis, Rituximab, and immune modulators were preferred in refractory cases (Bhatti and Gazali, 2015). In a study, treatment with IVIG demonstrated a significant reduction in patient's stiffness and reduced anti-GAD65 AAb titers to the lowest levels. Therefore, SPS could be a functional disorder due to disruption

in GABAergic neurotransmission, rather than a structural disorder (Dalakas et al., 2001). Compared with IVIG, plasmapheresis portrayed lower side effects and was better tolerated in patients (McLeod et al., 1999). Furthermore, treatment with Rituximab to deplete CD20+ B cells has been administered in some patients with considerable reductions in disease symptoms. Therefore, Rituximab could be considered a substitute to benzodiazepines or immune modulatory drugs, when the desired effects were not achieved. (Lobo et al., 2010). Despite only minimal symptomatic relief in some patients, early diagnosis and timely therapeutic interventions might help improve the quality of life of the affected patients (Bhatti and Gazali, 2015).

1.2.5. Pathogenic relevance of autoantibodies in SPS

The haunting question in SPS is the pathogenic significance of the anti-GAD AAbs. Some groups have hypothesized probable theories which include: (1) production of GAD65-specific AAbs within the CNS due to the intrathecal sensitization of GAD65-reactive CD4+ T cells and (2) antigen sensitization outside the CNS due to crossover of a CNS related antigen across the blood-brain barrier and recognition by specific AAbs (Vives-Pi and Sabater, 2010). The production of high-affinity AAbs is dependent on antigen-specific CD4+ T cells. However, in SPS there has been no indication of cellular infiltration or atrophic changes within the CNS, but only selective loss of Purkinje cells observed in one patient with cerebellar ataxia positive for anti-GAD AAbs (Ishida et al., 2007; Vives-Pi and Sabater, 2010). Furthermore, GAD-specific T-cells were observed only in few SPS patients and the levels were highly inconsistent (Dalakas, 2013). In addition, most autopsies showed a lack of lymphocyte infiltration, which could indicate that the synthesis of anti-GAD AAbs is not within the CNS parenchyma, but possibly in the meninges (Holmoy and Geis, 2011). On the contrary, autopsies and biopsies of T1DM patients have revealed leukocyte infiltration into the pancreatic islets cells and these were shown to include CD8+ T cells, recruitment of pro-inflammatory cytokines, and over-expression of human leukocyte antigen (HLA) and adhesion molecules (Vives-Pi and Sabater, 2010). Additionally, anti-GAD AAbs were also observed in other neurological diseases such as epilepsy, limbic encephalitis, myoclonus, Batten's disease, or abnormal eye movements, indicating that these AAbs do not define a unique clinical phenotype or that they identify different disease-specific GAD epitopes within the CNS (Brown and Marsden, 1999; Nemni et al., 1994; Saiz et al., 2008; Steffen et al., 1999; Vulliemoz et al., 2007).

All the standard methodologies used to prove brain autoimmunity have been fulfilled by many groups, but in vain. These include creation of an animal model by active immunization or

passive transfer, comparing antibody titers with disease severity and response, finding evidence of maternal transfer, determining the functional effect etc. (Alexopoulos and Dalakas, 2010). However, till date, the pathogenic significance of GAD AAbs in SPS has not yet been established. One hypothesis that comes close to explaining the pathogenic significance is the presence of a defective GABAergic inhibitory neuronal circuit that could result in the constant firing of alpha-motor neurons. GABA is the major inhibitory neurotransmitter in the brain and a dysfunction in its production/reuptake pathway could explain the continuous motor cortex hyper-excitability and muscle hyperactivity (Meinck et al., 1984; Sandbrink et al., 2000). Therefore, prohibition of GABA production and/or obstruction in the exocytosis of vesicles carrying GABA could explain how anti-GAD and anti-amphiphysin AAbs disrupt GABAergic neurotransmission (Dinkel et al., 1998; Geis et al., 2010; Ishida et al., 1999; Rakocevic and Floeter, 2012; Wu et al., 2007). A study reported decreased pre-synaptic GABAergic transmission as recorded by patch clamp readings of rat cerebellar slices following incubation with GAD-specific IgG from patient positive for cerebellar ataxia (Ishida et al., 1999). In another study, rats demonstrated stiffness-like tendency, disabled walking, and decreased grip strength after being injected with anti-GAD AAbs from a SPS patient with severe motor nerve damage into their lateral ventricle, but not intrathecally, suggesting GABAergic impairment in the supraspinal pathway (Hansen et al., 2013). In another study, repeated intrathecal injections of IgG from a SPS patient with high anxiety resulted in the transfer of only the anxiety and no motor symptoms to the rats (Geis et al., 2011).

Interneuron loss could also disrupt the function of central or spinal inhibitory circuits. However, reports of depletion of GABAergic neurons in the cerebral cortex or spinal motor neurons in the intermediate and medial ventral horn has been very minimal in SPS (n = 5). Additionally, perivascular inflammation was observed only in three patients (Meinck and Thompson, 2002). Manto *et al,* showed that the potentiation of the corticomotor response was blocked in rats following intracerebellar administration of anti-GAD65 AAbs from SPS patients. On the contrary, injecting it into the paraspinal region caused continuous firing of motor neurons and elevated excitability in the anterior horn neurons. No such result was observed on injecting the sera from SPS patients without any neurological symptoms (Manto et al., 2007). These results indicate the involvement of spinal neurons in SPS, specifically the inhibitory synapse.

Till date, there is no known evidence of genetic predisposition or maternal transfer of the disease to the offspring (Alexopoulos and Dalakas, 2010; Nemni et al., 2004; Vives-Pi and Sabater, 2010). A case report revealed that a mother with SPS having high titer anti-GAD AAbs did not transfer the disease to the offspring. The baby in fact showed high concentrations of

anti-GAD AAbs up to 24 months following birth, but a follow-up after six and eight years revealed no signs of SPS in the offspring (Nemni et al., 2004). These findings suggest that either the blood-brain barrier in the child was intact and prevented the AAb transfer into the CNS or that anti-GAD AAbs are not pathogenic. However, it is not easy to draw conclusions based on one study (Alexopoulos and Dalakas, 2010). On the contrary, an association with the HLA class II locus was reported in a study, wherein 72% of SPS patients carried the DQB1*0201 allele (Pugliese et al., 1993). Genes within the major histocompatibility complex (MHC) such as the HLA DR and DQ alleles are associated with genetic risks of developing various autoimmune diseases including SPS. A strong association between several DQB1 and DRB1 MHC-II alleles has been reported in both idiopathic and paraneoplastic SPS. Patients with the DQB1* 0201 allele are conferred to be at a higher risk of developing T1DM, which appropriately is also associated with AAbs against GAD (Ali et al., 2011).

The correlation between anti-GAD AAbs and the clinical parameters of SPS was analyzed in many studies in order to determine the pathogenic significance of these AAbs (Dalakas et al., 2001; Murinson et al., 2004; Rakocevic et al., 2004). Unfortunately, there was no association between the serum or the CSF anti-GAD AAb titers and the disease duration, severity, or treatment response, indicating that these AAbs are not pathogenic. It is indeed important to examine how these AAbs can target an intracellular antigen such as GAD65 (Alexopoulos and Dalakas, 2010).

The lack of a pathogenic relevance of the anti-GAD AAbs in SPS might point towards the existence of additional AAbs directed against other intracellular or cell-surface proteins in the GABAergic neurons, which on discovery might explain the etiology of the disease better. Therefore, the primary objective of the current study was to screen additional, unrevealed autoantigens in SPS and other associated hyperexcitability disorders.

1.3. Progressive encephalitis with rigidity and myoclonus

Hyperexcitability disorders associated with the CNS such as SPS, SLS, and PERM (SPS-plus) affect motor neuron excitability in different regions of the brain and spinal cord. Cumulatively, these disorders instigate painful spasms, stiffness, rigidity, and exaggerated startle in the truncal, spinal, and limbic muscles of the affected patients (McKeon et al., 2013). Even though PERM portrayed similar symptoms to SPS, patients diagnosed with PERM have added neurological and brainstem defects and its often considered more progressive, severe, and generally fatal (Brown and Marsden, 1999; Meinck and Thompson, 2002). Patients with PERM portray symptoms such as stiffness, rigidity, spasms, hyperekplexia, and myoclonus in addition

to brainstem and oculomotor malfunction. These patients may harbor AAbs against the GLRA1, with or without the presence of anti-GAD AAbs and the use of immunomodulatory drugs might be effective in them (Carvajal-Gonzalez et al., 2014; Hutchinson et al., 2008). A study proposed two hypotheses supporting the pathogenic significance of anti-GLRA1 AAbs in PERM. (1) Complemented-mediated mechanism: anti-GLRA1 AAbs deposited C3b and activated complement in live human embryonic kidney cells 293 (HEK293-cells) expressing GLRA1. (2) Antibody internalization: incubation of patients' sera on HEK293-cells expressing GLRA1 resulted in the internalization and loss of glycine receptors in these cells. These mechanisms could directly hinder the functioning of glycine receptors and in turn cause a malfunction in the inhibitory synaptic neurotransmission (Carvajal-Gonzalez et al., 2014). PERM patients portrayed variable prognosis with immunotherapies including a blend of plasma exchange, IVIG, corticosteroids, and cyclophosphamides. Even though many patients showed good response with immunomodulatory drugs, recommendation of early diagnosis and aggressive therapy is mandated for such rare diseases (Stern et al., 2014).

In comparison to the anti-GLRA1 AAbs, the pathogenic significance of anti-GAD AAbs still remain enigmatic in PERM and other anti-GAD associated movement disorders. Therefore, the search for additional autoantigens continues in PERM and other related hyperexcitability disorders such as cerebellitis, dystonia, hyperekplexia etc.

1.4. Neuronal cell-communication

Most antibody-associated disorders of the CNS, targeting primarily cell-surface proteins alter the function of the target proteins and block neuronal cell communication and transmission. For example, in anti-NMDAR encephalitis, antibody-mediated internalization and selective loss of NMDAR in the neurons abolishes normal NMDAR-mediated glutamate neurotransmission, resulting in cognitive and behavioral deficits in patients. Similarly, other neuronal AAbs could affect either GABAergic or glutamatergic neurotransmission by targeting receptors, synaptic proteins, or directly modulate the structure of neurons (Hughes et al., 2010; Irani et al., 2014).

Membrane trafficking is the primary means of communication in eukaryotic cells. Even though many cells undergo direct fission or fusion, dedicated trafficking vesicles are involved in well-developed organelles. These vesicles detach from the original compartment, then dock and fuse with the target compartment, transporting both membrane and soluble contents to the target side. The vesicles could be between 40-80 nm in size and in neurons they are termed as "synaptic vesicles" (Bonifacino and Glick, 2004; Takamori et al., 2006). Membrane trafficking in the neurons is the most complex, due to the rapid, yet highly regulated vesicular fusions and

reuptakes (Dulubova et al., 2007). Neurons communicate with one another though electrical and chemical signals known as quantal transmission. The chemical messengers are packed into the synaptic vesicles, which fuse with the plasma membrane at the nerve endings and release the signals into inter-neuronal point of contact at the axonal termini called neuronal synapse. Electrical impulses traverse at a speed of 100 m/s through the neurons and are converted into chemical signals at the pre-synaptic terminus. These chemical messengers or neurotransmitters are released into the synaptic cleft following calcium-dependent exocytosis of the synaptic vesicles (Holt et al., 2008; Hussain and Davanger, 2011; Nicholls et al., 1992). Subsequently, neurotransmitters bind to the appropriate receptors on the post-synaptic membrane and trigger a series of physiological changes depending on the membrane's electrical potential. To maintain normal synaptic function and to prepare for subsequent neurotransmitter release, the synaptic vesicles are recycled through clathrin-mediated endocytosis and pumped once again with neurotransmitters using the energy from electro chemical proton gradient (Nicholls et al., 1992). A sequential recruitment of various cytoplasmic protein complexes are observed during exocytosis, particularly for the recognition of target membrane, transport of synaptic vesicles, docking, priming, and fusion of the vesicles with the target membrane (Takamori et al., 2006). This group of conserved, 60-70 amino acid, membrane associated proteins is called Soluble NSF Attachment Protein Receptor (SNARE), where NSF stands for N-ethylmaleimide sensitive factor (Bonifacino and Glick, 2004; Hussain and Davanger, 2011; Jahn and Scheller, 2006; Südhof and Rothman, 2009; Whiteheart and Matveeva, 2004; Whiteheart et al., 2001).

2. Material and Methods

2.1. Materials

2.1.1. Antibodies

Table 1: List of primary antibodies purchased externally for identification of different SNARE proteins and other target antigens

Antibody target	Host / Isotype / clonality	Company	Product number	Molecular weight of target
Dynamin 1	Rabbit / IgG/ polyclonal	Sigma-Aldrich Chemie GmbH, Germany	HPA049910	≈ 97 kDa
EXOC4 or Sec8	Rabbit / IgG/ polyclonal	Sigma-Aldrich Chemie GmbH, Germany	HPA031443	≈ 122 kDa
GABARAP	Rabbit / IgG/ polyclonal	Antibodies-online GmbH, Germany	ABIN388564	≈ 13 kDa
NSF	Rabbit / IgG/ polyclonal	Atlas antibodies, Germany	HPA003154	≈ 82 kDa
Rab3A	Rabbit / IgG/ polyclonal	Sigma-Aldrich Chemie GmbH, Germany	HPA003160	≈ 24 kDa
SNAP25	Rabbit / IgG/ polyclonal	Sigma-Aldrich Chemie GmbH, Germany	HPA001830	≈ 25 kDa
STX1B	Mouse/ IgG/ monoclonal	R & D Systems GmbH, Germany	MAB6848	≈ 33 kDa
STXBP1 or Munc18	Rabbit / IgG/ polyclonal	Sigma-Aldrich Chemie GmbH, Germany	HPA008209	≈ 66 kDa
Synaptotagmin 1	Rabbit / IgG/ polyclonal	Sigma-Aldrich Chemie GmbH, Germany	HPA064788	≈ 47 kDa
Synaptophysin 1	Rabbit / IgG/ polyclonal	Sigma-Aldrich Chemie GmbH, Germany	HPA002858	≈ 38 kDa
VAMP2	Rabbit / IgG/ polyclonal	Sigma-Aldrich Chemie GmbH, Germany	V1389	≈ 12 kDa

Table 2: List of polyclonal rabbit antibodies generated by immunization with recombinant proteins (Euroimmun AG, Germany)

Antibody target	Designation	Molecular weight of target
GAD 65/67	EURab0022	≈ 65 and 67 kDa
GLRA1	EURab0033	≈ 52 kDa
NMDAR	EURab008	≈ 105 kDa

Table 3: List of recombinant monoclonal antibodies produced at Euroimmun AG, Germany

Antibody target	Host / Isotype / clonality	Designation	Molecular weight of target
GAD 65/67	Human / IgG / monoclonal	AK1242	≈ 65 & 67 kDa
Amphiphysin	Human / IgG / monoclonal	AK59	≈ 76 kDa
Metabotropic Glutamate Receptor 1 (GRM1)	Human / IgG / monoclonal Mouse / IgG / monoclonal	AK122 AK123	≈ 133 kDa

Table 4: List of secondary antibodies

Antibody	Conjugate	Company	Product number
Anti-human-IgG-B/E-AP	Alkaline Phosphatase	EUROIMMUN AG, Germany	AE-142-1030
Anti-human-IgG-FITC	Fluorescein isothiocyanate	EUROIMMUN AG, Germany	AF 102-0160
Goat anti-rabbit-IgG(H+L)-Cy2	Cyanine 2	Dianova GmbH, Germany	111-225-045
Goat anti-rabbit-IgG(H+L)-Cy3	Cyanine 3	Dianova GmbH, Germany	111-165-045
Polyclonal goat anti-mouse-IgG(H+L)-Alexa488	Alexa488	Jackson ImmunoResearch Europe Ltd.	115-545-062
Polyclonal goat anti-mouse-IgG(H+L)-AP	Alkaline Phosphatase	Jackson ImmunoResearch Europe Ltd.	115-055-062
Polyclonal goat anti-rabbit-IgG(H+L)-AP	Alkaline Phosphatase	Sigma-Aldrich Chemie GmbH, Germany	A3812

2.1.2. Chemicals

Table 5: List of chemicals

Chemical Name	Company
Acetic acid (100%)	Merck KGaA, Germany
Acetonitrile	Merck KGaA, Germany
Acetone	Merck KGaA, Germany
Alpha-Cyano-4-hydroxycinnamic acid	Bruker Corporation, Germany
Aluminum sulfate Hydrate, 98%	Sigma-Aldrich Chemie GmbH, Germany
Ammonium hydrogen carbonate (NH_4HCO_3)	Merck KGaA, Germany

Ammonium phosphate monobasic	Sigma-Aldrich Chemie GmbH, Germany
Amphotericin B (100 x stock solution)	PAA Laboratories, Germany
Benzonase	Merck KGaA, Germany
Bicinchoninic acid Solution (BCA)	Sigma-Aldrich Chemie GmbH, Germany
Bromophenol blue	Merck KGaA, Germany
Copper sulfate ($CuSO_4$)	Merck KGaA, Germany
Coomassie brilliant blue G250	Merck KGaA, Germany
Dithiothreitol (DTT)	Gerbu Biotechnik GmbH, Germany
Ethanol	Merck KGaA, Germany
Ethylenediaminetetraacetic acid (EDTA)	Gerbu Biotechnik GmbH, Germany
Hydrogen peroxide (30%)	Carl Roth GmbH & Co. KG, Germany
Iodoacetamide	Bio-Rad Laboratories GmbH, Germany
Isopropanol	Serva Electrophoresis GmbH, Germany
Methanol	Merck KGaA, Germany
n-Octyl-β-D-glucopyranoside	Carl Roth GmbH & Co. KG, Germany
Ortho-Phosphoric acid	Merck KGaA, Germany
Peptide Calibration Standard II	Bruker Corporation, Germany
Phenylmethylsulfonyl fluoride (PMSF)	Sigma-Aldrich Chemie GmbH, Germany
Phosphate buffered saline (PBS) ready-to-use	Euroimmun AG, Germany
Ponceau S	Sigma-Aldrich Chemie GmbH, Germany
Protease inhibitor cocktail	Sigma-Aldrich Chemie GmbH, Germany
Sodium chloride (NaCl)	Merck KGaA, Germany
Sodium deoxycholate monohydrate, 98%	Abcr GmBh, Germany
Sodium dodecyl sulfate (SDS)	Carl Roth GmbH & Co. KG, Germany
Thiourea	Sigma-Aldrich Chemie GmbH, Germany
Trifluoro acetic acid (25% solution in water)	Merck KGaA, Germany
Tris(hydroxymethyl)aminomethane (Tris)	Gerbu Biotechnik GmbH
Triton X-100	Sigma-Aldrich Chemie GmbH, Germany
Trypsin (Sequencing grade modified)	Promega GmbH, Germany
Tween® 20	Gerbu Biotechnik, Germany
Urea	Gerbu Biotechnik GmbH, Germany
Urea Zoom	Thermo-Fisher Scientific GmbH, Germany
Water for chromatography	Merck KGaA, Germany
Western blot substrate (NBT/BCIP)	Euroimmun AG, Germany
ZOOM Carrier Ampholytes pH 3–10	Thermo-Fisher Scientific GmbH, Germany
ZOOM CHAPS	Thermo-Fisher Scientific GmbH, Germany

2.1.3. Buffers

Table 6: List of buffers

Buffer Type	Buffer Composition
BCA - BSA-Standard Stock	5 mg/ml BSA 0.9% (w/v) NaCl
BCA - BSA-Standard - 31 µg/ml	31 µg/ml BSA 0.9 % (w/v) NaCl
BCA - BSA-Standard - 63 µg/ml	63 µg/ml BSA 0.9% (w/v) NaCl
BCA - BSA-Standard - 125 µg/ml	125 µg/ml BSA 0.9% (w/v) NaCl
BCA - BSA-Standard - 250 µg/ml	250 µg/ml BSA 0.9% (w/v) NaCl
BCA - BSA-Standard - 500 µg/ml	500 µg/ml BSA 0.9% (w/v) NaCl
BCA-$CuSO_4$ solution	4% (w/v) $CuSO_4$
Blue silver de-staining solution	10% (v/v) Ethanol 2% (v/v) Ortho-Phosphoric acid
Blue silver fixating solution	50% (v/v) Methanol 10% (v/v) acetic acid
Blue silver staining solution	0.02% (w/v) Coomassie brilliant blue 5% (w/v) Aluminum sulfate Hydrate 10% (v/v) Ethanol 2% (v/v) Ortho-Phosphoric acid
CHAPS sample buffer	7 M Urea 2 M Thiourea 4% (v/v) CHAPS 0.5% (v/v) Carrier Ampholyte pH 3-10 1% (v/v) Bromphenol blue
Cryo-IP-PBS buffer	1 x PBS 0.1% (w/v) Tween-20 2.5 mM EDTA 1 mM PMSF
Iso-electric focusing (IEF) NH_4HCO_3	200 mM NH_4HCO_3

IEF sample buffer	1.5 mg DTT 500 µl CHAPS sample buffer 2 µl 1% bromophenol blue 2.5 µl ZOOM Carrier Ampholyte pH 3-10
IEF Urea	10 M urea
Matrix Assisted Laser Desorption/Ionization (MALDI) 23	650 mM Iodoacetamide
MALDI de-staining solution 1	30% (v/v) Acetonitrile 25 mM NH_4HCO_3 Water for chromatography
MALDI de-staining solution 2	50% (v/v) Acetonitrile 10 mM NH_4HCO_3 Water for chromatography
MALDI-extraction solution	5 mM n-Octyl-β-D-glucopyranoside 50% (v/v) Acetonitrile 0.3% (v/v) Trifluoro acetic acid Water for chromatography
MALDI-matrix solution	1.4 mg/ml α-Cyano-4-hydroxycinnamic acid 85% (v/v) Acetonitrile 0.1% (v/v) Trifluoro acetic acid 1 mM Ammonium phosphate monobasic
MALDI-peptide calibration/matrix	10% (v/v) Peptide calibration II 1.4 mg/ml α-Cyano-4-hydroxycinnamic acid 85% (v/v) Acetonitrile 0.1% (v/v) Trifluoro acetic acid 1 mM Ammonium phosphate monobasic
MALDI-peptide calibration II	Peptide calibration standard II 1% (v/v) Trifluoro acetic acid
MALDI-trypsin stock solution	10 µg/ml Trypsin 3 mM Tris-HCl pH 8.5
PBS/Tween	1 x PBS 0.2% Tween® 20 in PBS
PMSF 100 mM	100 mM PMSF 100% (v/v) Isopropanol
Ponceau S solution	0.2% (w/v) Ponceau S 7% (v/v) Acetic acid

Ponceau S de-staining solution	50 mM Tris-base
Protein G elution buffer	1x NuPAGE® sample buffer 250 mM DTT
Solubilization buffer	100 mM Tris, pH 7.4 150 mM NaCl 2.5 mM EDTA 1% (w/v) Triton-X-100 0.5% (w/v) Deoxycholate

2.1.4. Miscellaneous

Table 7: List of additional reagents and lab equipment

Instruments/Materials	Supplier
Analytical balance ACJ/ACS	KERN & SOHN GmbH, Germany
Confocal laser scanning microscope LSM700- Axio Imager	Carl Zeiss Microscopy GmbH, Germany
CO_2 Incubator BBD 6220	Thermo-Fisher Scientific GmbH, Germany
DMEM high glucose medium	PAA Laboratories, Germany
Embedding medium	Euroimmun AG, Germany
Eppendorf® Thermomixer Compact	Eppendorf AG, Germany
Fetal bovine serum (Mycoplex)	PAA Laboratories, Germany
Fluorescence microscope EUROStar II	Euroimmun AG, Germany
Dounce cylinder (15 ml) with plunger sizes: large and small	Sartorius Stedim Biotech GmbH, Germany
Dynabeads® His-Tag Isolation and Pulldown	Thermo-Fisher Scientific GmbH, Germany
Dynabeads® Protein G for Immunoprecipitation	Thermo-Fisher Scientific GmbH, Germany
DynaMag™-2 Magnetic separator	Thermo-Fisher Scientific GmbH, Germany
Heraeus Fresco 21 Refrigerated Microcentrifuge	Thermo-Fisher Scientific GmbH, Germany
Hyperflasks (T75) -Corning®	Omnilab-Laborzentrum, Germany

Lab pH meter InoLab® pH 7110 with pH-Electrode	Xylem Analytics Germany Sales GmbH & Co. KG, WTW, Germany
MALDI TOF/TOF MS, Autoflex III smartbeam	Bruker Daltonik GmbH, Germany
Magnetic stirrer and Stirring Bar - cylindrical shape	Heidolph Instruments GmbH, Germany
MICCRA D-9 Homogenizer	Miccra GmBH, Germany
MICCRA Dispersing tool for small volumes (1-100 ml): DS-8/P	Miccra GmBH, Germany
Microtome - Leitz 1720 Cryostat	Leica Microsystems, Germany
Microtiter plates, 96-well, natural, and sterile	Greiner Bio-one GmbH, Germany
Mini Lab Roller™ Dual Format Rotator	Labnet International, USA
Mini shaker IKA MS 3 Basic	IKA®-Werke GmbH & Co. KG, Germany
Nitrocellulose Blotting Membrane (UniSart® 0.22µm)	Sartorius Stedim Biotech GmbH, Germany
NuPAGE® 4-12% Bis-Tris Gel 1.0 mm	Thermo-Fisher Scientific GmbH, Germany
NuPAGE® LDS Sample Buffer (4 x)	Thermo-Fisher Scientific, Germany
NuPAGE® MOPS SDS Running Buffer (20 x stock solution)	Thermo-Fisher Scientific GmbH, Germany
NuPAGE® Transfer Buffer (20 x stock solution)	Thermo-Fisher Scientific GmbH, Germany
Penicillin/streptomycin (100 x stock solution)	PAA Laboratories, Germany
PowerPac Basic Power Supply	Bio-Rad Laboratories GmbH, Germany
PROTEAN® i12™ Isoelectric Focusing (IEF) Cell	Bio-Rad Laboratories GmbH, Germany
PROTEAN® i12™ IEF cleaning concentrate	Bio-Rad Laboratories GmbH, Germany
PROTEAN® i12™ IEF electrode Assembly Pair	Bio-Rad Laboratories GmbH, Germany
PROTEAN® i12™ IEF focusing Tray (11 cm)	Bio-Rad Laboratories GmbH, Germany
PROTEAN® i12™ IEF gel side down electrode wicks	Bio-Rad Laboratories GmbH, Germany
PROTEAN® i12™ IEF mineral oil	Bio-Rad Laboratories GmbH, Germany
PROTEAN® i12™ IEF rehydration/equilibration trays	Bio-Rad Laboratories GmbH, Germany
PROTEAN® i12™ IEF retainers	Bio-Rad Laboratories GmbH, Germany
Precision balance PES/PEJ	KERN & SOHN GmBH, Germany
Readystrip IPG strips 7 cm pH 3-10 NL (nonlinear)	Bio-Rad Laboratories GmbH, Germany
Rocking shaker BIOMETRA® WT16	Biometra GmbH, Germany
Sonicator Branson 250 Sonifer	Branson ultrasonics corportation, USA
Spectrafuge™ Mini Laboratory Centrifuges	Labnet International, USA
TE22 small transfer tank unit	Hoefer Inc., USA

Tecan Sunrise™ Microplate reader	Tecan GmbH, Germany
Universal blot buffer plus (10 x stock solution)	Euroimmun AG, Germany
Universal blot wash buffer (10 x stock solution)	Euroimmun AG, Germany
Water bath WB14	Memmert GmbH +Co. KG, Germany
XCell SureLock® Mini-Cell	Thermo-Fisher Scientific GmbH, Germany

2.1.5. Patients

Anonymized serum samples from clinically-characterized patients (n = 100) diagnosed with SPS, PERM and various neurological-related hyperexcitability disorders were a kind donation from Prof. Dr. Hans-Michael Meinck from the Department of Neurology, University of Heidelberg, Germany **(Table 8).** These patient' sera were analyzed in various tests methods in comparison with arbitrary controls including sera from neurological and healthy controls. Neurological controls included patients (n = 65) having AAbs against other well-known neuronal candidate antigens **(Table 9)** and sera from healthy blood donors (n = 70) were classified as the healthy controls. All control serum samples were obtained internally at EUROIMMUN AG, Germany and all sera samples were made into 30 µl aliquots stored at −20°C until further use.
Testing was approved by the institutional review boards of the participating institutions. Informed consent was obtained from all patients whose serum was used in this study (University of Heidelberg).

Table 8: Clinical characteristics of patients (n = 100) included in this study

Patient diagnosis	Number of patients	Gender (female: male)
SPS	51	37: 14
Stiff-Limb Syndrome (SLS)	3	2: 1
PERM	24	15: 9
Cerebellitis	2	2: 0
Hyperekplexia	6	2: 4
Dystonia	5	2: 3
Anxiety and other associated movement disorders	9	3: 6

Table 9: Neurological controls (n = 65) included in this study: patients' sera with AAbs against NMDAR, CASPR2, LGl1, Rho GTPase-activating protein 26 (ARHGAP26), Hu, Ri, Yo, GLRA1, GABA-A receptor subunit α1 (GABAR-A1), Glutamate receptor ionotropic delta-2 (GLUDR2), Purkinje cell cytoplasmic antibody type 2 (PCA-2), AQP4, Flotillin, Titin, and Transcription factor SRY-Box 1 (SOX1)

Patients with AAbs against	Number of patients	Plausible disorder
• Anti-NMDAR • Anti-CASPR2 • Anti-LGl1 • Anti-ARHGAP26	5 5 6 4	Limbic encephalitis
• Anti-Hu • Anti-Ri • Anti-Yo	7 6 4	Associated tumor
• Anti-GLRA1 • Anti-GABAR-A1 • Anti-GLUDR2	2 2 2	AAbs against receptors involved in neurotransmission
• Anti-PCA2	4	AAbs against Purkinje cells of cerebellum
• Anti-AQP4 • Anti-Flotillin	4 4	Neuromyelitis optica
• Anti-Titin • Anti-SOX1	6 4	Myasthenia gravis \ Lambert-Eaton myasthenic syndrome

2.2. Methods

In section 2.2 only the methods are explained. For the exact composition of buffers or source of a material, please refer to the section 2.1.

2.2.1. Indirect Immunofluorescence Assay on customized EUROIMMUN BIOCHIP Mosaics™

Indirect Immunofluorescence Assay (IFA) was performed as described by Probst et al. (Probst et al., 2015), with a minor modification in the BIOCHIP Mosaics™ that were implemented. In general, EUROIMMUN BIOCHIP Mosaics™ contain biochips from tissue sections belonging to different animal species, antigen dots, or transfected cells **(Figure 3A)** that are fixed by covalent bonding to an activated glass surface (Stöcker, 1987)**.** Such BIOCHIP Mosaics™ aid in the simultaneous evaluation of an antibody binding to different substrates, which can be visualized concomitantly using a small volume of patients' sera or an antibody sample. The Mosaics™ are customized depending on the study under consideration.

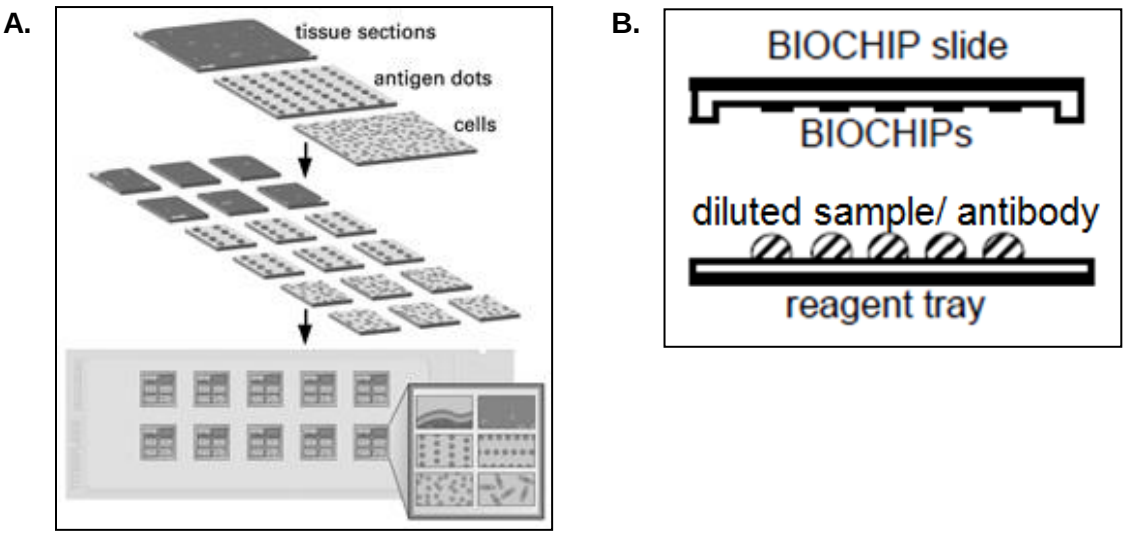

Figure 3: Representation of the BIOCHIP Mosaics™ Technology and the TITERPLAN™ Technique
Adapted from www.euroimmun.de (EUROIMMUN; Stöcker, 1987)
A) Representation of a reaction field in a customized EUROIMMUN slide with several biochips side by side. It is possible to study the detailed antibody profiles against various organs or antigenic substrates simultaneously and compare them by implementing minimal effort. **B)** The Titerplane technique was developed by EUROIMMUN AG, Germany to control immunological investigations. The diluted serum samples or antibodies are pipetted on to the reagent tray and the prepared slides are placed facing down on them, where they come in contact directly with the samples, ensuring simultaneous commencement of all the reactions.

In the present study, two BIOCHIP Mosaics™ were customized and the representative images of the two slides are depicted in **Figure 4**. The first BIOCHIP Mosaics™ (GAD65ko slide mosaic) consisted of nine biochip substrates including standard cerebellum cryosections (4 µm, unfixed snap-frozen) from adult wild-type mouse, rat, pig, and rhesus monkey (Euroimmun AG, Germany). Additionally, this slide included cerebellar cryosections from a GAD65 knock-out (ko) mouse to study novel AAb patterns within the patient cohort **(Figure 4A).** The GAD65ko mouse cerebellum was kindly donated by Prof. Dr. Oliver Stork, Otto-von-Guericke-University, Magdeburg, Germany. Furthermore, this slide incorporated acetone-fixed HEK293 cells transfected with plasmids coding for GAD65, GAD67, and no antigen (mock-transfected).
The second slide (SNARE slide mosaic) contained seven biochip substrates comprising of acetone-fixed HEK293 cells transfected with plasmids coding for SNARE proteins namely synaptosomal-associated protein 25 (SNAP25), VAMP2, syntaxin-binding protein 1 (STXBP1), wild-type NSF (WT NSF), and mutant NSF (K266A). In addition, acetone-fixed HEK293 cells concurrently transfected with plasmids coding for the cognate SNARE proteins: syntaxin (STX) 1B, SNAP25, and VAMP2 were included **(Figure 4B)**.

A standard neurology BIOCHIP Mosaics™ (Euroimmun AG, Germany) was employed for the initial screening of the patients' sera to determine the presence of AAbs against well-known neuronal autoantigens.

A.

GAD65 ko mice cerebellum	Monkey cerebellum	HEK293T-pTriEx-1-GAD2 (Typ1)
Mice cerebellum	Pig cerebellum	HEK293T-pTriEx-1-GAD1 (Typ1)
Rat cerebellum	HEK293T-pTriEx-1 (Typ 1)	

B.

HEK293T-pTriEx-1-SNAP25 (Typ1)	HEK293T-pTriEx-1-NSF (K266A) (Typ1)	HEK293T-pTriEx-1 (Typ 1)
HEK293T-pTriEx-1-VAMP2 (Typ1)	HEK293T-pTriEx-1-NSF(human) (Typ1)	
HEK293T-pTriEx-1-STXBP1 (Typ1)	HEK293T-pTriEx-1-STX1B+SNAP25+ VAMP2 (Typ1)	

Figure 4: Representation of the customized BIOCHIP Mosaics™

A) The GAD65ko BIOCHIP Mosaics™ consisted of standard animal cerebellum cryosections from wild-type mouse, rat, pig, and monkey in addition to a GAD65ko mouse cerebellum. The slide also included HEK293 cells transfected with plasmids coding for GAD65 (GAD2), GAD67 (GAD1), and no antigen. **B)** The SNARE BIOCHIP Mosaics™ consisted of acetone fixed HEK293 cells transfected with plasmids coding for SNARE proteins such as SNAP25, VAMP2, STXBP1, WT NSF, NSF (K266A), and no antigen in addition to co-expressed STX1B + SNAP25 + VAMP2. Typ 1 indicates fixation of substrates with acetone

For all IFA experiments, a standard EUROIMMUN protocol implementing the TITERPLANE™ technique (Euroimmun AG, Germany) was followed **(Figure 3B).** In the first step, sera from patients and healthy subjects in addition to monospecific animal antibodies against the antigens under investigation were diluted 1:10 and 1:100 in PBS/Tween. In total, 30 µl of each of the diluted sample was pipetted on to the reaction fields of a reagent tray (Euroimmun AG, Germany) and incubated with the BIOCHIP Mosaic™ facing downwards. Care should be taken to ensure that the biochips are in contact with their respective samples in order to commence all the reactions simultaneously. Additionally, there was no requirement of a standard "humidity chamber" since the fluids are confined to an enclosed space. The samples were then incubated

at room temperature for 30 minutes. Subsequently, the slides were washed with PBS/Tween and immersed in a cuvette containing PBS/Tween for five minutes. In the second step, binding of the human IgG was visualized by incubating with fluorescein isothiocyanate conjugated polyclonal goat anti-human-IgG (ready-to-use). Similarly, binding of the monospecific animal antibodies was detected using appropriate secondary antibodies such as: polyclonal goat anti-mouse-IgG-Alexa 488 (1:400) or polyclonal goat anti-rabbit-IgG-Cy2/Cy3 (1:500). Incubation with the respective secondary antibodies was performed in dark at room temperature for 30 minutes. A list of the different primary and secondary antibodies employed is provided in **Table 1 and Table 4.** After 30 minutes, the slides were given a final wash with PBS/Tween and immersed in a cuvette containing PBS/Tween for five minutes. Subsequently, each field was embedded with ≈ 20 µl of embedding medium and covered with a cover glass. Examination of the slides was performed using a EUROStar II fluorescence microscope with 460-490 nm LED excitation and the images were captured with the help of Europicture software (Euroimmun AG, Germany). To obtain high-quality images, some pictures were captured using the LSM 700 confocal microscope (Carl Zeiss, Germany) using the ZEN 2009 software. A scoring system based on the EUROIMMUN AG recommended semi-quantitative evaluation method (www.euroimmun.com) was implemented to classify patients as positive or negative for AAbs against GAD65/67 depending on the immunofluorescence signal observed in the tissue cryosections as well as on the HEK293-cell transfectants. Based on the intensity of the immunofluorescence signal, patients' sera versus control sera were assigned a score between one and five, with five indicating the highest immunofluorescence reactivity and one indicating lowest detectable fluorescence signal. The slides were evaluated within 24 hours of incubation and all test results were also assessed by another independent observer having more than 10 years of professional experience in the field of florescence staining.

2.2.2. Preparation of the pig cerebellum lysate

Cerebellum from the pig was dissected after slaughtering the animal and was snap-frozen at -80°C until further use. The lysate preparation was conducted at 4°C as described by Miske et al. (Miske et al., 2017). In brief, the tissue was weighed in the frozen state, defrosted, and cut into small pieces using a scalpel. The mashed tissue was transferred to a falcon tube (Sarstedt AG & Co, Germany) and added five-times the volume of a detergent-based solubilization buffer per gram of the tissue together with protease inhibitor cocktail. The mixture was then homogenized to a pulp using the MICCRA D-9 homogenizer. The homogenization step was performed twice (level C) with a five-minute pause between each cycle. Subsequently,

the cells were further lysed using a Dounce homogenizer with two different pestle (plunger) sizes, each implemented 10 times. The pestle size “large” was used to generate a homogenous mixture and the pestle size “small” was implemented to generate maximum friction and cell disruption. Care was taken to avoid too much frothing while homogenizing the cerebellum lysate mixture. This homogenate was then incubated on a bench rotor at 4°C for three hours. Following incubation, the homogenate was centrifuged at 21,000 x g at 4°C for 15 minutes and the clear supernatant containing solubilized proteins was carefully pipetted and transferred into fresh Eppendorf microfuge tubes (Eppendorf GmbH, Germany) and stored at -80°C until further use.

2.2.3. Determination of total protein concentration of the lysate

A Bicinchoninic Acid Protein (BCA) assay was used to determine the total protein concentration of the cerebellum lysate mixture (Smith et al., 1985; Walker, 1994). This method is based on the ability of the proteins to reduce Cu^{+2} to Cu^{+1} in an alkaline solution to form a purple-blue complex with Bicinchoninic acid. The extent of reduction is proportional to the protein concentration and four amino acid residues including cysteine or cysteine, tyrosine, and tryptophan help in reducing Cu^{+2} to Cu^{+1} (Wiechelman et al., 1988). The protocol was conducted as described by He (He, 2011). The stock solution of bovine serum albumin (BSA) was serially diluted to obtain BCA-BSA working standards between the ranges of 31-500 µg/ml. The BCA working solution was prepared by diluting 50 parts of the BCA reagent with one part of BCA-$CuSO_4$ solution resulting in a clear green solution. In a sterile 96-well microtiter plate, 20 µl of the standards as well as the cerebellum lysate diluted 1:100 in distilled water was pipetted in duplicates in addition to distilled water as blank for the standard curve. Subsequently, 200 µl of the BCA working reagent was added to each well and incubated at 37°C for 30 minutes. The plate was kept at room temperature for 10 minutes before measuring the absorbance at 570 nm using a Tecan Sunrise™ Microplate reader using the Magellan™ 7.1 Data Analysis Software (Tecan GmbH, Germany).

2.2.4. Immunoprecipitation

2.2.4.1. Total lysate immunoprecipitation

Following IFA, a total lysate immunoprecipitation was implemented to identify the unknown antigens targeted by patients’ AAbs. This test was performed as described previously by Miske et al. (Miske et al., 2017). The lysate preparation was performed as described in section 2.2.2. Subsequently, 500 µl of the lysate was incubated with 15 µl of a monospecific antibody as the

positive control. The positive controls included a human monoclonal anti-GAD65/67-IgG antibody and a human anti-metabotropic glutamate receptor 1 (GRM1)-IgG antibody **(Table 3)** when screening for GAD65 and GAD67, and the SNARE proteins, respectively. Additionally, equal volume of the lysate was incubated with 30 µl of sera each from the patients, neurological, and healthy controls. To prevent degradation of proteins by active proteases, 100 mM PMSF was added to the lysate mixture. The mixtures were vortexed gently and incubated in a bench rotor at 4°C for three hours to allow formation of immune complexes. These immune complexes were captured using Dynabeads® Protein G for immunoprecipitation, which are superparamagnetic beads (2.8 µm) covalently bound to the recombinant protein G (www.thermofisher.com). In brief, 50 µl of the beads suspension was transferred into a new Eppendorf tube and placed on the DynaMag™ magnetic separator. The sample buffer was discarded and the beads were equilibrated with the solubilization buffer. Subsequently, the beads were incubated with the sera/antibody-lysate mixture at 4°C, overnight. The following day, the beads were washed thrice with the same solubilization buffer and eluted with 40 µl protein G elution buffer and incubated at 70°C in a thermomixer for 10 minutes. To prevent re-formation of the disulfide bridges, 4 µl 650 mM Iodoacetamide was added to the eluate and incubated in the dark for 30 minutes. This step is essential when the samples are specially processed for mass spectrometry (MS). Following incubation, the eluates were loaded on a NuPAGE® 4-12% Bis-Tris gel and were either processed for direct staining with Coomassie Brilliant Blue and subsequent MS analysis or transferred onto a nitrocellulose membrane for Western blot (WB) analysis.

2.2.4.2. Cryo-immunoprecipitation

Another variant of the immunoprecipitation analysis designated as “cryo-immunoprecipitation” was performed as a complementation to the previous method. This protocol is a slight modification to the Histo-immunoprecipitation as described by Scharf et al. (Scharf et al., 2015). Similar to the previous technique, pig cerebellum was dissected and shock-frozen in liquid nitrogen. The cerebellum was then serially cut into 25 x 25 µm cryosections using a Leitz 1720 Cryostat microtome and added to a four-well plate (Sarstedt AG & Co, Germany) containing 3 ml of cryo-IP-PBS buffer per well. In total, 30 µl of sera from patients versus controls were added to the respective wells and incubated on a rocking platform at 4°C for three hours. Subsequently, the contents of each well were transferred to a fresh 2 ml Eppendorf tubes and centrifuged at 2500 rpm at 4°C for five minutes. The supernatant was discarded and the pellet was subsequently washed three times with 1 ml PBS/Tween with a similar centrifugation step

between each cycle. The pellets were then solubilized with 1 ml of the solubilization buffer plus protease-inhibitor cocktail and homogenized well using a pipette. The mixture was incubated at 4°C for one hour and centrifuged at 16,000 x g at 4°C for 20 minutes. The supernatants were collected in separate Eppendorf tubes and pellet was stored at -20°C for analysis. As performed in the previous method, 50 µl of Dynabeads® Protein G beads were incubated with the supernatants at 4°C, overnight to capture immune complexes. Following incubation, the beads were washed and eluted as described previously.

2.2.5. Analysis of the immunoprecipitated eluates

2.2.5.1. Sodium dodecyl sulfate polyacrylamide gel electrophoresis (SDS-PAGE)

Following immunoprecipitation, the eluates were separated based on their size by gel electrophoresis using NuPAGE® 4-12% Bis-Tris gels in NuPAGE® MOPS SDS running buffer. The gels were placed in an XCell SureLock® Mini-Cell tank and run at 150 V for 90 minutes or until the blue front ran out of the gel. Following SDS-PAGE, the gels were either stained with blue silver stain or transferred to a nitrocellulose membrane (0.22 µm) for subsequent WB analysis.

2.2.5.2. Blue silver staining

After SDS-PAGE, the gels were fixed with blue silver-fixating solution for one hour followed by an overnight incubation with the staining solution. The following day, the gels were de-stained for 30 minutes and subsequently, washed with distilled water. The gels were scanned using a CanoScan 9000FMark II scanner, and stored at 4°C. Following staining, the gels were examined to spot unique and interesting protein bands in patients' sera lanes in comparison with controls, which were then identified by MS analysis.

2.2.5.3. Western blot analysis

Alternatively, the SDS-PAGE separated proteins were transferred onto a nitrocellulose membrane for subsequent WB analysis. WB and MS analyses were conducted as described by Scharf et al. (Jarius et al., 2014; Scharf et al., 2015). In brief, the proteins were electro-transferred onto a nitrocellulose membrane by the tank blotting technique. The electro-transfer was performed at 400 mA for 60 minutes using NuPAGE® Transfer Buffer in a TE22 small transfer tank unit. Subsequently, the membrane was stained with Ponceau S solution for 10 minutes to verify the protein transfer. The membrane was then de-stained using 50 mM Tris-base and blocked at room temperature for 15 minutes using 1 x universal blocking

buffer. Following blocking, the membrane was incubated either with monospecific primary antibodies against the antigens under study or with sera from patients versus controls. All samples were all diluted in the universal blocking buffer and incubated at room temperature, overnight on a shaker. The list of different antibody dilutions used in this study is provided in **Table 10**. All serum samples were diluted either 1:350 or 1:1000 depending on the antigen under investigation. The following day, the membrane was washed thrice with 1 x universal blot wash buffer and incubated with corresponding secondary antibodies conjugated with alkaline phosphatase for 30 minutes on a shaker **(Table 11)**. The membranes were given a final wash (three times) with the wash buffer and subsequently incubated with the WB substrate nitro-blue tetrazolium chloride / 5-bromo-4-chloro-3'-indolyphosphate p-toluidine salt (NBT/BCIP) for ≈ 10 minutes. On reacting with the alkaline phosphatase, NBT / BCIP produces an insoluble black-purple precipitate corresponding to the position of respective target antigens on the membrane (De Jong et al., 1985). The reaction was stopped by washing the membrane thrice with distilled water and air dried prior to being scanned.

Table 10: List of primary antibody dilutions used in the WB analysis

Antibody target	Dilution	Molecular weight of target	Species
Amphiphysin	1:500	≈ 76 kDa	Human monoclonal
Dynamin 1	1:1000	≈ 97 kDa	Rabbit polyclonal
EXOC4 (or Sec8)	1:250	≈ 122 kDa	Rabbit polyclonal
GABARAP	1:250	≈ 13 kDa	Rabbit polyclonal
GAD65 and GAD67 (EURab0022)	1:20,000	≈ 65 and 67 KDa	Rabbit polyclonal
GRM1	1:250	≈ 133 KDa	Human monoclonal
NSF	1:650	≈ 82 kDa	Rabbit polyclonal
Rab3A	1:250	≈ 24 kDa	Rabbit polyclonal
SNAP25	1:1000	≈ 25 kDa	Rabbit polyclonal
STX1B	1:2000	≈ 33 kDa	Mouse monoclonal
STXBP1 (or Munc18)	1:500	≈ 66 kDa	Rabbit polyclonal
Synaptotagmin 1	1:250	≈ 47 kDa	Rabbit polyclonal
Synaptophysin 1	1:250	≈ 38 kDa	Rabbit polyclonal
VAMP2	1:250	≈ 12 kDa	Rabbit polyclonal

Table 11: List of secondary antibody dilutions used in the WB analysis

Antibody	Conjugate	Dilution
Anti-human-IgG-B/E-AP	Alkaline Phosphatase	1:10
Polyclonal goat anti-mouse-IgG(H+L)-AP	Alkaline Phosphatase	1:20,000
Polyclonal goat anti-rabbit-IgG(H+L)-AP	Alkaline Phosphatase	1:20,000

2.2.6. Matrix Assisted Laser Desorption/Ionization-Time of Flight Mass Spectrometry (MALDI-TOF-MS)

Preparation of samples for the MS analysis was performed as described by Koy et al. (Koy et al., 2003). In short, prior to SDS-PAGE, the samples were reduced with DTT and carbamidomethylated with Iodoacetamide. The gels were stained with Coomassie Brilliant Blue G-250 to visualize the proteins and the indicated protein bands were excised and de-stained. In brief, each excised gel band was placed in a 96-well, non-skirted plate (0.3 ml, Thermo-Fisher Scientific GmbH, Germany) which was in turn placed in a 96-well deep well microplate (MASTERBLOCK®, 2 ml, Greiner Bio-One International GmbH, Germany). The de-staining protocol included: incubation with 100 µl MALDI de-staining solution 1 for 20 minutes (two-times) followed by 100 µl MALDI de-staining solution 2 for 20 minutes and a final incubation with 100 µl acetonitrile for 10 minutes. The protein samples were then digested with 15 µl MALDI-trypsin stock solution at 37°C for three hours in a humid chamber. Following trypsin digestion, peptides were extracted with 10 µl MALDI-extraction solution at room temperature for 45 minutes. In total, 0.8 µl of each peptide was spotted with α-cyano-4-hydroxycinnamic acid onto a MTP AnchorChip™ 384 TF target (Bruker Corporation, USA). Subsequently, 0.5 µl MALDI-matrix solution was added to each sample on the target and 0.5 µl MALDI-peptide calibration/matrix was applied on calibration spots on the target. Autoflex™ III Smartbeam MALDI-TOF/TOF200 was used to conduct MALDI-TOF/TOF measurements using the software FlexControl™ 3.4 (Bruker Corporation, USA). MS spectra for peptide mass fingerprinting were recorded in positive ion reflector mode with 500 shots and in a mass range from 700 Da to 4000 Da. A commercially available Peptide Calibration Standard II was used to calibrate the spectra externally and analyzed by software BioTools™ 3.2 (Bruker Corporation, USA). Protein identification was performed using the Mascot search engine Mascot Server 2.3 (Matrix Science, London, UK) by searching against the NCBI database limited to Mammalia. The search parameters are as indicated: Mass tolerance was set to 80 ppm, one missed cleavage site was accepted, and carbamidomethylation of cysteine residues as well as oxidation of methionine residues were set as fixed and variable modifications, respectively. A significance threshold of $p<0.05$ was selected to evaluate the protein hits. Two peptides of each identified protein were selected for MS/MS measurements using the WARP feedback mechanism of BioTools™ to further confirm the peptide mass fingerprinting hits. Parent and fragment masses were recorded with 400 and 1000 shots, respectively. Spectra were processed and analyzed as described above with a fragment mass tolerance of 0.7 Da.

2.2.7. Cloning and recombinant expression of GAD and the SNARE proteins

The cloning and expression of recombinant proteins was performed as described by Radzimski et al. (Radzimski et al., 2013) by the Molecular Biology Department at EUROIMMUN AG, Germany. The coding DNAs for GAD65 (UNIPROT acc. # Q05329), GA67 (Q99259), NSF (WT; P46459), NSF (mutant; K266A), NSF (mutant; E329Q), SNAP25 (P60880), STX1A (Q16623), STX1B (P61266), STXBP1 (P61764) and VAMP2 (P63027) were obtained by polymerase chain reaction from commercially available cDNA (BioSource, Germany) as given in **Table 12.** Each amplified product was then digested with appropriate restriction enzymes and ligated with NcoI/XhoI-linearized pTriEx-1 (Merck Biosciences, Germany).

In this study, apart from the WT NSF, two mutant versions of NSF were included: NSF (K266A) and NSF (E329Q). In the NSF (E329Q), a point mutation was introduced at position 329 to replace glutamic acid to glutamine and in NSF (K266A), the lysine at position 266 was replaced with alanine. Generally, mutant versions of a protein are included in the BIOCHIP Mosaics™ to obtain better expression of the protein in the HEK293 cell system.

Table 12: List of cDNA clones ordered

Protein expressed (without His-tag)	cDNA clone	Genbank accession number	Plasmid name
GAD65	IRAKp961I2248Q	BC029517	pTriEx-1- GAD65 (dHis)
GAD67	IRATp970D1022D	BC026349	pTriEx-1- GAD67 (dHis)
NSF (WT)	IRATp970E0728D	BC030613.2	pTriEx-1-NSF[human] (dHis)
NSF mutant (E329Q)	pTriEx-1-NSF[human] (dHis)	-	pTriEx-1-NSF(E329Q) (dHis)
NSF mutant (K266A)	pTriEx-1-NSF[human] (dHis)	-	pTriEx-1-NSF(K266A) (dHis)
SNAP25	IRATp970D118D	BC010647	pTriEx-1- SNAP25 (dHis)
STX1A	IRATp970A0185D	BC064644	pTriEx-1- STX1A (dHis)
STX1B	IRAUp969B07110D	BC062298	pTriEx-1- STX1B (dHis)
STXBP1	IRAUp969B0273D	BC015749	pTriEx-1- STXBP1 (dHis)
VAMP2	IRATp970E0540D	BC019608	pTriEx-1- VAMP2 (dHis)

A list of the primers along with their sequence and restriction enzymes are mentioned in **Table 13.** Following ligation, 100% transformation was performed using heat competent *E. coli* cells (NEB 5 alpha, New England Biolabs, Germany). Following cloning, the plasmids with the correct insert were purified and transfected into a mammalian cell line (HEK293 cells).

Table 13: List of primers used for the amplification of the proteins

List of primers	Sequence	Restriction Enzymes
sense GAD65	TATCCATGGCATCTCCGGGCTCTGGCTTTTGGTC, TTTCCAGAAGTCAAGGAGAAGGGGATGGCAGCACTTCCCAG GCTCATCG, TTGAAGCCAAACAGAAAGGATTTGTTCCTTTC	NcoI/ XhoI/ DpnI
asense GAD65	CTCCTTGACTTCTGGAAACATCTTAAAGCGGGCAATCATCAT GGCATAC, AACAAATCCTTTCTGTTTGGCTTCAAGGATTCTTCTTTC, TATCTCGAGATCTTGTCCGAGGCGTTCGATTTC	NcoI/ XhoI/ DpnI
sense GAD67	TTAACGTCTCCCATGGCGTCTTCGACCCCATCTTCGTC	Esp3I/XhoI
asense GAD67	TATCTCGAGCAGATCCTGGCCCAGTCTTTCTATC	Esp3I/DpnI
sense NSF	ATACGTCTCACATGGCGGGCCGGAGCATGCAAG	Esp3I/DpnI
asense NSF	TATCGTCTCCTCGACATCAAAATCAAGGGGGCTAG	Esp3I/DpnI
asense NSF(Stop)	TATCGTCTCCTCGATCAATCAAAATCAAGGGGGCTAG	Esp3I/DpnI
sense NSF(K266A)-ZF2	ATACGTCTCAGTGCTACTCTCTTGGCTCGACAGATTGGC	Esp3I/DpnI
asense NSF(K266A)-ZF1	ATACGTCTCAGCACCACAACCTGGGGGTCCATATAACAG	Esp3I/DpnI
sense NSF(E329Q)-ZF2	ATACGTCTCGATCAGATTGATGCCATCTGCAAGCAGAGAGG	Esp3I/DpnI
asense NSF(E328Q)-ZF1	ATACGTCTCCTGATCAAAGATGATGATGTGCAAACCAC	Esp3I/DpnI
sense SNAP25	ATACGTCTCACATGGCCGAAGACGCAGACATGCGCAATGAG C	Esp3I/DpnI
asense SNAP25-Stop	ATACGTCTCCTCGATTTAACCACTTCCCAGCATCTTTGTTGC	Esp3I/DpnI
sense STX1A	ATACGTCTCACATGAAGGACCGAACCCAGGAGCT	Esp3I/DpnI
asense STX1A-Stop	ATACGTCTCCTCGAGCTAGGCGAAGATGCCCCCAACAGTG	Esp3I/DpnI
sense STX1B	ATACGTCTCACATGAAGGATCGGACTCAAGAGCTGC	BsmBI/DpnI
asense STX1B-Stop	ATACGTCTCCTCGAGCTACAAGCCCAGCGTCCCCCCAATG	BsmBI/DpnI

sense STX1B (ic)	ATACGTCTCACATGAAGGATCGGACTCAAGAGCTGC	Esp3I/DpnI
asense STX1B (ic)	ATACGTCTCCTCGAGTTTCTTCCTCCGGGCCTTGCTCTG	Esp3I/DpnI
sense STXBP1	ATACGTCTCACATGGCCCCCATTGGCCTCAAAGCTG	Esp3I/DpnI
asense STXBP1-Stop	GGCCGTCTCCTCGATTAACTGCTTATTTCTTCATCTGTTTTATTC	Esp3I/DpnI
sense VAMP2	ATACGTCTCTCATGTCTGCTACCGCTGCCACGGCCC	Esp3I/DpnI
asense VAMP2-Stop	ATACGTCTCCTCGAGTTAAGTGCTGAAGTAAACTATGATG	Esp3I/DpnI

2.2.7.1. Transfection of HEK293 cells

All the plasmids coding for recombinant proteins such as GAD65, GA67, WT NSF (human), NSF (K266A), NSF (E329Q), SNAP-25, STX1A, STX1B, STXBP1, and VAMP2 were expressed without a histidine-tag (His-tag) in HEK293 cells. Furthermore, plasmids coding for STX1B, SNAP25, and VAMP2 were transfected together in HEK293 cells to identify possible AAbs against the SNARE complex. The substrates for the BIOCHIP mosaics™ were prepared as follows: HEK293 cells with a density of 3.0 x 10^5 cells/cm^2 were seeded on sterile glass slides (Euroimmun AG, Germany) with DMEM high glucose supplemented with 10% fetal bovine serum, penicillin (100 U/ml), streptomycin (0.1 mg/ml) and amphotericin B (2.5 µg/ml). The plates were incubated at 37°C for four hours and subsequently transfected with appropriate plasmids implementing the ExGen500-mediated transfection protocol (Fermentas, Germany) based on the manufacturer's instructions. Subsequently, the cells were cultured at 37°C, 95% humidity, and 8.5% CO_2 for two days to express the corresponding recombinant protein. The negative control for the substrates was pTriEx-1.1 without any inserts. After 48 hours, the glass slides were washed twice with PBS and fixed with acetone at room temperature for 10 minutes and stored at -20°C until used for the mosaics production (Stöcker, 1987). In addition to the above-mentioned proteins, WT NSF was expressed with a His-tag in HEK293 cells (HEK293-NSF[human]) and the intracellular(ic) domain of STX1B was expressed in *E. coli* (STX1B(ic)). These proteins were then purified by immobilized metal ion affinity chromatography (IMAC) by the Immunobiochemistry department (Euroimmun AG, Germany) and subsequently used for downstream experiments.

The lysates of HEK293 cells expressing recombinant proteins was prepared as depicted previously (Radzimski et al., 2013). In brief, the cells were cultured and transfected in standard Corning® T75 HYPER Flasks using a similar protocol as mentioned above. After 72 hours, the

medium was removed and the cells were harvested by scraping in PBS. The cells were then washed thrice with 20 mM Tris-HCl pH 7.4, 150 mM NaCl, 5 mM EDTA, and 1 mM PMSF and finally re-suspended in 10 µl/cm^2 culture surface of the solubilization buffer. The lysates were stored in -80°C until used for immunoprecipitation experiments as described in section 2.2.4.1.

2.2.8. Immobilized metal ion affinity chromatography

IMAC is a highly effective and rapid method for purifying or enriching a desired biomolecule (Porath and Olin, 1983). This protocol relies on the principle that some amino acids, particularly histidine, have an affinity towards metals. In short, the separation of proteins is dependent on the expression of electron donor groups such as histidine, thiol, phenylalanine, and tryptophan residues on the protein surface, which can bind to transition metal ions such as Co^{2+}, Cu^{+2} or Ni^{+2}, which are strong electron acceptors. These metal ions are immobilized on a stationary phase using strong metal chelators such as Iminodiacetic acid or Nitrilotriacetic acid. The specific coordinate covalent bond between the protein and the metal ion is pH dependent and the strongest interaction is observed at a neutral pH. Desorption is achieved by reducing the pH to 4.0 or by using a strong electron donor competitor such as imidazole. In this study, IMAC protocol was implemented to enrich SNARE proteins from the brain tissue lysate using magnetic beads coated with Co^{2+} incorporating the IMAC chemistry. Approximately 50 µl (2 mg) of the Dynabeads® for His-Tag Isolation and Pulldown were transferred to a new Eppendorf tube and placed on the DynaMag™ magnetic separator. The sample buffer was discarded and the beads were equilibrated with 200 µl PBS. The beads were then incubated with 30 µl, 1:1 PBS diluted His-tagged mouse GRM1 antibody **(Table 3)**. The mixture was vortexed gently and incubated in a bench rotor at 4°C for one hour to allow binding of the His-tagged antibody to the beads. The beads were then washed thrice with 200 µl PBS and subsequently incubated with 300 µl 0.03% hydrogen peroxide (Carl Roth GmbH, Germany). Hydrogen peroxide oxidizes the cobalt from $Co^{2+} \rightarrow Co^{3+}$ state, which makes the His-tagged antibody-beads interaction stable and kinetically inert to ligand-exchange (Wegner and Spatz, 2013). The tube was then incubated in a bench rotor at room temperature for one hour and then washed thrice with 500 µl PBS and equilibrated once with 500 µl solubilization buffer. Thereafter, 500 µl pig cerebellum tissue lysate, as prepared in section 2.2.2, was added to the antibody-beads mixture and incubated at 4°C, overnight. The following day, the beads were washed thrice with 1 ml solubilization buffer and eluted with 50 µl protein G elution buffer at room temperature (Elution 1). Following elution 1, the beads were re-incubated with protein G elution buffer and heated at 70°C for 10 minutes to elute all the bound proteins (Elution 2). Subsequently, eluates of elution 1 were

also heated at 70°C for 10 minutes in a thermomixer and both eluates were incubated with 4 µl 650 mM Iodoacetamide for 30 minutes in the dark. Predominantly, the elution 1 eluate was used for downstream experiments such as immunoblotting tests with the patient cohort.

2.2.9. Neutralization test using the recombinant NSF

A neutralization test was performed using the HEK293-NSF[human] as the antigen source to nullify the patients' sera reactivity against NSF. The molecular biology department (Euroimmun AG, Germany) cloned and transfected plasmids coding for His-tagged WT NSF in HEK293 cells and the Immunobiochemistry department (Euroimmun AG, Germany) purified the NSF from the HEK293-NSF[human] by IMAC to a final concentration of 13 mg/ml. The purified NSF was pre-diluted 1:10 in PBS and incubated with the anti-NSF antibody as well as with sera from patients versus controls to a final dilution of 1:100. As the control, the anti-NSF antibody and the serum samples were diluted 1:100 in PBS buffer alone. All samples with/without the antigen (Neutralized samples) were pre-incubated at room temperature for one hour. Subsequently, all samples were diluted with the universal blot wash buffer plus to a final dilution of 1:2000 and 1:1000 for the anti-NSF antibody and the serum samples, respectively. Approximately 5 µg of the IMAC purified NSF was transferred onto a nitrocellulose membrane and the WB analysis was performed as depicted in section 2.2.5.3. All samples that were pre-incubated with the antigen (neutralized) as well as those that were pre-incubated with PBS alone (non-neutralized) were immunoblotted in parallel against the WT NSF to determine whether the antigen (NSF) was able to neutralize the reactivity of the anti-NSF antibody as well as serum samples against NSF.

2.2.10. Isoelectric Focusing

Isoelectric focusing (IEF) involves separation of proteins based on their isoelectric point (pI) and is based on the principle that the overall charge of the protein is dependent on the pH of its surroundings. The charge of a protein is determined by the acidic and basic side chains of the amino acids of the proteins. The pI of a protein would be at a low pH value when there are more acidic groups compared to basic groups with the overall charge of the protein being positive and vice versa. In a pH region below the pI of a protein, proteins would move towards the cathode during electrophoresis due to its positive charge. Alternatively, the proteins having a negative charge will migrate towards the anode (Garfin, 2003; Righetti, 1983). As the proteins move through a gradient pH their overall charge decreases and at a particular pH the overall charge reaches zero ceasing further migration of the proteins. The pH at which a protein has no net

charge is termed as the pI of the protein. The proteins ultimately separate into sharp stationary bands each relative to its pI in this region (Garfin, 2003). In this study, the IEF experiment was conducted as follows: a total lysate immunoprecipitation protocol was performed using the mouse anti-GRM1 antibody plus the lysates from the pig cerebellum tissue or the HEK293-NSF[Human] as prepared in sections 2.2.2 and 2.2.7.1, respectively. Approximately 100 µl of each eluate obtained following the immunoprecipitation was taken in separate Eppendorf tubes and incubated with 8 µl of 250 mM DTT and an equal volume of 10 M urea to obtain a final concentration of 2 mM DTT and 5 M urea, respectively. The mixture was incubated at room temperature for 30 minutes to allow protein denaturation. Subsequently, 7 mg Iodoacetamide was dissolved in 100 µl of 200 mM Ammonium hydrogen carbonate solution (pH 8) and 25 µl of the solution was added to the mixture and incubated in the dark for 30 minutes. Approximately four-times the volume of acetone was added to the above sample and incubated at -20°C for one hour to precipitate all proteins. Following incubation, the tube was centrifuged at 20,000 x g at 4°C for 30 minutes and the supernatant was discarded. The pellet was air dried for 10 minutes and then re-suspended in 270 µl IEF sample buffer. In case there was any difficulty in dissolving the pellet, a short sonication step was implemented (Duty Cycle: 10, Output Control: 1). Approximately 125 µl of each of the dissolved protein sample was pipetted on a PROTEAN® i12™ IEF rehydration tray and incubated with a 7 cm nonlinear immobilized pH gradient strip (pH 3-10). Each eluate sample was processed in duplicates by incubating two strips per 270 µl IEF sample buffer. The strips were then overlaid with 3 ml mineral oil and incubated on a levelled surface at room temperature, overnight. The following day, the PROTEAN® i12™ IEF electrode assembly was assembled appropriately on an IEF focusing tray. Thereafter, the electrode wicks were moistened with 9 µl distilled water and carefully positioned on the positive and negative ends of the tray. Following the overnight rehydration step, oil from the strips was drained and the strips were placed on the focusing tray with the gel side facing downwards. Care was taken to position the strips in constant touch with the wicks on the tray. The strips were once again overlaid with 3 ml mineral oil and the IEF tray was fixed on the PROTEAN® i12™ IEF Cell with proper retainers to maintain position of the strips. The PROTEAN® i12™ cell was run with a standard program from Bio-Rad (Germany):

250 V, 15 minutes
Gradient to 4000 V, 60 minutes
4000 V to 15,000 V
500 V, Hold
Total power: 15,000 V

After the run, the strips were carefully removed from the IEF tray and stored at -20°C until further use. Alternatively, the strips were prepared for downstream analysis by incubating with 1x NuPAGE® LDS sample buffer for 15 minutes. Each strip was then placed on a NuPAGE® 4-12% Bis-Tris 2D Gel such that proteins from one strip was transferred onto a nitrocellulose membrane for WB analysis and the other one was processed for direct staining with Coomassie Brilliant Blue.

2.2.11. Enzyme linked immunosorbent assay

An indirect enzyme linked immunosorbent assay (ELISA) was performed to quantitatively measure the amount of AAbs in the patient versus control sera. In ELISA, the antigen in question is immobilized on a solid surface by passive adsorption and is incubated with the test serum (Bidwell et al., 1976). The plate is then incubated with an enzyme-labelled anti-human IgG and finally a visible signal, corresponding to the amount of AAbs in the sample, is observed upon the addition of an enzymatic substrate. In this study, an ELISA was performed to determine the concentration of the anti-GAD65 AAbs in the patient cohort. Characterization of the patients' sera to determine the levels of anti-GAD65 AAbs was performed by the Immunobiochemistry Department at EUROIMMUN AG, Germany using the gold standard anti-GAD ELISA (Euroimmun AG, Germany) by following the company guidelines. The plates were read at an absorbance of 450 nm using a Tecan Sunrise™ Microplate reader using the Magellan 7.1 software (Tecan, Germany) and a cut-off of 5 International units (IU)/ml was implemented.

2.2.12. Statistics

Statistical comparisons and graphs were created using the GraphPad prism 5 software (GraphPad, USA). Image J was used to quantify the intensity of the WB blot images and different sample groups were compared with Kruskal-Wallis test and Dunn's multiple comparisons to determine the relative density of the WB bands. Graphs report mean ± standard deviation (SD) if not stated otherwise.

3. Results

3.1. Characterization of the patients' sera

Sera from patients (n = 100) clinically diagnosed with SPS, SLS, PERM, cerebellitis, dystonia, hyperekplexia, and anxiety related disorders were included in this study **(Table 8)**. The gold-standard anti-GAD ELISA was implemented to determine the concentrations of anti-GAD65 AAbs in the patient cohort (section 2.2.11). In total, 63 patients' sera were positive for anti-GAD65 AAbs and of them, 58 patients' sera possessed values > 2000 IU/ml, indicating high titer anti-GAD65 AAbs **(Table 21)**. Additionally, patients' sera were tested for AAbs against various well-characterized neuronal antigens in IFA using the standard neurology BIOCHIP Mosaics™ **(Table 14)**. The most frequently detected AAbs, following anti-GAD AAbs, were directed against amphiphysin (n = 7), which is commonly detected in the paraneoplastic variant of SPS. Additionally, some patients were also positive for AAbs against GLRA1 (n = 5), gephyrin (n = 1), dipeptidyl aminopeptidase-like protein 6 (DPPX, n = 2), and sodium-and chloride-dependent glycine transporter 2 (SLC6A5, n = 2). AAbs against gephyrin and glycine receptors are well-characterized in patients with SPS and PERM (Figure 2).

Table 14: Patients' sera tested in IFA for the detection of AAbs against neuronal antigens: acetone fixed HEK293 cells transfected with plasmids coding for amphiphysin, D(2) dopamine receptor (DRD2), DPPX, gephyrin, glycine receptor subunit β (GLRB), NMDAR subtype 1a (NR1a), Rho guanine nucleotide exchange factor 9 (ARHGEF9), SLC6A5 and formalin fixed HEK293 cells transfected with CASPR2, DRD2, GABA-A receptor subunit α1 + β3 (GABAR-A1+B3), GABA-B receptor subunit B1/2 (GABARB1_2), GLRA1, LGI1.

Antigens Tested	Number of positive patients
Amphiphysin	7
GLRA1	5
DPPX	2
SLC6A5	2
Gephyrin	1
ARHGEF9	0
CASPR2	0
DRD2	0
GABAR-A1+B3	0
GABARB1_2	0
GLRB	0
LGI1	0
NR1a	0

3.2. Screening for novel AAb patterns using the GAD65ko BIOCHIP Mosaics™

Sera from patients (n = 100) in comparison with healthy controls (n = 50) were screened in IFA using the GAD65ko BIOCHIP Mosaics™ **(Figure 4A)** to detect novel AAb patterns. This slide included cryosections from wild-type mouse, rat, pig, and monkey cerebellum in addition to a GAD65ko mouse cerebellum to identify patterns other than the classical GAD65-specific AAb pattern. Additionally, the slides also included acetone fixed HEK293 cells transfected with plasmids coding for GAD65 (HEK293-GAD65) and GAD67 (HEK293-GAD67), and no antigen to classify patients positive or negative for AAbs against GAD65 and/or GAD67. IFA was performed as mentioned in section 2.2.1. A humanized monoclonal antibody against GAD65/67 (anti-GAD65-IgG1[human]) was included as a positive control in addition to screening sera from patients versus controls. **Figure 5** depicts a representative incubation of a patient serum positive for anti-GAD AAbs on the GAD65ko slide. Following incubation, a blotchy florescence staining pattern of the granular layer (GL) and grain-like appearance of the molecular layer (ML) characteristic for anti-GAD65 AAbs was observed on all wild-type cerebellar cryosections **(Figure 5B-E)**. The GAD65-specific pattern was noted in the positive control and in the majority of the patients' sera positive for anti-GAD65 AAbs, as verified by the anti-GAD ELISA. Overall, 39 patients' sera were positive for AAbs against GAD65 and GAD67. On scoring the intensity of the observed immunofluorescence signal as indicated in section 2.2.1, 25 patients' sera received a score in the range of 3-4 in HEK293-GAD65 cells, 2-4 in HEK293-GAD67, and 2-4 in tissue substrates, indicating the presence of high-titer anti-GAD65/GAD67 AAbs. Additionally, 14 patients' sera were positive only for anti-GAD65 AAbs and of them, 10 sera received a score in the range of 2-4 in both the tissue and HEK293-GAD65 cells and 4 patients' sera received a score of 1. One patient serum amongst them showed a positive immunofluorescence signal only on the HEK293-GAD65 cells (patient number: 41, Table 21), suggesting presence of very low anti-GAD65 AAbs titers, which matched with the anti-GAD ELISA test results. In comparison with the ELISA test results, 10 patients' sera positive for anti-GAD65 AAbs were negative in IFA and five sera amongst them had levels > 2000 IU/ml **(Table 15)**.

Overall, sera from 47 patients and 50 controls were negative for AAbs against GAD65/GAD67 in IFA. Additionally, anti-nuclear antibody, anti-mitochondrial antibody, and antibodies against myelin, neurofilament, and endothelial cells were observed in some patients. Of the seven patients' sera positive for anti-amphiphysin AAbs, only one serum portrayed a typical amphiphysin-specific pattern on the tissue substrates. The florescence staining pattern of the GL of the wild-type animal tissue substrates following the incubation with anti-amphiphysin

AAbs is similar to that observed with the anti-GAD65 AAbs. However, the ML portrays a higher fluorescence staining intensity compared with the GL.

Simultaneously, the slides were further evaluated to identify any unknown or novel AAb patterns in the GAD65ko substrate, wherein no classical GAD65-specific pattern was observed and therefore, was suitable to screen for unrevealed AAb patterns. However, no new AAb patterns were identified in the GAD65ko substrate following incubation with the entire cohort **(Figure 5A)**. Additionally, no specific pattern was observed on the GAD65ko substrate after incubation of patients' sera positive for anti-GAD67 AAbs. All the control sera were negative for anti-GAD AAbs and did not portray any specific fluorescence pattern on the tissue substrates.

Table 15: Number of patients' sera positive for anti-GAD AAbs using ELISA and IFA (n = 100)

Test method	Detection of AAbs against	Number of positive patients		Total number of positive patients
		Titers: > 2000 IU/ml	Titers: < 2000 IU/ml	
ELISA	GAD65	58	5	**63**
		Scores: ≥ 2 (2-5)	Score: 1	
IFA	GAD65 and GAD67	25	14	**39**
	GAD65 alone	10	4	**14**
				53

In short, following screening of the patient versus control sera on the GAD65ko BIOCHIP Mosaics™, 53 patients' sera were identified positive for anti-GAD65/GAD67 AAbs and 47 sera were devoid of such AAbs. Additionally, no unique AAb patterns were detected on the GAD65ko substrate following screening of the patient cohort. These results probably indicate that additional unknown AAbs, if present, appear in very low concentrations or as observed with the anti-GAD67 AAbs, wherein no GAD67-specific pattern was detected, these AAbs might not produce any specific pattern on the tissue substrates in IFA. Furthermore, some epitopes were probably hidden or masked in IFA and could not be accessible by patients' AAbs to produce a positive immunofluorescence signal. Keeping these reasons in mind, the search for additional autoantigens was continued using other immuno-biochemical assays such as immunoprecipitation.

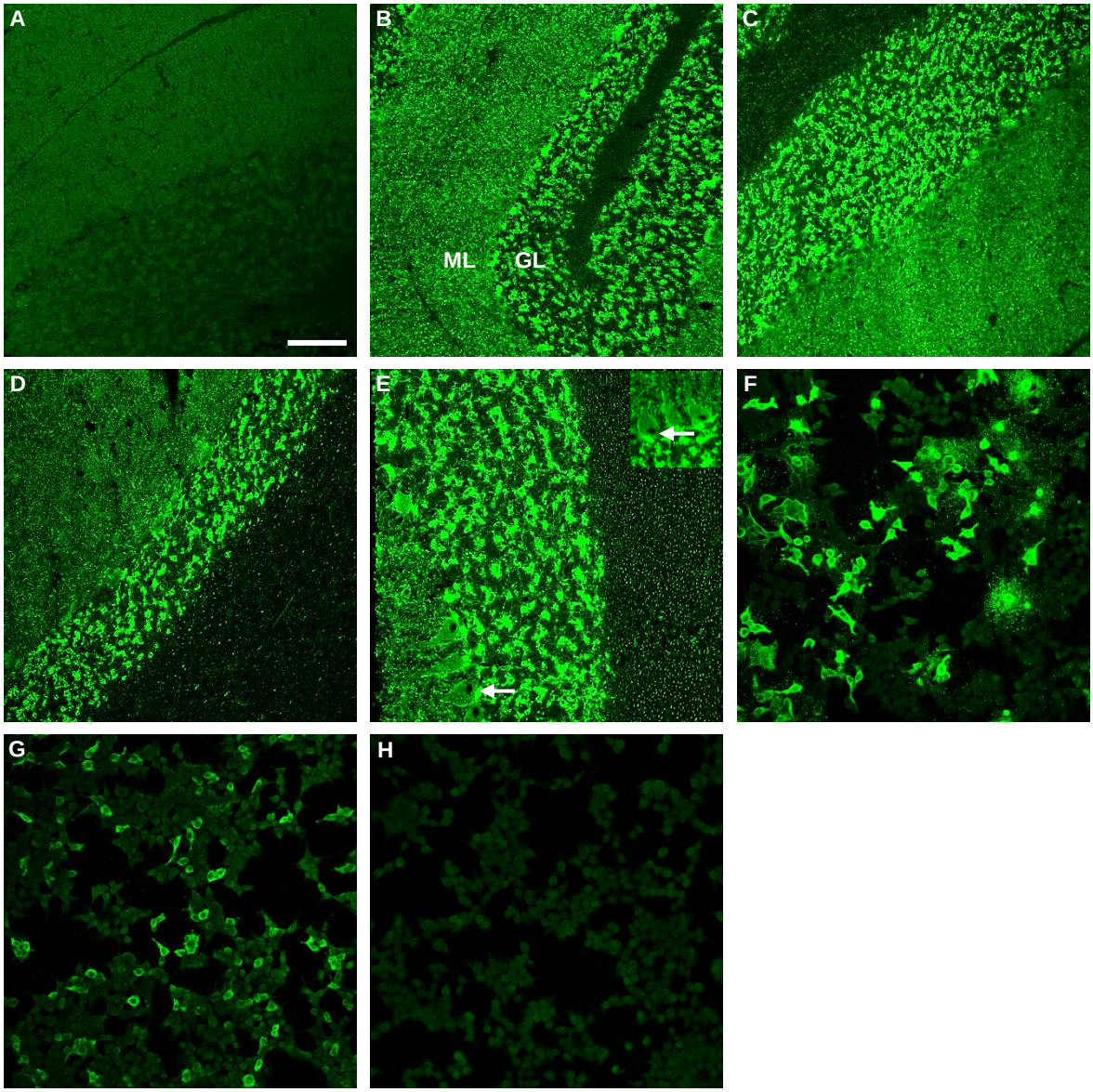

Figure 5: Representation of a GAD65-Specific pattern on wild-type animal cerebellar cryosections by incubating patient serum positive for anti-GAD65 and -GAD67 AAbs on a GAD65ko slide

Patient serum (1:10) positive for anti-GAD AAbs was incubated on a GAD65ko slide, including different wild-type animal cerebellum cryosections, a GAD65ko mouse cerebellum cryosection, and HEK293-GAD65, -GAD67, and mock transfected cells. GAD65-specific pattern is described as a blotchy florescence pattern of the granular layer (GL) and grain-like appearance of the molecular layer (ML). This pattern was observed on wild-type animal cerebellar cryosections including mouse **(B, GL and ML)**, rat **(C)**, monkey **(D)**, and pig **(E)**. Additionally, a positive staining of the Purkinje cells was observed on all wild-type cerebellum cryosections **(E, inset, arrows)**. A positive immunofluorescence signal was observed only on the HEK293-GAD65 and -GAD67 cells **(F-G)**, but not on the mock transfected cells **(H).** Following screening of the patient cohort, no new AAb pattern was detected in the GAD65ko substrate **(A)**. Additionally, patients' sera positive for anti-GAD67 AAbs did not produce any GAD67-specific pattern on the GAD65ko substrate. (Magnification: 200X, scale bar: 100 µm)

3.3. Immunoprecipitation of NSF and Dynamin 1 from the cerebellum by the patients' sera

Incubation with the patient cohort did not reveal any interesting pattern on the GAD65ko substrate. Therefore, an immunoprecipitation analysis using the patients' sera and the pig cerebellum lysate was implemented to identify additional target auto-antigens, other than GAD65 and GAD67. The total protein concentration of the pig cerebellum lysate as determined by the BCA assay (section 2.2.2) was ≈ 20-23 mg/ml during every preparation. In this study, two types of immunoprecipitation protocols were implemented.

The total lysate immunoprecipitation was performed as mentioned in section 2.2.4.1. The immunoprecipitated proteins were then resolved by gel electrophoresis and stained with blue silver stain to identify bands unique to the sera from patients compared with controls, which were subsequently identified by MS. A representative image of a blue silver stained gel following total lysate immunoprecipitation is shown in **Figure 6**.

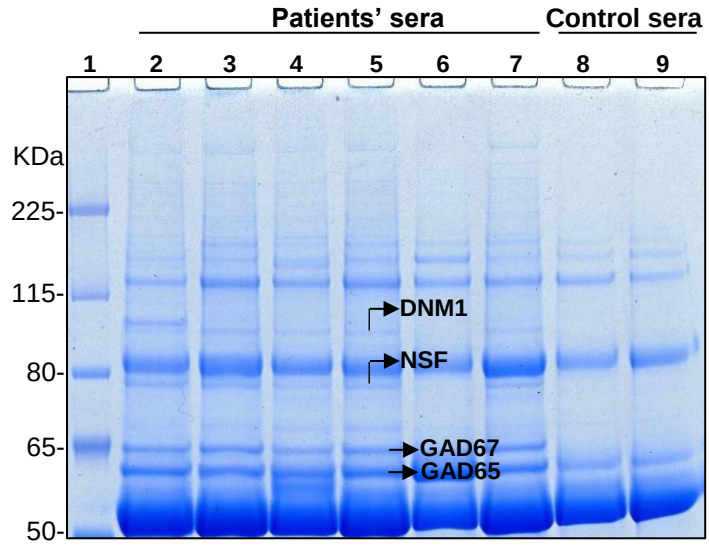

Figure 6: Representative image of a blue silver stained gel following total lysate immunoprecipitation to demonstrate pull-down of GAD65, GAD67, NSF, and DNM1 by the patients' sera

Sera from patients versus healthy subjects were incubated with the pig cerebellum lysate to form immune complexes. The bound antibody-antigen complex was then pulled down using protein G coated magnetic beads and separated by gel electrophoresis. The gel was subsequently stained with blue silver stain and the unique bands identified in the patients compared with control lanes were picked and identified by MS. In addition to GAD65 and GAD67 antigens at positions ≈ 65 kDa and ≈ 67 kDa, respectively **(lanes: 2-7, line arrows)**, proteins such as NSF (≈ 82 kDa) and DNM1 (≈ 97 kDa) were exclusively identified in the patients' sera **(lanes: 2, 3, 4, 5 and 7, elbow arrows)**, but not in the controls **(lanes: 8-9)**. Additionally, one anti-GAD positive patient serum did not pull-down NSF or DNM1 **(lane 6)**.

In this experiment, sera from six patients positive for anti-GAD65 and –GAD67 AAbs compared with two healthy controls were included. Following staining of the gel, the pull down of the primary target antigens: GAD65 and GAD67 at positions ≈ 65 kDa and ≈ 67 kDa, respectively were observed in all patients' sera lanes (Figure 6, line arrows), but not in the sera from controls. Additionally, two other bands unique to the patients' sera lanes were identified as NSF and dynamin 1 (DNM1) at positions ≈ 82 kDa and ≈ 97 kDa, respectively (Figure 6, elbow arrows). However, these bands were not observed in one anti-GAD positive patient serum (Figure 6, lane 6), indicating that the pull down of these proteins could be independent of the GAD antigens. Furthermore, the pull-down of above-mentioned proteins were not observed in any sera from controls.

Therefore, patients' sera specifically immunoprecipitated NSF and DNM1 in addition to GAD65 and GAD67. These results were verified by the second immunoprecipitation method; cryo-immunoprecipitation.

In this method, the pig cerebellum cryosections were used instead of the tissue lysate (section 2.2.4.2). Comparable to the above method, the immunoprecipitated proteins were resolved in a gel and stained with blue silver stain **(Figure 7)**. In this experiment, four patients' sera positive and one negative for anti-GAD65 and –GAD67 AAbs in addition to three sera from healthy controls were included for representation purposes. The results from the two immunoprecipitation methods were comparable. The pull-down of the primary target antigens namely GAD65 (≈ 65 kDa) and GAD67 (≈ 67 kDa) was observed in all patients' sera positive for anti-GAD AAbs (Figure 7, line arrows), but not in the patient serum negative for anti-GAD AAbs (Figure 7, lane 4). Furthermore, a strong pull-down of NSF (≈ 82 kDa) and DNM1 (≈ 97 kDa) was observed in all anti-GAD AAb positive patients' sera (Figure 7, arrows), except one, wherein the pull-down was weaker (Figure 7, lane 5). Remarkably, NSF and DNM1 were immunoprecipitated in the patient serum negative for anti-GAD AAbs, suggesting that these proteins might not be co-immunoprecipitated with the GAD antigens (Figure 7, lane 4). Additionally, there was no pull-down of the above-mentioned proteins with the healthy controls. The patient serum negative for the pull-down of NSF and DNM1 in the total lysate immunoprecipitation experiment (Figure 6, lane 6) was also negative in this test (data not shown). The pull-down of GAD65 and GAD67 and other possible target antigens were minimal with in the cryo-immunoprecipitation analysis and therefore, the remaining immunoprecipitation experiments were carried out only with the total lysate immunoprecipitation analysis.

In short, apart from GAD antigens, proteins such as NSF and DNM1 were immunoprecipitated specifically by the patient cohort, but not by the controls in both the test methods. The

immunoprecipitation of NSF and DNM1 was observed in patients' sera both positive and negative for anti-GAD AAbs and not all anti-GAD AAb positive sera precipitated the proteins in question, indicating that these proteins were pulled down independent of the GAD antigens.

NSF and DNM1 are pre-synaptic vesicle associated proteins and they play a very important role in trafficking of vesicles carrying neurotransmitters. NSF is associated with the superfamily of proteins called SNARE proteins and it could be possible additional SNARE proteins were precipitated in the form of a complex in the patient cohort. As a subsequent step, screening for additional SNARE proteins as possible auto-antigens in the patient cohort and determination of the direct AAb target was mandated.

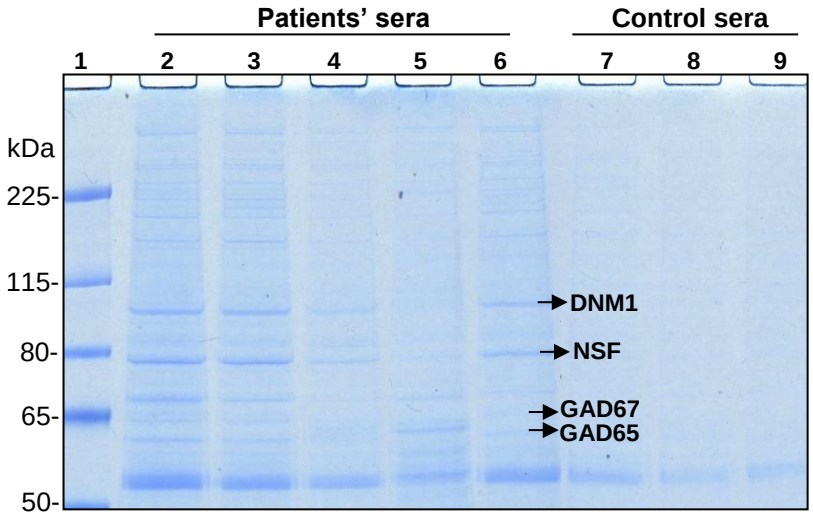

Figure 7: Representative image of a blue silver stained gel to show pull-down of NSF, DNM1, GAD65, and GAD67 following cryo-immunoprecipitation

Sera from patients versus healthy subjects were incubated with pig cerebellum tissue cryosections resulting in the formation of immune complexes. The mixture was solubilized and incubated with protein G coated magnetic beads to bind immune complexes. Subsequently, the immunoprecipitated eluates were separated by gel electrophoresis and stained with blue silver stain to identify unique bands in the patients' sera compared with control sera. The pull-down of GAD65 (≈ 65 kDa) and GAD67 (≈ 67 kDa) was observed in all anti-GAD positive patients' sera **(Lanes: 2, 3, 5, and 6, arrows)**, but not in the negative serum **(lane 4)** or control sera **(lanes: 7-9)**. In addition to the GAD antigens, unique proteins such as NSF and DNM1 at positions ≈ 82 kDa and ≈ 97 kDa, respectively were exclusively identified in the patients' sera **(lanes: 2-6, arrows)**, but not in controls. The pull-down of NSF and DNM1 were independent of the GAD antigens since the patient serum negative for anti-GAD AAbs also immunoprecipitated the proteins in question **(lane 4)**.

3.4. Verification of the pull-down of synaptic proteins by the patient cohort

Following immunoprecipitation, the proteins were electro-transferred onto nitrocellulose membranes (section 2.2.5.3) and analyzed with different commercial antibodies **(Table 10)**. Representative images of the immunoprecipitation followed by WB (IP-WB) analysis are depicted in **Figure 8**. In this experiment, a humanized monoclonal antibody against GAD65/67 was used as a positive control for immunoprecipitation (Figure 8, PC1) in addition to five patients' sera positive for anti-GAD65 and -67 AAbs and one patient serum negative for these AAbs as well as two sera from healthy controls. The Ponceau S stained membrane was cut sequentially at the regions: 115-80 kDa, 80-65 kDa, 65-50 kDa, 35-30 kDa (Figure 8A, dotted lines) and incubated with primary antibodies such as DNM1, NSF, GAD65/67, and STX1B, respectively depending on the position of their target antigens (Table 10). Syntaxins are important membranes of the SNARE proteins and its isoform STX1B is specifically observed in neurons (Bennett et al., 1992). Determination of AAbs against STX1B was simultaneously being researched at EUROIMMUN AG (Germany) and therefore, was additionally included in this analysis. As a size control, 8 µg of total protein from the pig cerebellum tissue lysate was loaded (Figure 8, Lys). Reactivities against DNM1 (≈ 97 kDa), NSF (≈ 82 kDa), GAD67 (≈ 67 kDa), GAD65 (≈ 65 kDa), and STX1B (≈ 33 kDa) were detected in the lysate (Figure 8B, lane 2), revealing the presence of these proteins in the included tissue lysate. Reactivity against GAD65 and GAD67 was observed in the positive control and in all patients' sera positive for anti-GAD AAbs (Figure 8B, lanes: 3, 4-6, 8-9), but not in the serum negative for anti-GAD AAbs (Figure 8B, lane 7) or in the control sera (Figure 8B, lane: 10-11). Furthermore, a strong reactivity against DNM1 and NSF was observed in all patients' sera positive for anti-GAD AAbs (Figure 8B, lanes: 4-6), except in two sera (Figure 8B, lanes: 8-9), suggesting that the pull-down of these proteins were observed only with some anti-GAD positive patients' sera. Additionally, patient serum negative for anti-GAD AAbs also pulled down DNM1 and NSF (Figure 8B, lane 7), as observed in the cryo-immunoprecipitation analysis (Figure 7, lane 4). No reactivity against NSF or DNM1 was observed with the anti-GAD65/67 antibody or controls. Furthermore, the pull-down of STX1B at ≈ 33 kDa was observed in patients' sera both positive and negative for anti-GAD AAbs (Figure 8B, lanes: 4-7), but in reduced amounts compared to NSF and DNM1.

IP-WB analysis revealed that the pull-down of SNARE proteins like NSF and STX1B and another vesicle associated protein, DNM1, might be independent of the well-known target antigens; GAD65 and GAD67. Immunoprecipitation of these antigens was observed in patients' sera both positive and negative for anti-GAD AAbs, but not in the control cohort.

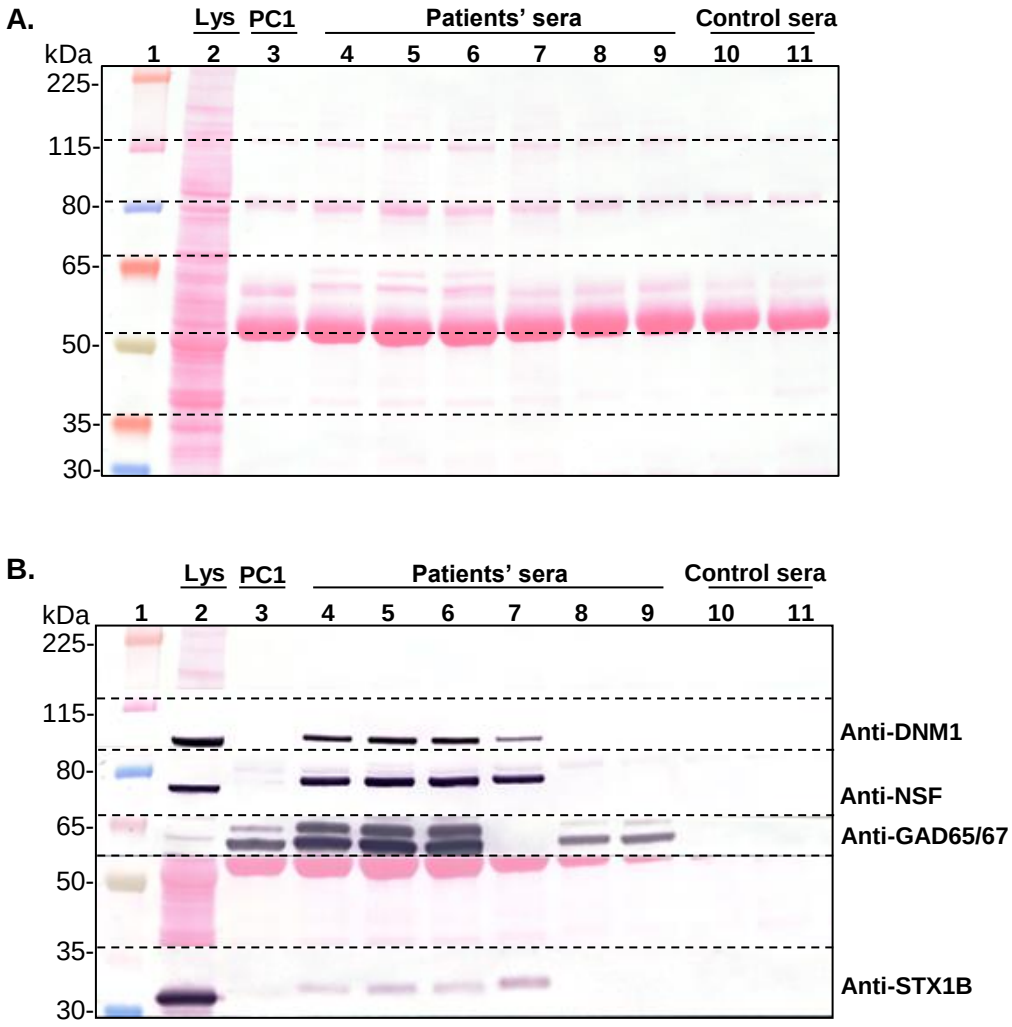

Figure 8: IP-WB analysis showing the pull-down of GAD, DNM1, NSF, and STX1B by the patients' sera

Immunoprecipitation analysis was performed using sera from patients both positive (n = 5) and negative (n = 1) for anti-GAD65 and -67 AAbs as well as from healthy controls (n = 2). Additionally, a monospecific antibody directed against GAD65/57 was included as a positive control **(PC1)** and ≈ 8 µg of total protein from the tissue lysate was loaded as the size control **(Lys)**. The immunoprecipitated proteins were transferred onto nitrocellulose membranes, cut sequentially at the dotted lines, and immunoblotted with primary antibodies against DNM1 (1:1000), NSF (1:650), GAD65/67 (1:20,000), and STX1B (1:2000) depending on the position of their respective target antigens. In the lysate, presence of DNM1 (≈ 97 KDa), NSF (≈ 82 KDa), GAD67 (≈ 67 KDa) and GAD65 (≈ 65 KDa), and STX1B (≈ 33 KDa) was noted **(lane 2)**. Reactivity against GAD65/67 was observed in all anti-GAD AAb positive patients' sera **(lanes: 4-6 and 8-9)** and in the positive control **(lane 3)**. Additionally, reactivity against DNM1 and NSF was observed in three anti-GAD AAb positive patients' sera **(lanes: 4-6)** as well as in the anti-GAD AAb negative serum **(lane 7)**, suggesting a pull-down of these proteins. No reactivity against NSF or DNM1 was observed in two anti-GAD AAb positive patients' sera **(lanes: 8-9)**, anti-GAD65/67 antibody **(lane 3)**, and in controls **(lanes: 10-11)**. Additionally, the pull-down of STX1B was observed in four patients' sera **(lanes: 4-7),** but in reduced amounts.

3.4.1. The rate of pull-down of GAD and SNARE proteins in the entire cohort

On screening the entire patient cohort (n = 100) in comparison with healthy controls (n = 50) in IP-WB analysis using an anti-GAD65/67 antibody, 52 patients' sera were positive for anti-GAD AAbs **(Table 16A).** Overall, 36 patients' sera were positive for anti-GAD65 and -GAD67 AAbs and 16 patients' sera only for anti-GAD65 AAbs. In the IFA, 53 patients' sera were positive for anti-GAD AAbs and it was observed that one patient serum (patient number: 41) positive for anti-GAD65 AAbs in the HEK-GAD65 cells alone, was negative for anti-GAD65 AAbs in the IP-WB analysis (Table 21). Additionally, two patients' sera (patients' number: 55 and 90) negative for anti-GAD67 AAbs in IFA were positive for anti-GAD67 AAbs in IP-WB analysis and five patients' sera positive for anti-GAD65 and GAD67 AAbs (patients' number: 10, 20, 46, 47, 63) in IFA were positive only for anti-GAD65 AAbs in IP-WB analysis **(Table 16B).** However, these patients' sera portrayed a weak reactivity against GAD67 in IFA (score: 1). Altogether, detection of AAbs against GAD65 and GAD67 was more sensitive in IFA compared with immunoblotting tests.

Table 16: Comparison of IFA and WB analysis to depict number of patients positive for anti-GAD AAbs (n = 100)

A.

Test methods	**Number of patients' sera positive for AAbs against**		**Total**
	GAD65 and GAD67	GAD65 alone	
IFA	39	14	**53**
WB	36	16	**52**

B.

	IFA: sera positive for AAbs against		**WB:** sera positive for AAbs against	
	GAD65 and GAD67	**GAD65 alone**	**GAD65 and GAD67**	**GAD65 alone**
	34	11	34	11
	X	1	X	Negative
	Negative for GAD67	2	2	X
	5	X	Negative for GAD67	5
Total	**39**	**14**	**36**	**16**

The IP-WB analysis revealed that patients' sera additionally immunoprecipitated possible target antigens such as NSF, STX1B, and DNM1, independently of the GAD antigens. In patients' sera positive for anti-GAD AAbs (n = 52), the pull-down of NSF and STX1B was observed in 23 and 37 patients, respectively **(Figure 9A)** and in those negative for anti-GAD AAbs (n = 48), six patients' sera immunoprecipitated NSF and 22 pulled down STX1B **(Figure 9B)**.

A.

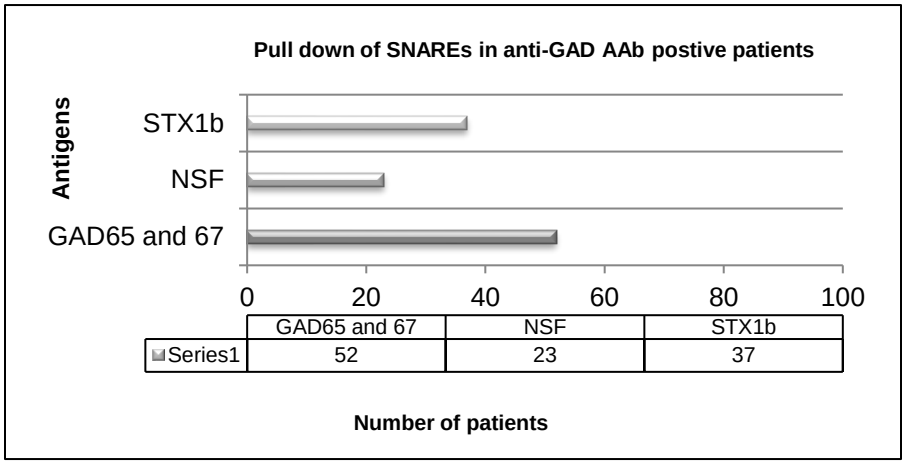

B.

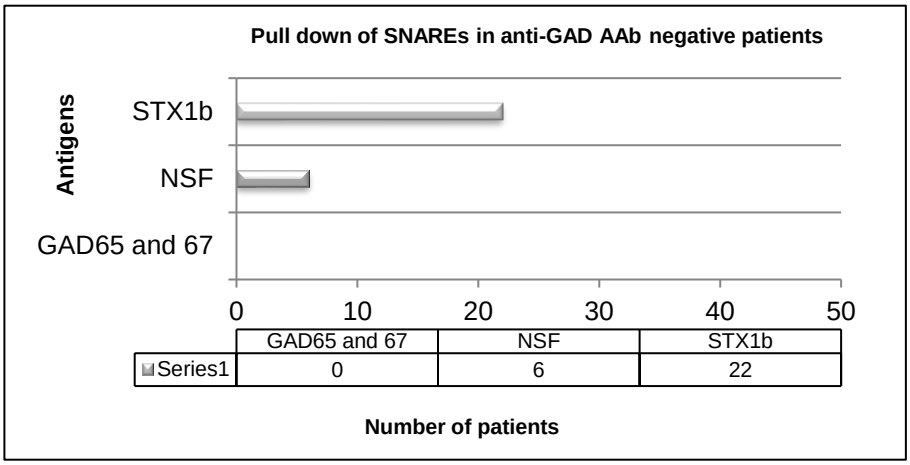

Figure 9: Graphical representation of the rate of pull-down of GAD, NSF, and STX1B in IP-WB

IP-WB analysis using animal antibodies against NSF, GAD65 and GAD67, and STX1B revealed the pull-down off NSF and STX1B in 23 and 37 patients, respectively, in patients' sera positive for anti-GAD AAbs (n = 52) and in six and 22 patients, respectively, in those negative for anti-GAD AAbs (n = 48). Even though the rate of pull-down of STX1B was higher, the intensity of reactivity was weaker compared with NSF.

Data is not represented for DNM1 because the antigen was identified later during the project and could not be represented for the entire patient cohort. However, in a subset of patients the immunoprecipitation of DNM1 was close to that of NSF, indicating comparable immunoprecipitation results between the two proteins (Figure 8). Additionally, dynamin is closely

associated with amphiphysin, which is a pre-synaptic protein that binds with dynamin during vesicular endocytosis (Takei et al., 1999). However, the immunoprecipitation of DNM1 was independent of amphiphysin (data not shown), indicating that DNM1 could be another individual candidate antigen in this patient cohort.

In short, possible target antigens such as NSF, STX1B, and DNM1 were identified exclusively in the patient cohort, independently of the well-known candidate antigens such as GAD and amphiphysin. Therefore, these proteins could be a common, yet independent biomarker in patients diagnosed with SPS, PERM and associated movement disorders. However, it could be possible that different SNARE proteins were co-immunoprecipitated as a complex, mandating the need to identify the direct and individual AAb targets.

3.4.2. No immunoprecipitation of GABARAP by the patients' sera

Raju et al identified GABARAP as a possible target antigen in SPS patients harboring anti-GAD65 AAbs using immunoprecipitation analysis (Raju et al., 2006). Furthermore, studies have shown a direct interaction between GABARAP and NSF and that these two proteins exist in a complex in the brain (Chen et al., 2007; Kittler et al., 2001). Therefore, to verify whether patients' sera pulled down GABARAP and if NSF was co-immunoprecipitated with it, WB analysis using anti-GABARAP antibody was performed. The blot from the previous experiment (Figure 8) was cut at the 15 kDa region and incubated with anti-GABARAP antibody (Table 10).

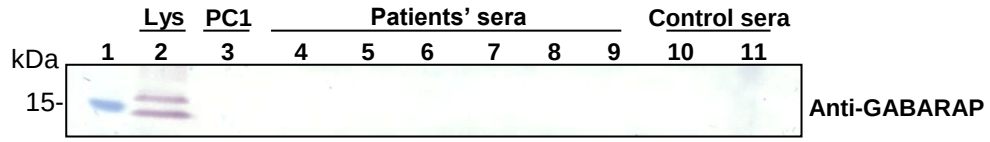

Figure 10: GABARAP was not immunoprecipitated by the patient cohort

The blot from section 3.4 was cut at ≈ 15 kDa regions and incubated with rabbit anti-GABARAP antibody (1:250). GABARAP was detected at ≈ 13 KDa in the lysate alone **(Lys, lane 2)**. Reactivity against GABARAP was not observed in the anti-GAD65/67 antibody **(PC1, lane 3)** and in sera from patients or controls **(lanes: 4-11)**.

Reactivity against GABARAP (≈ 13 kDa) was observed in the lysate, demonstrating the presence of the protein in the tissue **(Figure 10**, **Lys)**. However, neither the anti-GAD65/67 antibody nor the serum samples pulled down GABARAP (Figure 10, lanes: 3-11). Therefore, GABARAP might not be a possible candidate antigen in these patients. Specifically, GABARAP was not detected in any patients' sera that immunoprecipitated NSF, suggesting that the pull-down of NSF was independent of GABARAP. In short, NSF, STX1B, and/or DNM1 could be possible additional, independent candidate antigens in the patient cohort.

3.4.3. Investigation of the pull-down of SNARE proteins in the neurological and healthy controls

Total lysate immunoprecipitation was performed including sera from patients in comparison with healthy as well as neurological controls. Neurological controls included patients' sera positive for AAbs against other well-known neuronal target antigens as mentioned in **Table 9**. Overall, 30 neurological controls harboring AAbs against NMDAR (n = 7), CASPR2 (n = 7), LGI1 (n = 7), Hu (n = 5), and Ri (n = 4) were tested for the pull-down of SNARE proteins such as NSF and STX1B in the IP-WB analysis. A representative image of the IP-WB analysis is depicted in **Figure 11**. In this test, seven neurological controls including three patients' sera positive for anti-LGI1 AAbs, two patients' sera positive for anti-NMDAR AAbs, two patients' sera positive for anti-Hu AAbs, and two sera from healthy controls were included. Additionally, a patient serum that immunoprecipitated the SNARE proteins was used as the positive control (Figure 11, PC). The Ponceau stained membrane (Figure 11A) was cut at the dotted lines at the regions: 115-65 kDa, 65-50 kDa, and 35-30 kDa and incubated with antibodies against NSF, GAD65/67, and STX1B, respectively (Table 10). Reactivity against NSF (≈ 82 kDa), GAD67 (≈ 67 kDa), GAD65 (≈ 65 kDa), and STX1B (≈ 33 kDa) were observed only in the positive control (Figure 11B, lane 2), but not in any of the neurological or healthy controls (Figure 11B, lanes: 3-12). Therefore, immunoprecipitation of SNARE proteins including NSF and STX1B might be specific to the patient cohort alone and not in controls. As a subsequent step, it was important to screen the patient cohort for the pull-down of different SNARE proteins and accordingly determine which of the SNARE proteins could be possible direct target antigens of patient AAbs.

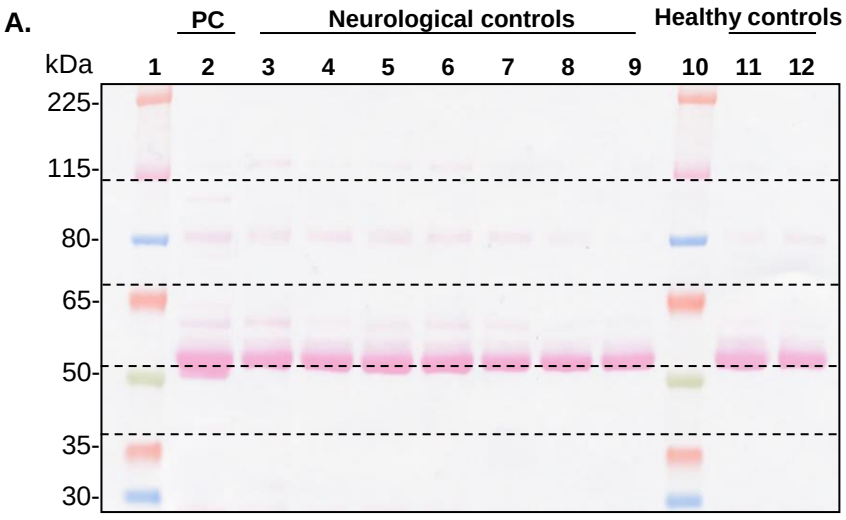

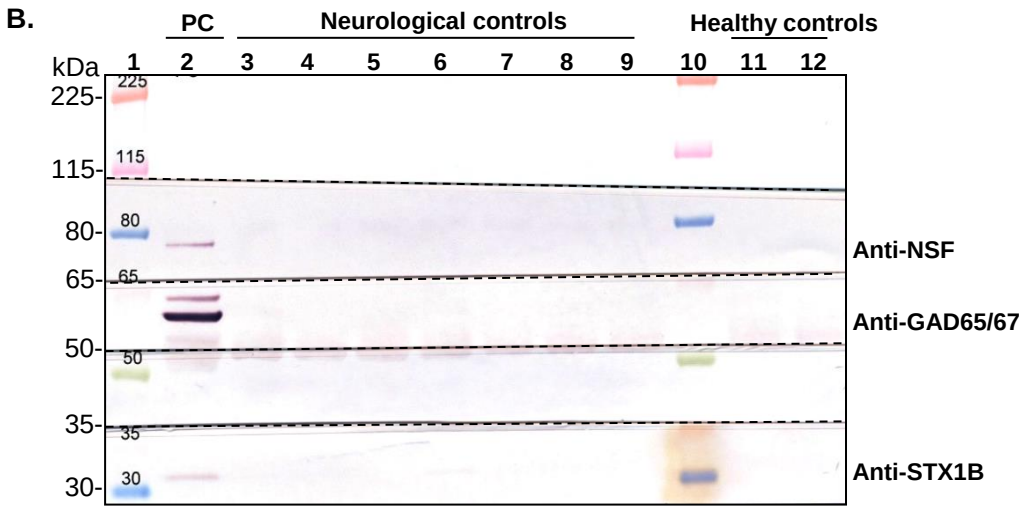

Figure 11: WB analysis to show neurological and healthy controls do not pull-down GAD, NSF, or STX1B
A) Patient serum positive for AAbs against GAD65/67 **(PC, lane 2)**, LGI1 **(lanes: 3-5)**, NMDAR **(lanes: 6-7)**, Hu **(lanes: 8-9)**, and sera from controls **(lanes: 11-12)** were included in the immunoprecipitation analysis. Subsequently, the immunoprecipitated proteins were transferred onto blots and stained with Ponceau S. **B)** The blot was cut at the dotted lines and incubated with commercial antibodies namely anti-NSF (1:650), anti-GAD65/67 (1:20,000), and STX1B (1:2000) depending on the position of the respective target antigens. Reactivity against NSF (≈ 82 KDa), GAD (≈ 65/67 KDa), and STX1B (≈ 33 KDa) was identified only in the positive control **(lane 2)**, but not in neurological or healthy controls **(lanes: 3-12)**.

3.5. Characterization of antibodies against the SNARE proteins

IP-WB analysis revealed that the immunoprecipitation of vesicular proteins including DNM1, NSF, and STX1B even though specific to the patient cohort, could be immunoprecipitated as a complex with other SNARE proteins. Therefore, the pull-down of seven additional proteins associated with the synaptic vesicular trafficking namely exocyst complex component 4 (EXOC4/Sec8), Rab3A, SNAP25, STXBP1 (or Munc18), synaptotagmin 1, synaptophysin 1, and VAMP2 were screened with the patient cohort as possible additional target antigens **(Table 1)**.

3.5.1. Determination of the Western blot reactivity of commercial antibodies against synaptic proteins in the pig cerebellum

Commercial animal antibodies against further SNARE proteins in addition to other proteins associated with synaptic vesicular trafficking were tested in WB analysis using the pig cerebellum lysate. **Figure 12** portrays the WB reactivity of various antibodies against appropriate antigens (arrows) such as anti-SNAP25 at ≈ 25 kDa (strip 1), anti-VAMP2

at ≈ 12 kDa (strip 2), anti-synaptotagmin 1 at ≈ 47 kDa (strip 3), anti-synaptophysin 1 at ≈ 38 kDa (strip 4), anti-STXBP1 at ≈ 66 kDa (strip 5), anti-EXOC4 at ≈ 122 kDa (strip 6), anti-Rab3A at ≈ 24 kDa (strip 7), anti-GAD65 and GAD67 at ≈ 65 and 67 kDa (strip 8), anti-NSF at ≈ 82 kDa (strip 9), and anti-STX1B at ≈ 33 kDa (strip 10). The reactivity against various SNARE proteins such as NSF, STX1B, SNAP25, and VAMP2 and other regulatory proteins associated with the SNARE proteins including EXOC4, Rab3A, STXBP1, synaptotagmin 1, and synaptophysin 1 were verified in the pig cerebellum lysate. The reactivity against synaptotagmin 1 (strip 3) was weaker compared with other proteins, probably indicating a lower concentration of the protein in the tissue source. Subsequently, all antibodies were analyzed in IFA to determine their reactivity against tissue substrates.

A collective term **"anti-SNARE antibodies"** would be used for simplicity to depict all above-mentioned commercial antibodies against proteins associated with synaptic vesicular trafficking.

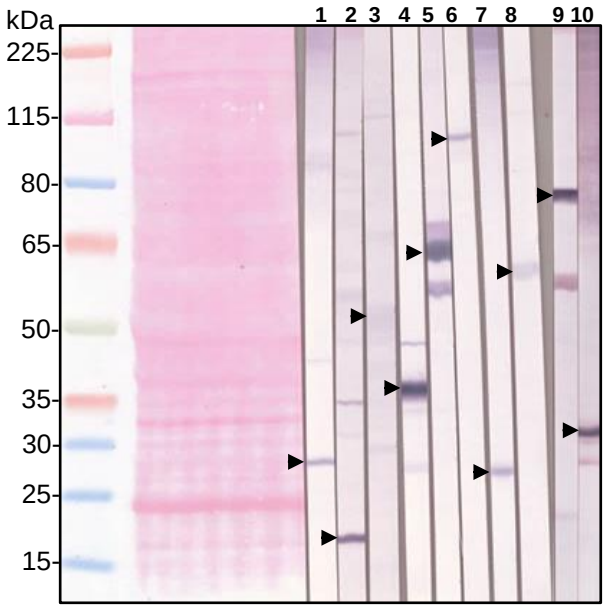

Figure 12: WB reactivity of externally purchased animal antibodies against synaptic proteins in the pig cerebellum

Approximately 8 µg of total protein from pig cerebellum tissue lysate was transferred onto membranes and immunoblotted using various animal antibodies. Reactivities against appropriate antigens **(arrows)** were detected for all antibodies namely anti-SNAP25 (≈ 25 kDa, strip 1), anti-VAMP2 (≈ 12 kDa, strip 2), anti-synaptotagmin 1 (≈ 47 kDa, strip 3), anti-synaptophysin 1 (≈ 38 KDa, strip 4), anti-STXBP1 (≈ 66 kDa, strip 5), anti-EXOC4 (≈ 122 kDa, strip 6), anti-Rab3A (≈ 24 kDa, strip 7), anti-GAD65 and GAD67 (≈ 65 and 67 kDa, strip 8), anti-NSF (≈ 82 kDa, strip 9), and anti-STX1B (≈ 33 kDa, strip 10). The reactivity against synaptotagmin (strip 3) was weaker compared with other SNARE proteins.

3.5.2. Determination of reactivity of anti-SNARE antibodies on the GAD65ko BIOCHIP Mosaics™

All anti-SNARE antibodies (1:10) were also screened on the GAD65ko BIOCHIP mosaics™ to identify specific antibody patterns on the tissue substrates **(Figure 13).** For representation purposes, images from the cerebellum cryosections from the GAD65ko mouse in addition to the wild-type mouse and pig are portrayed here.

Following incubation with the anti-NSF antibody, a weak staining of the GAD65ko substrate with a blotchy GL and no staining of the ML was observed (Figure 13, 1A). The intensity of staining on the mouse and pig cerebellum sections was brighter with a blotchy GL and plain-green, even staining of the ML (Figure 13, 1B-C). In contrast, the anti-STX1B antibody portrayed a brightly stained GAD65ko substrate (Figure 13, 2A). Additionally, all substrates demonstrated bright, even, and plain-green staining of the ML compared with a lower intensity staining of the GL (Figure 13, 2A-C). The staining pattern of anti-SNAP25 antibody was comparable with that of anti-STX1B antibody, but with higher staining intensities (Figure 13, 3A-C). With the anti-VAMP2 antibody, a speckled staining pattern of the GL and light-green, plain pattern of the ML was noted (Figure 13, 4A-B). However, the staining pattern on the pig cerebellum was weaker compared with the other substrates (Figure 13, 4C). The anti-EXOC4 (Sec8) antibody produced an interesting staining pattern on all substrates. The Purkinje cells were densely stained and portrayed visible dendrites in the ML, which was particularly evident in GAD65ko substrate (Figure 13, 5A). Additionally, no staining of the GL and uneven light-green staining of the ML was noted (Figure 13, 5A-C). Antibodies against STXBP1, Rab3A, synaptophysin 1, and synaptotagmin 1 produced no significant staining patterns on the tissue cryosections (Data not shown). However, WB reactivity of all the above-mentioned antibodies were detected on the pig cerebellum tissue (Figure 12, lanes: 3, 4, 5, and 7), probably suggesting that their epitopes could be masked in IFA interfering with the antibody-antigen binding.

Patterns produced by different anti-SNARE antibodies could be useful to determine AAbs against the SNARE proteins, if present in the patients' sera. However, screening of the patient cohort using the GAD65ko slide did not reveal any specific pattern on the GAD65ko substrate, that could be matched with the patterns observed with anti-SNARE antibodies (Figure 5A). Additionally, it was difficult to screen for underlying SNARE antibody patterns on the wild-type animal tissue substrates, since majority of patients' sera positive for anti-GAD AAbs predominantly portrayed a GAD65-specific pattern on these tissue substrates. Therefore, implementation of other immunoassays was mandated since it was difficult to identify antibodies against the SNARE proteins in the patient cohort under IFA conditions.

Results

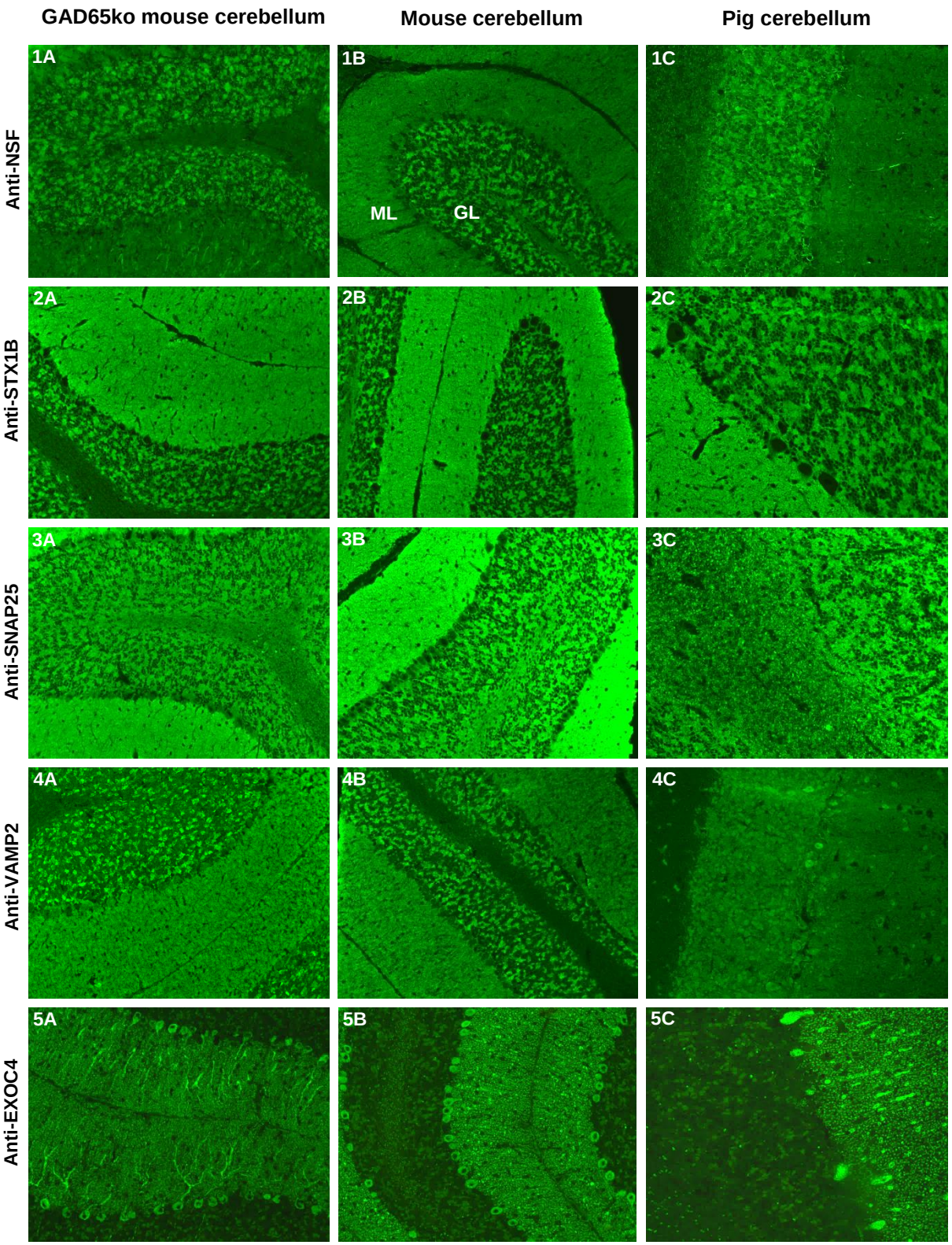
GAD65ko mouse cerebellum
Mouse cerebellum
Pig cerebellum
Anti-NSF
Anti-STX1B
Anti-SNAP25
Anti-VAMP2
Anti-EXOC4
1A
1B
1C
2A
2B
2C
3A
3B
3C
4A
4B
4C
5A
5B
5C
ML
GL

Figure 13: Fluorescence patterns produced by different anti-SNARE antibodies on the cerebellar cryosections in the GAD65ko BIOCHIP mosaics™

Representative images of patterns produced on the GAD65ko mouse cerebellum **(A)**, wild-type mouse **(B)**, and pig cerebellum **(C)** following incubation with anti-SNARE antibodies (1:10) on the GAD65ko slide. The primary antibodies were detected using appropriate secondary antibodies and examined under EUROStar II fluorescence microscope. Anti-NSF antibody: light staining of the GAD65ko substrate with a blotchy GL and no staining on the ML **(1A)**. Staining of the wild-type mouse and pig substrates were brighter with a blotchy GL and even, plain-green ML **(1B-C)**. Anti-STX1B antibody: bright, even, plain-green staining of the ML compared with a lower intensity, blotchy signal in the GL **(2A-C)**. Anti-SNAP25 antibody: pattern of staining was similar to the anti-STX1B antibody, but with higher signal intensities **(3A-C).** Anti-VAMP2 antibody: speckled GL and light-green, plain pattern on the ML **(4A-C).** Anti-EXOC4 (Sec8) antibody: Purkinje cells were stained bright green with visible dendrites in the ML of the GAD65ko substrate **(5A)**. Additionally, there was no staining of the GL and the ML was stained uneven and light-green **(5A-C).** Antibodies against STXBP1, Rab3A, synaptophysin 1, and Synaptotagmin 1 produced either weakly stained tissue substrates or produced no pattern at all (Data not shown). (Magnification: 200X)

3.6. Immunoprecipitation of the SNARE proteins by an antibody against the metabotropic glutamate receptor 1

A panel of monoclonal antibodies (Euroimmun AG, Germany) against various well-known neurological target antigens (Table 9), was also screened in the IP-WB analysis as a control to verify the pull-down of SNARE proteins. It was observed that none of the included antibodies, expect the antibody against GRM1, interacted with the SNARE proteins and resulted in the pull-down of NSF and STX1B (data not shown). **Figure 14** portrays a representative image of an immunoprecipitation experiment that was performed using a human monoclonal anti-GRM1-IgG antibody (Table 3) and an isotype control. Approximately 8 µg of total protein from pig cerebellum tissue lysate was loaded as a size control and to detect the presence of various proteins under study. After electro-transfer, the blot was sequentially cut depending on the position of target antigens at the following regions: 225-115 kDa, 115-80 kDa, 80-65 kDa, 65-50 kDa, 35-30 kDa, 30-25 kDa, and 25-10 kDa and incubated with antibodies directed against GRM1, DNM1, NSF, GAD65/67, STX1B, SNAP25, and VAMP2, respectively (Table 10). In the tissue lysate, reactivity against all antigens including GRM1 (≈ 132 kDa), DNM1 (≈ 97 kDa), NSF (≈ 82 kDa), GAD65/GAD67 (≈ 65/67 kDa), STX1B (≈ 33 kDa), SNAP25 (≈ 25 kDa), and VAMP2 (≈ 12 kDa) were observed (Figure 14, lane 2). The anti-GRM1 antibody pulled down GRM1 from the tissue (Figure 14, black arrow), but in reduced amounts, probably due to presence of lower concentrations of the protein in the lysate. Additionally, the antibody immunoprecipitated different SNARE proteins such as NSF, STX1B, SNAP25, and VAMP2 (weak) as well as DNM1 (Figure 14, lane 3). However, there was no precipitation of the GAD

antigens (Figure 14, red arrow). The control antibody did not immunoprecipitate any of the above-mentioned proteins (Figure 14, lane 4), indicating that the pull-down was specific to the GRM1 antibody alone.

In short, the anti-GRM1 antibody immunoprecipitated different SNARE proteins from the cerebellum tissue, without any interference from the GAD antigens.

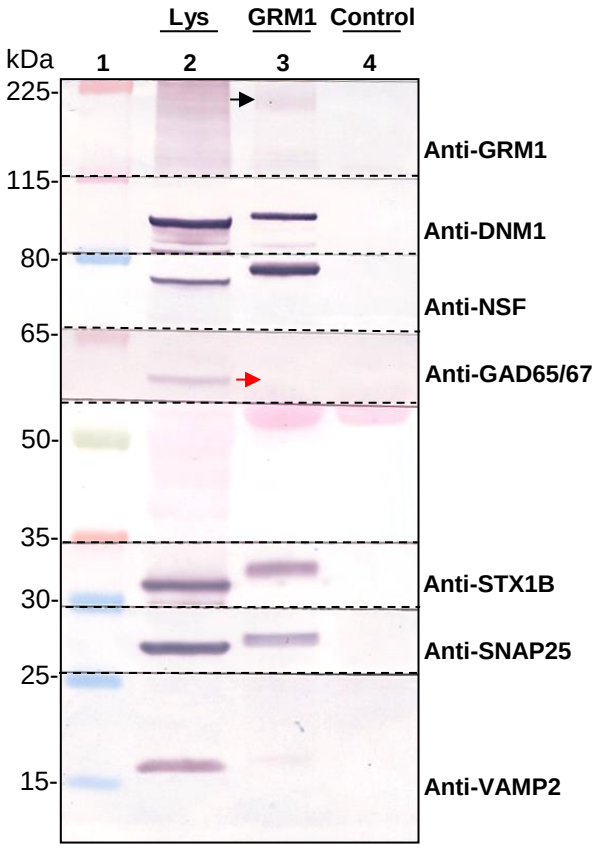

Figure 14: Anti-GRM1-IgG antibody augments the pull-down of the SNARE proteins

A monoclonal anti-GRM1-IgG antibody enriched the pull-down of different SNARE proteins in total lysate immunoprecipitation. Approximately 8 µg of total protein from the pig cerebellum lysate was transferred onto a nitrocellulose membrane as the size control **(Lys, lane 2).** Immunoprecipitation was performed using a anti-GRM1-IgG antibody **(lane 3)** and an isotype control **(lane 4)**. Subsequently, the membrane was cut at the dotted lines depending on the position of different antigens in question and incubated with antibodies against GRM1 (1:250), DNM1 (1:1000), NSF (1:650), GAD65 and GAD67 (1:20,000), STX1B (1:2000), SNAP25 (1:1000), and VAMP2 (1:250). On comparing with the tissue lysate, an enriched pull-down of NSF (≈ 82 kDa), followed by DNM1 (≈ 97 kDa), STX1B (≈ 33 kDa), and SNAP25 (≈ 25 kDa), and to a minor extent VAMP2 (≈ 12 Da) was observed with the anti-GRM1 antibody **(lane 3 versus lane 2)**. However, the pull-down of the primary antigen, GRM1 **(lane 3, black arrow)** was lower compared with the other mentioned proteins. Furthermore, no pull-down of GAD65/67 antigens was observed with the anti-GRM1 antibody **(lane 3, red arrow)**. The control antibody did not pull-down any of the proteins in question **(lane 4)**.

3.6.1. Analysis of the immunoprecipitation of GRM1 by the patient cohort

The previous experiment revealed that the anti-GRM1 antibody directly or indirectly interacted with the SNARE proteins and enriched their pull-down. Additionally, immunoprecipitation experiments showed that several patients' sera immunoprecipitated NSF and STX1B. Therefore, it was important to verify whether patients' AAbs directly targeted GRM1 and if, NSF and STX1B were co-immunoprecipitated with it**.** An immunoprecipitation analysis was performed including the monoclonal anti-GRM1 antibody as the positive control (PC2) as well as seven anti-GAD AAb positive sera and two sera from healthy controls **(Figure 15)**. WB analysis with antibodies against GRM1, NSF, and GAD65/67 revealed reactivity against GAD antigens (≈ 65 and 67 kDa) in the patients' sera (Figure 15, lanes: 3-9), but not in the sera from controls or the anti-GRM1 antibody. Additionally, NSF (≈ 82 kDa) was immunoprecipitated with the patients' sera as well as the anti-GRM1 antibody (Figure 15, lanes: 2-9). However, the reactivity against the GRM1 antigen (≈ 133 kDa) was detected only with the anti-GRM1 antibody (Figure 15, red arrow), but not in any of the serum samples, suggesting that the GRM1 antigen was not a common AAb target in these patients. Therefore, it could be possible that NSF, and/or other SNARE proteins could be additional candidate antigens in the patient cohort.

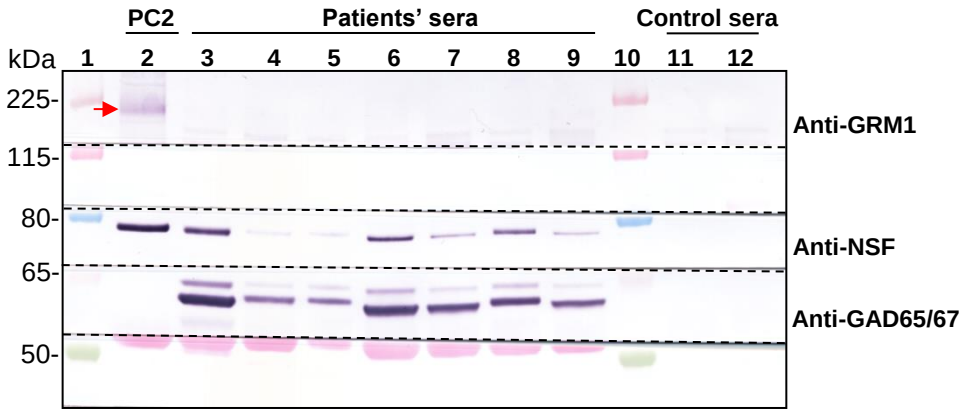

Figure 15: GRM1 was not a common AAb target in the patient cohort

An immunoprecipitation experiment was performed including the anti-GRM1 antibody **(PC2)**, seven anti-GAD positive patients' sera **(lanes: 3-9),** and two sera from healthy controls **(lanes: 11-12)**. The membrane was cut along the dotted lines and incubated with antibodies against GRM1 (1:250), NSF (1:650), and GAD65 and GAD67 (1:20,000). Reactivity against the GAD antigens (≈ 65 and 67 kDa) was observed in all patients' sera **(lanes: 3-9).** Additionally, the pull-down of NSF (≈ 82 kDa) was detected in all patient's sera as well as in the anti-GRM1 antibody **(lanes: 2-9)**. However, the reactivity against the GRM1 antigen at ≈ 133 kDa was observed only with the anti-GRM1 antibody **(lane 2, red arrow)**, but not in sera from patients or controls **(lanes: 3-12)**.

3.7. Immunoprecipitation of different SNARE proteins by the patient cohort

The patient cohort was tested in IP-WB analysis for the pull-down of the SNARE proteins such as EXOC4, SNAP25, STXBP1, synaptophysin 1, and VAMP2, in addition to the already detected possible AAb targets DNM1, NSF1, and STX1B. Immunoprecipitation was performed including monoclonal antibodies against GAD65/67 (PC1) and GRM1 (PC2) in addition to three anti-GAD65 and -GAD67 positive patients' sera and three sera from healthy controls. The immunoprecipitated proteins along with 8 µg total protein from cerebellum tissue lysate (size control) were transferred onto a membrane **(Figure 16)**. The membrane was cut at the dotted lines at the regions 115-80 kDa, 80-65 kDa, 65-50 kDa, 50-35 kDa, 35-30 kDa, 30-25 kDa, 25-15 kDa and incubated with antibodies against EXOC4, NSF, STXBP1, synaptophysin 1, STX1B, SNAP25, and VAMP2, respectively depending on the position of their respective targets (Table 10). Antibodies against DNM1 and GAD65/67 were avoided since these antigens were present in similar molecular weight regions as EXOC4 and STXBP1, respectively. Reactivity against the SNARE proteins namely EXOC4, NSF, STXBP1, synaptophysin 1, STX1B, SNAP25, and VAMP2 was detected in the tissue lysate at positions ≈ 122 kDa, ≈ 82 kDa, ≈ 66 kDa, ≈ 38 kDa, ≈ 33 kDa, ≈ 25 kDa, and ≈ 12 kDa, respectively (Figure 16, Lys). A strong pull-down of various SNARE proteins was observed with the anti-GRM1 antibody, but not with the anti-GAD65/67 antibody (Figure 16, lane 4 versus lane 3). Furthermore, all three patients' sera portrayed mild to strong reactivities against STXBP1 and SNAP25 in addition to NSF and STX1B, indicating the pull-down of these proteins by the patients' sera. There was no precipitation of EXOC4, synaptophysin 1, and VAMP2 (Figure 16, lanes: 5-7) or synaptotagmin 1 and Rab 3A (data not shown) by the patients' sera. Furthermore, no control sera immunoprecipitated any of the above-mentioned proteins. The results for the pull-down of different SNARE proteins by the entire cohort are depicted in **Table 21**.

These results suggest that the anti-GRM1 antibody in addition to the patients' sera immunoprecipitated different SNARE proteins, probably in the form of a complex. In addition to the immunoprecipitation of NSF and STX1B, pull-down of other SNARE proteins such as SNAP25 and STXBP1 was strongly observed with the patients' sera. There is a possibility that patients' sera possess multiple AAbs targeting the GAD antigens as well as different SNARE proteins and therefore, it was important to determine the direct targets of patient AAbs in the subsequent experiments.

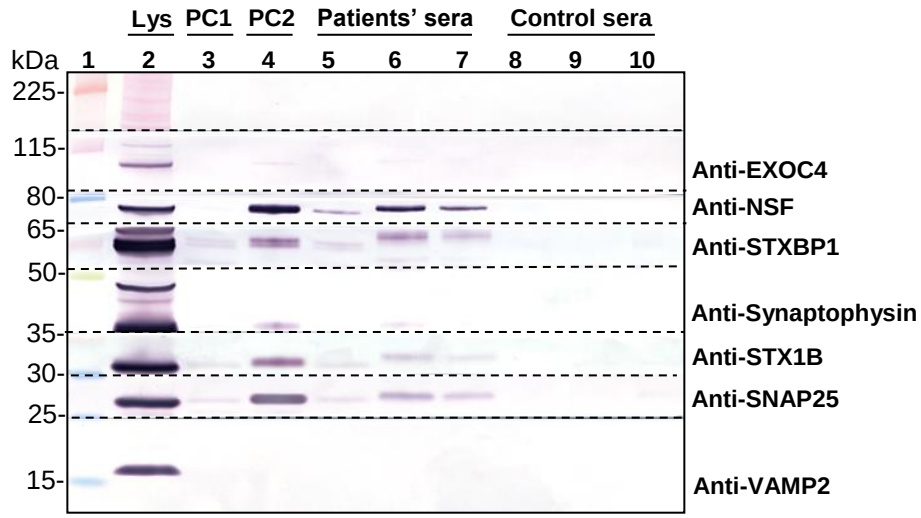

Figure 16: Patients' sera immunoprecipitated STXBP1 and SNAP25 in addition to NSF and STX1B

Total lysate immunoprecipitation was performed using sera from patients versus controls in addition to monoclonal antibodies against GAD65/67 **(PC1)** and GRM1 **(PC2)**. The membrane was cut sequentially at the dotted lines and incubated with antibodies against EXOC4, NSF, STXBP1, synaptophysin 1, STX1B, SNAP25, and VAMP2 depending on the position of target antigens at ≈ 122 kDa, ≈ 82 kDa, ≈ 66 kDa, ≈ 38 kDa, ≈ 33 kDa, ≈ 25 kDa, and ≈ 12 kDa, respectively. Reactivity against all SNARE proteins was detected in the lysate **(Lys, lane 2)**. Additionally, pull-down of various SNARE proteins was stronger with the anti-GRM1 antibody **(lane 4)** compared with the anti-GAD65/67 antibody **(lane 3)**. All patients' sera demonstrated mild to strong reactivity against STXBP1 and SNAP25 in addition to NSF and STX1B **(lanes: 5-7)**. No reactivity against the SNARE proteins was detected in the controls **(lanes: 8-10)**.

3.8. Recombinant expression of the SNARE proteins in HEK293 cells

The majority of the patients' sera immunoprecipitated proteins associated with vesicular trafficking such as NSF, SNAP25, STXBP1, and STX1B in addition to DNM1. However, DNM1 is not classified as a SNARE protein and hence, was not included as a substrate in the preparation of the SNARE BIOCHIP Mosaics™ (Figure 4B). The recombinant expression of various SNARE proteins was performed as mentioned in section 2.2.7. SNARE proteins including WT NSF, NSF (K266A), NSF (E329Q), SNAP25, STX1B, STXBP1, and VAMP2 were cloned and expressed in HEK296 cells. The mutant versions of NSF (K266A and E329Q) affected only the function of the enzyme, but not its structure (Whiteheart and Matveeva, 2004). Furthermore, to identify possible AAbs targeting the SNARE complex, the cognate SNARE proteins namely SNAP25, STX1B, and VAMP2 were co-transfected in HEK293 cells. Additionally, His-tagged HEK293-NSF[human] (13 mg/ml) and STX1B(ic) (0.93 mg/ml) expressed in *E. coli* were prepared to be used in other downstream experiments such as immunoblotting tests.

3.8.1. Evaluation of the expression of recombinant SNARE proteins using respective anti-SNARE antibodies

A preliminary IFA was performed to determine the reactivity of commercial anti-SNARE antibodies against the prepared recombinant SNARE substrates. An IFA was conducted using selected antibodies directed against NSF, SNAP25, STX1B, STXBP1, and VAMP2 (Table 1). The reactivity against respective SNARE antigens was verified in the individual substrates as well as in the co-expressed substrates. A representative incubation of the antibodies diluted 1:10 in PBS/Tween is depicted in **Figure 17**. A strong reactivity against all individual substrates as well as the co-expressed substrates was observed with the antibodies directed against STX1B and SNAP25, but not VAMP2, wherein only a weak reactivity was detected. This could probably be due to reduced expression of the protein by the HEK293 cells or that it requires additional modifications to be stably expressed. Antibody directed against NSF portrayed a strong reactivity against the WT NSF as well as in one of the mutant substrates, NSF (K266A). However, the expression of the second mutant substrate, NSF (E329Q), was not optimal and hence was not included in the in the final preparation of the BIOCHIP mosaics™ (data not shown). Additionally, no reactivity was observed with the mock-transfected substrates with any antibody, confirming the specificity of the reactivity of the antibodies against respective SNARE antigens.

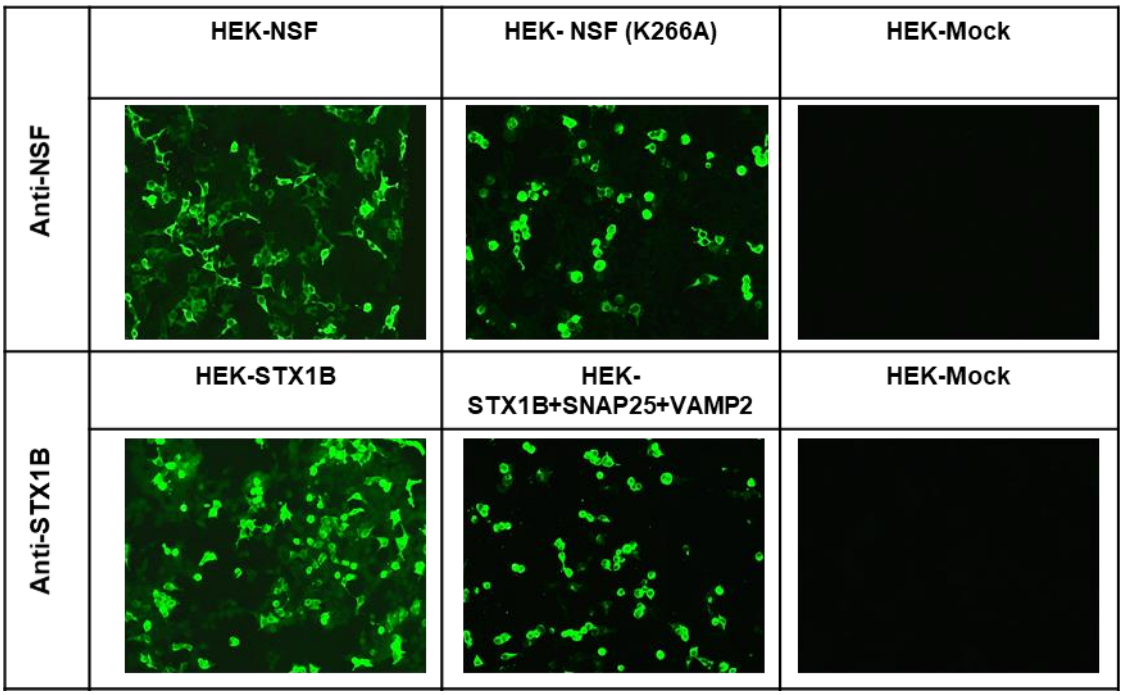

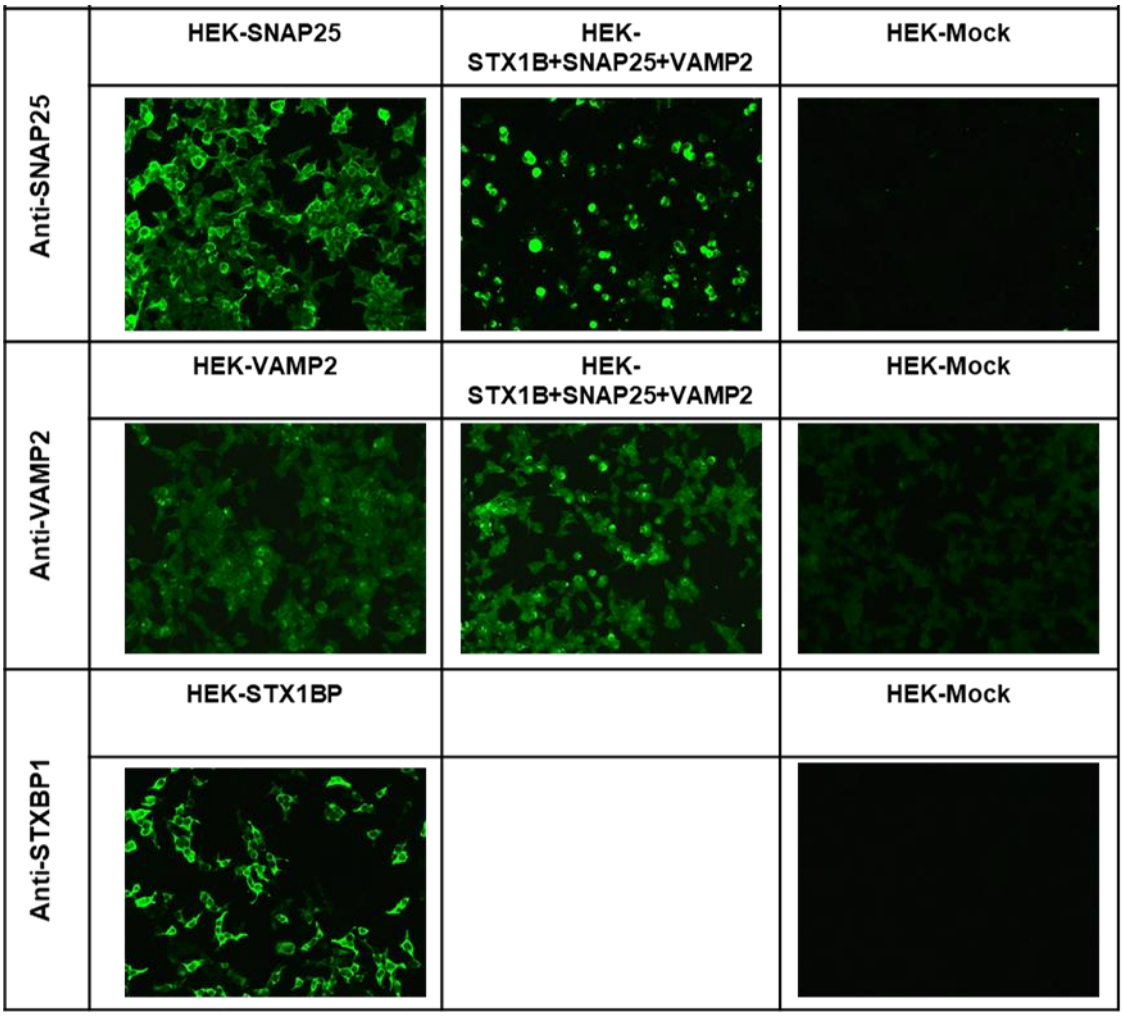

Figure 17: Reactivity of various anti-SNARE antibodies against the prepared recombinant SNARE substrates
IFA was performed using antibodies against SNARE proteins such as anti-NSF, anti-STX1B, anti-SNAP25, anti-VAMP2, and anti-STXBP1 all diluted 1:10 in PBS/Tween and incubated against the recombinant substrates. The slides were examined under EUROStar II florescence microscope and pictures were captured using the Europicture software. Strong reactivity was observed with all the antibodies against their respective substrates. However, only a weak reactivity was detected in the HEK-VAMP2. (Magnification: 200x)

3.9. IFA with the patient cohort using the SNARE BIOCHIP mosaics™

To precisely identify AAbs against individual SNARE proteins in the patient cohort, an IFA was performed using the SNARE BIOCHIP Mosaics™ (Figure 4B). Sera from patients (n = 100) versus controls (n = 50) were screened on the SNARE slides for the detection of AAbs against specific SNARE proteins. During screening of the cohort, if a serum was negative in the SNAP25 and VAMP2 substrate, but demonstrated even weak reactivity in the STX1B + SNAP25 + VAMP2 substrate **(Figure 18, 2B)**, then these sera were additionally screened in

another syntaxin-specific BIOCHIP mosaics™ (Euroimmun AG, Germany) prepared previously for another study. This mosaic included HEK293 cells expressing STX1A, STX1B and mock antigen. Following screening of the patient cohort in the SNARE slide, the number of patients' sera positive for AAbs against NSF, STXBP1, and VAMP2 were two, one, and one, respectively. On additionally screening the selected patient' sera on the syntaxin BIOCHIP mosaics™, three patients' sera were positive for AAbs against STX1A and STX1B, six patients' sera were positive for AAbs against STX1B and one patient serum was immunoreactive against STX1A alone. No reactivity was observed in the mock transfectants. Furthermore, AAbs against NSF, but not against any other SNARE proteins, were detected in the sera from two healthy controls **(Table 17)**. Representative images for patients' sera positive for AAbs against NSF and STX1B are depicted in **Figure 18.**

Table 17: Screening of sera from patients versus controls on the SNARE and syntaxin BIOCHIP mosaics™

	IFA: To screen for AAbs against the SNARE proteins					
Subjects Tested	**NSF**	**STX1A/B**	**STX1B**	**STX1A**	**VAMP2**	**STXBP1**
Patients' sera (n=100)	2 (2%)	3 (3%)	6 (6%)	1(1%)	1 (1%)	1 (1%)
Healthy sera (n=50)	2 (4%)	0	0	0	0	0

Although only few patients' sera portrayed an immunoreactivity against the SNARE proteins, these results were in agreement with the results observed with the GAD65ko BIOCHIP mosaics™, wherein patients' sera did not reveal any new AAb pattern that matched with SNARE antibody patterns (Figure 5A and Figure 13). However, results the from total lysate immunoprecipitation experiments revealed that patients' sera immunoprecipitated various SNARE proteins, particularly NSF, from the cerebellum lysate (Figure 8). Therefore, as the subsequent step, it was important to verify if patient AAbs could access their target antigens better in the lysates of the recombinant proteins under conditions similar to the immunoprecipitation analysis conducted with the pig cerebellum tissue (section 3.3).

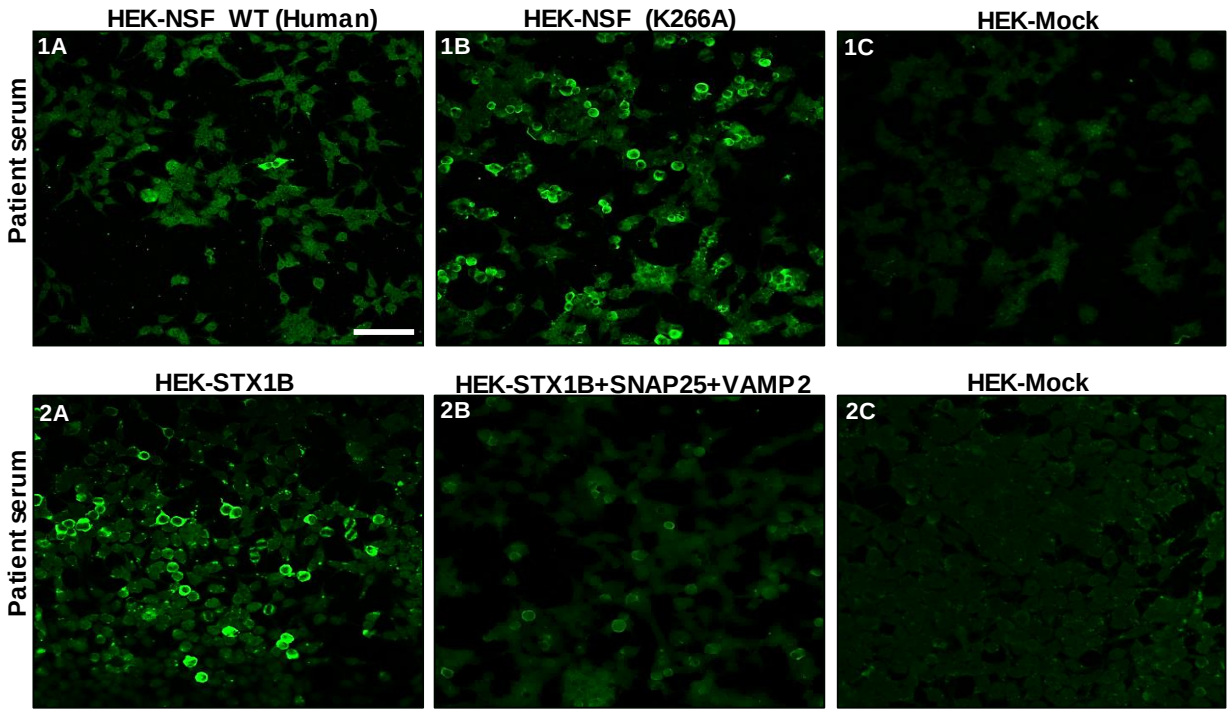

Figure 18: Images representing serum samples positive for AAbs against NSF and STX1B

Sera from patients versus controls (1:10) were incubated on the SNARE BIOCHIP mosaics™ to identify AAbs against different SNARE proteins. The slides were examined under the LSM 700 confocal microscope and the images were captured using the ZEN software. In total, two patients' sera were positive for AAbs against NSF **(1A-B)** and one against STXBP1. Additionally, one patient serum showed a weak immunoreactivity against VAMP2 (data not shown). Some sera portrayed a weak reactivity in the HEK293 cells co-expressed with STX1B + SNAP25 + VAMP2 **(2B)**, but were negative against SNAP25 and VAMP2. These sera were subsequently screened in another syntaxin-specific BIOCHIP mosaics™ prepared previously. Using this slide, three patients' sera were positive for AAbs against STX1A and STX1B, six patients' sera against STX1B **(2A),** and one patient serum against STX1A. No reactivity was observed in the mock transfectants **(1C and 2C)**. (Magnification: 200X and scale bar: 100 µm).

3.10. Immunoprecipitation of NSF from the HEK293-NSF[human] lysate by the patients' sera

Lysates of HEK293 cells expressing WT NSF were prepared as mentioned in section 2.2.7.1. In IFA, most patients' sera were not immunoreactive against HEK293 cells expressing NSF. However, 29 patients' sera had immunoprecipitated NSF from the cerebellum tissue in the immunoprecipitation tests (Figure 9). Therefore, to ensure accessibility of all target epitopes to patient AAbs, an immunoprecipitation analysis was performed using the HEK293-NSF lysate to verify if patients' sera could pull-down NSF as observed in with the cerebellum tissue. The analysis was performed with the monoclonal human anti-GRM1-IgG antibody (PC2) as well as

with six patients' sera that immunoprecipitated NSF and three sera from healthy controls **(Figure 19)**. The immunoprecipitated proteins in addition to 10 µl of the prepared lysate (HEK-NSF) were transferred onto a membrane and incubated with the anti-NSF antibody (Table 10) to verify the pull-down of NSF at ≈ 82 kDa. A strong reactivity against NSF was observed in the lysate and with the anti-GRM1 antibody (Figure 19, lanes: 2 and 3), indicating that the human anti-GRM1-IgG antibody immunoprecipitated NSF from the HEK293-NSF lysate, similar to the cerebellum tissue (Figure 14). Additionally, a weak reactivity against NSF was observed in the majority of the patients' sera, indicating the pull-down of NSF by these sera (Figure 19: lanes 4, 5, 7, 8, and 9). However, patients' sera probably have very low AAb titers against NSF, causing only detection of a weak signal. No reactivity against NSF was detected in the control sera lanes. Additionally, the blot was incubated with the anti-DNM1 antibody as a control. No reactivity against DNM1 was detected in any sample, suggesting there was no endogenous expression of DNM1 in the HEK293 cells, and that the reactivity against NSF was specific.

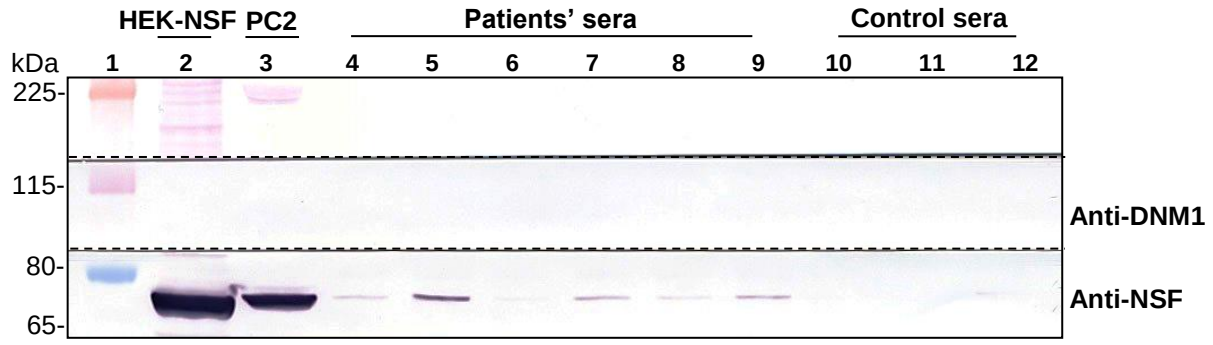

Figure 19: Patients' sera immunoprecipitated NSF from HEK293-NSF[human] lysate, but in reduced amounts

A total lysate immunoprecipitation was performed using HEK293-NSF lysate plus monoclonal human anti-GRM1-IgG antibody **(PC2)**, sera from six patients that immunoprecipitated NSF, and three sera from healthy controls. The immunoprecipitated proteins were transferred onto a nitrocellulose membrane, cut sequentially at the dotted lines, and immunoblotted with antibodies against NSF (1:650), and DNM1 (1:1000). Presence of NSF was detected at ≈ 82 kDa in the HEK-NSF **(lane 2)**. Additionally, a strong reactivity against NSF was observed with the anti-GRM1 antibody **(PC2, lane 3)**, suggesting that the antibody immunoprecipitated NSF, comparable to the results observed with the cerebellum. Furthermore, five patients' sera revealed a weak reactivity against NSF **(lanes: 4, 5, 7, 8, and 9)**. None of the control sera immunoprecipitated NSF **(lanes: 10-12)** and a reactivity against DNM1 was not detected in any lane.

3.11. IMAC enrichment of SNARE proteins using a mouse anti-GRM1-IgG antibody

Immunoprecipitation tests revealed that patients' sera bound weakly to the recombinant NSF and therefore, it was analyzed whether the patients' sera were better immunoreactive against NSF from the cerebellar tissue. An IMAC protocol was performed using the mouse anti-GRM1-IgG antibody to obtain enriched fractions of the SNARE proteins from the cerebellum. Subsequently, these fractions were immunoblotted with the patients' sera to determine their immunoreactivity against different SNARE proteins. The IMAC protocol was implemented using a His-tagged mouse anti-GRM1-IgG antibody (Table 3), instead of the human anti-GRM1 antibody, to prevent any interaction or cross reactivity with the human sera during immunoblotting. The experiment was performed as described in section 2.2.8. The first elution **(Elution 1)** ensured maximum elution of the bound SNARE proteins alone, with minimal elution of the bound anti-GRM1 antibody. A second elution was conducted to elute all bound proteins **(Elution 2)**. Both the eluates as well as 8 µg of total protein from pig cerebellum lysate were transferred onto a nitrocellulose membrane and stained with Ponceau S to verify the transfer of proteins onto the membrane **(Figure 20A)**. The amount of antibody eluted in Elution 1 (E1) was lower compared with Elution 2 (E2), indicating that eluate E1 would have lower interference due to the immunoglobulin heavy and light chain bands at ≈ 50 and ≈ 23 kDa, respectively, during immunoblotting experiments (Figure 20A, arrows). The membrane was then cut depending on the position of the antigens under investigation at regions 225-115 kDa, 115-80 kDa, 80-65 kDa, 35-30 kDa, 30-25 kDa, 25-15 kDa. Subsequently, the individual membranes were incubated with antibodies directed against GRM1, DNM1, NSF, STX1B, SNAP25, and VAMP2 to detect their target antigens at positions ≈ 133 kDa, ≈ 97 kDa, ≈ 82 kDa, ≈ 33 kDa, ≈ 22 kDa, ≈ 12 kDa, respectively. The presence of all SNARE proteins in question was observed in the lysate **(Figure 20B, Lys)**. An enriched pull-down of the proteins, primarily NSF and DNM1, was observed with E1 in comparison with E2. Additionally, SNARE proteins such as STX1B and SNAP25, but not VAMP2, was observed in E1 alone. The presence of GRM1 antigen was detected in all sample lanes. Furthermore, the eluate E1 was stained with blue silver stain, to verify the identity of proteins by MS analysis **(Figure 20C)**. In E1, the concentration of NSF and DNM1 were higher compared with other proteins and only these two proteins could be verified by MS (Figure 20C, bands: 2 and 3). All other bands identified by MS analysis are listed in **Table 18**.

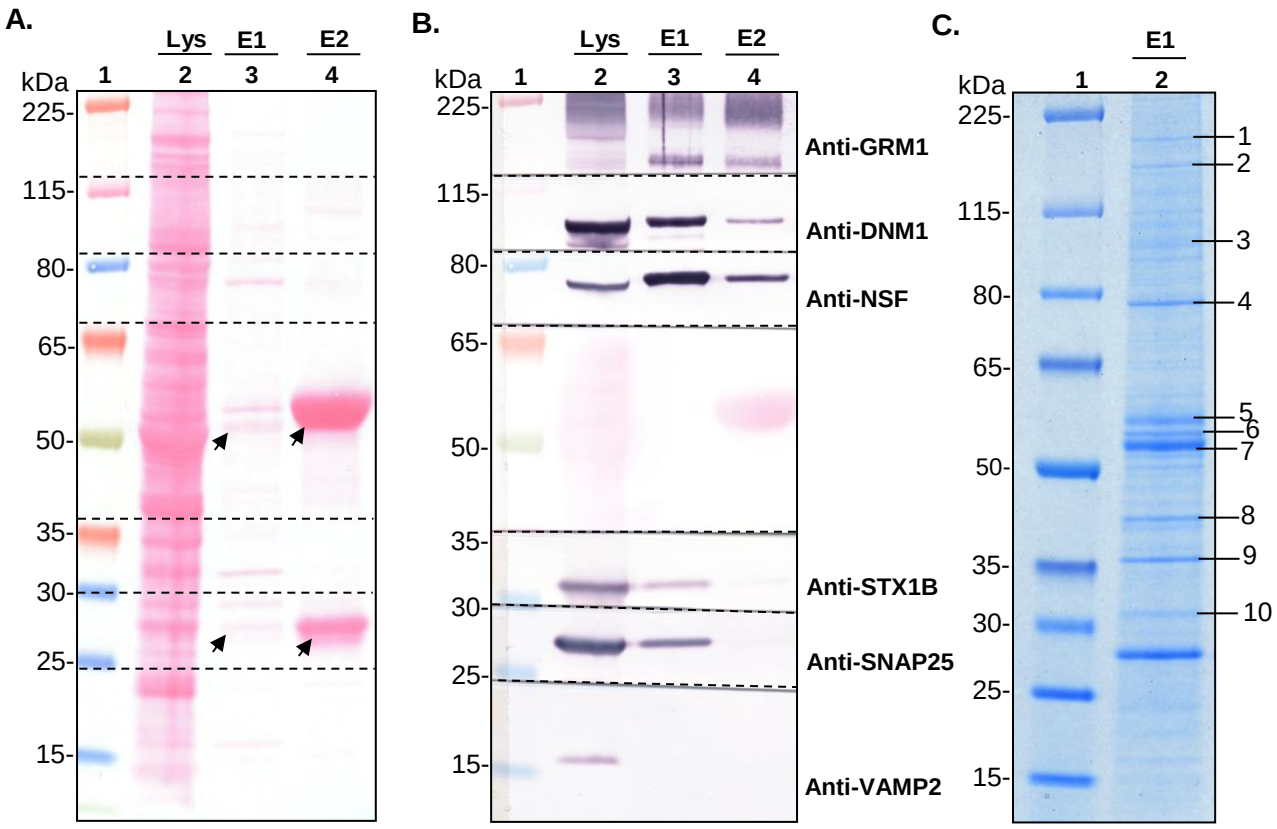

Figure 20: Enrichment of SNARE proteins using His-tagged mouse anti-GRM1-IgG antibody by IMAC

Dynabeads® coated with Co^{2+} incorporating the IMAC chemistry were incubated with a his-tagged mouse anti-GRM1 antibody. The binding was stabilized by oxidizing the cobalt from Co^{2+} →Co^{3+} using 0.03% hydrogen peroxide. Subsequently, the antibody-loaded beads were incubated overnight with the pig cerebellum lysate to allow formation of immune complexes. The following day, only the bound antigens were eluted with protein G elution buffer at room temperature **(E1)**. The beads were then re-incubated with protein G elution buffer and heated at 70°C to elute all the remaining bound proteins **(E2)**. **(A)** The eluates E1 and E2 in addition to 8 µg total protein from cerebellum tissue lysate were transferred onto a nitrocellulose membrane and stained with Ponceau S to detect the protein transfer. The blot portrayed minimal antibody elution in E1 compared with E2 **(lane 3 versus lane 4, arrows),** and therefore would have a reduced interference due to the antibody bands at ≈ 50 and ≈ 23 kDa regions. **(B)** The membrane was subsequently cut at the dotted lines and incubated with various anti-SNARE antibodies. Reactivity against GRM1 (≈ 132 kDa), DNM1 (≈ 97 kDa), NSF (≈ 82 kDa), STX1B (≈ 33 kDa), SNAP25 (≈ 25 kDa), and VAMP2 (≈ 12 kDa) were observed in the lysate **(lane 2, Lys)**. An enriched pull-down of the proteins, particularly NSF and DNM1, were observed with E1 compared with E2 **(lane 3 versus lane 4)**. Reactivity against STX1B and SNAP25, but not VAMP2 was observed with E1 alone and a reactivity against GRM1 was observed in all lanes. **(C)** Proteins eluted in E1 were stained with blue silver stain and the observed bands were marked **(1-10)** and verified by MS. Only, NSF and DNM1 were identified by MS analysis **(bands: 2 and 3)**.

Altogether, the IMAC experiment with a mouse anti-GRM1 antibody enriched the pull-down of majority of SNARE proteins such as NSF, STX1B, SNAP25 in addition to DNM1. The first elution had minimal interference from the antibody heavy and light chains (≈ 50 and ≈ 23 kDa) in addition to no interference from the GAD antigens (≈ 65/67 KDa). Therefore, reactivity against additional underlying antigens with similar molecular weights could be clearly identified during immunoblotting tests with the patient cohort. MS analysis identified only NSF and DNM1 proteins since they were enriched in higher concentrations compared with other SNARE proteins. The additional proteins bands detected in MS were frequently identified during pull-down assays and hence, were not considered vital in immunoprecipitation tests. Patients' sera never immunoprecipitated VAMP2 and therefore, failure to detect VAMP2 in this experiment was not a major setback.

Table 18: List of antigens identified by MS in E1 following IMAC

Band	Name	Score/ cut-off	Mass (Da)	Database
1	Clathrin heavy chain 1 isoform 1 [Homo sapiens]	143/78	193260	NCBInr_sub_Mammalia
2	PREDICTED: ATP-dependent RNA helicase A [Sus scrofa]	126/78	142595	NCBInr_sub_Mammalia
3	**PREDICTED: dynamin-1 isoform X5 [Sus scrofa]**	**64/78**	**97730**	**NCBInr_sub_Mammalia**
4	**vesicle-fusing ATPase [Sus scrofa] or N-ethylmaleimide sensitive factor**	**261/78**	**84007**	**NCBInr_sub_Mammalia**
5	Immunoglobulin gamma 2A chain, partial [Mus musculus domesticus]	86/78	36865	NCBInr_sub_Mammalia
6	Tubulin alpha-1C chain [Myotis brandtii]	99/78	52877	NCBInr_sub_Mammalia
	PREDICTED: ATP synthase subunit alpha, mitochondrial [Panthera tigris altaica]	90/78	60258	NCBInr_sub_Mammalia
	PREDICTED: vimentin isoform X1 [Sus scrofa]	92/78	53692	NCBInr_sub_Mammalia
	Tubulin beta-2B chain [Myotis brandtii]	91/78	50174	NCBInr_sub_Mammalia
7	PREDICTED: tubulin beta-2A chain isoform X2 [Mandrillus leucophaeus]	158/78	47565	NCBInr_sub_Mammalia
	PREDICTED: tubulin alpha-1 chain isoform X3 [Colobus angolensis palliatus]	122/78	48122	NCBInr_sub_Mammalia
	PREDICTED: ATP synthase subunit beta, mitochondrial [Sus scrofa]	82/78	56300	NCBInr_sub_Mammalia
8	ACTB protein, partial [Homo sapiens]	38/51	40536	NCBInr_sub_Mammalia
9	glyceraldehyde-3-phosphate dehydrogenase [Sus scrofa]	23/49	36041	NCBInr_sub_Mammalia
10	PREDICTED: LOW QUALITY PROTEIN: zinc finger protein 879 [Miniopterus natalensis]	88/78	107752	NCBInr_sub_Mammalia
	ADP/ATP translocase 3 [Sus scrofa]	57/78	33117	NCBInr_sub_Mammalia

3.12. Detection of AAbs against cerebellar enriched NSF and DNM1 by immunoblotting with the patients' sera

Enriched fractions of the SNARE proteins were transferred onto a membrane and incubated with an antibody mixture consisting of anti-DNM1, anti-NSF, and anti-STX1B as well as with an internal anti-GAD65 and -GAD67 positive reference patient serum (Euroimmun AG, Germany) as positive control that was borderline positive for AAbs against NSF and STX1B in the SNARE slide (data not shown) in addition to sera from patients versus neurological and healthy controls. The antibody mixture was considered as the loading control to ensure similar distribution of respective antigens across different incubations **(Figure 21, arrows)**.

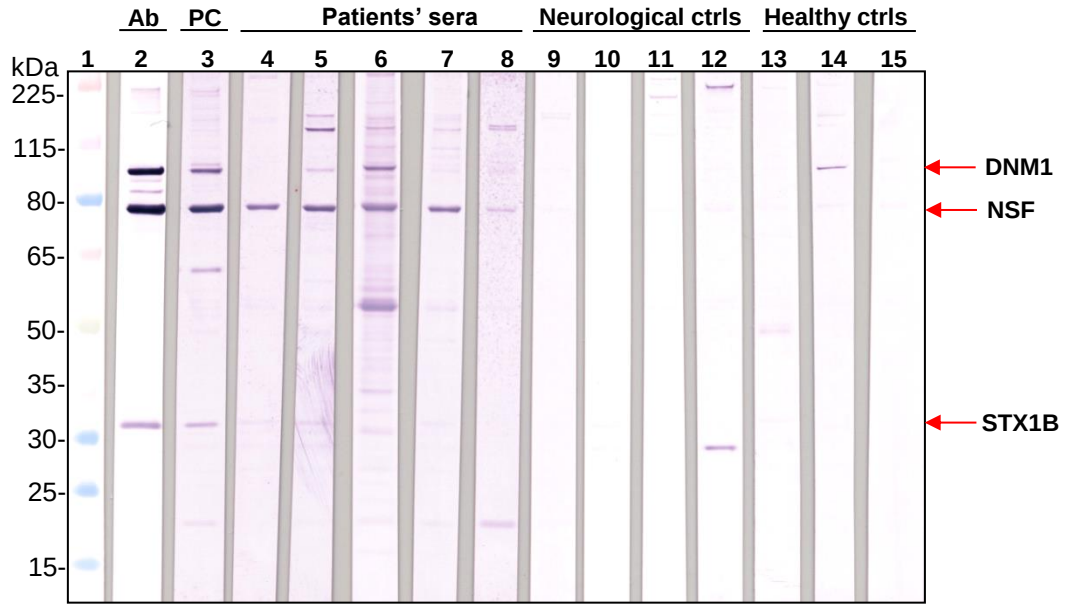

Figure 21: Patients' sera exhibited reactivity against NSF and DNM1 enriched from the cerebellum

The IMAC enriched SNARE protein fractions were separated by gel electrophoresis and transferred onto a nitrocellulose membrane. The membrane was cut vertically into strips and incubated with an antibody mixture containing anti-DNM1 (1:1000), anti-NSF (1:1000), and anti-STX1B (1:2000) **(Ab, lane 2)**, an internal reference patient serum (1:350) from Euroimmun AG that was positive for AAbs against GAD, NSF, and STX1B as the positive control **(PC, lane 3)**, and a panel of sera (1:350) from the patients **(lanes: 4-8)** versus neurological **(lanes: 9-12)** and healthy **(lanes: 13-15)** controls. The internal reference serum was immunoreactive against NSF and STX1B in the cell-based assays (data not shown). Reactivities against DNM1 (≈ 97 kDa), NSF (≈ 82 kDa), and STX1B (≈ 33 kDa) were observed with the antibody and the reference serum **(lanes: 2 and 3, red arrows)**. Furthermore, all patients' sera portrayed a reactivity against NSF and to a minor extent against DNM1 **(lanes: 4-8)**. No neurological controls **(lanes: 9-12)** or healthy controls, except one **(lane 14)**, portrayed any reactivity against NSF or DNM1. Reactivity against STX1B could not be determined in this experiment. (Abbreviations ctrls: controls)

Reactivities against DNM1 (≈ 97 kDa), NSF (≈ 82 kDa), and STX1B (≈ 33 kDa) were observed in the antibody lane (Figure 21, Ab) and in the positive control (Figure 21, PC). Furthermore, all patients' sera demonstrated a strong reactivity against NSF and some sera were also reactive against DNM1 (Figure 21, lanes: 4-8). For comparison, four neurological controls consisting of patients' sera positive for AAbs directed against CASPR2, Hu, Ri, and LGI1 were included. The neurological controls did not exhibit any reactivity against NSF or DNM1 (Figure 21, lanes: 9-12). However, one serum from the healthy control revealed a weak reactivity against DNM1 (Figure 21, lane: 14). A specific reactivity against STX1B could not be determined in this experiment and hence, AAbs against STX1B were analyzed in a separate WB analysis since 10% of the patient cohort were immunoreactive against the syntaxins in IFA (Table 17). No patients' sera portrayed any reactivity against SNAP25 in IFA or immunoblotting tests and therefore, this protein was not included in further analysis.

In short, this experiment revealed that the patients' sera were primarily immunoreactive against NSF, followed by DNM1. In the immunoprecipitation tests, both NSF and DNM1 were pulled down by the patients' sera and it could be possible that these proteins were co-immunoprecipitated. However, the above test revealed that NSF and DNM1 were individually targeted by patients' AAbs. Subsequently, their prevalence was determined for the entire patient cohort **(Table 21)**.

The intensities of the bands detected on the immunoblots were quantified using the Image J software, version 1.51n (https://imagej.nih.gov/ij/download.html accessed May 2017). The internal reference serum (Euroimmun AG, Germany), which was borderline positive for AAbs against GAD, NSF, and STX1B in cell-based assays, was used to normalize the intensities of all samples included in this study. In the Image J software, a rectangular region of interest (ROI) with consistent size was set for the reference serum and used as the standard ROI for the quantification of all band intensities. The ROI was moved over each band to measure each band's average pixel intensity. Similarly, the background adjacent to the bands was quantified using the ROI and subtracted from the respective band intensities to obtain the average intensity of each band above the background signal. Subsequently, the relative intensity of each band was expressed as a percentage of the average intensity of the reference serum using the formula:

$$Realtive\ intensity\ of\ band\ (\%) = \frac{Average\ intesnity\ of\ sample\ band}{Average\ intensity\ of\ reference\ band} \cdot 100$$

The reference serum was assigned a relative intensity of 100 and the remaining sample band intensities were normalized to that of the reference serum. The relative intensities of different groups were compared by implementing Kruskal-Wallis test followed by Dunn's multiple comparisons using Graph Pad prism 5 software (Graph Pad, USA). The graphs report mean ± SD of each group and a cut-off of 3SD above the mean of the healthy controls was implemented to determine the number of positive patients having relative intensities above the cut-off of 20% for NSF and 15% for DNM1 for screening purposes alone (Figure 22, dashed blue line). The relative intensity of the reference serum was indicated as the red dot in the graphs. For AAbs against NSF, 30 patients in the patient cohort, two patients in the neurological control, and one subject in the healthy control exhibited relative intensity values above the 20% cut-off **(Figure 22A)**. With respect to AAbs against DNM1, the relative intensity values of 23 patients in the patient cohort, zero in the neurological control, and one subject in the healthy control were above the 15% cut-off **(Figure 22B)**. One patient serum exhibited a higher relative intensity value above that of the reference serum for reactivity against DNM1 (patient number: 49, Table 20). Additionally, the AAbs against DNM1, unlike amphiphysin, were not restricted to paraneoplastic patients and were distributed across the patient cohort with and without underlying cancers. Of the seven patients positive for anti-amphiphysin AAbs, three patients were positive for AAbs against DNM1, indicating that these AAbs were observed independently of anti-amphiphysin AAbs. This is comparable to the immunoprecipitation results, wherein DNM1 was not co-immunoprecipitated with amphiphysin in the patient cohort. Therefore, patients' sera might have AAbs targeting individual synaptic proteins such as NSF and DNM1.

Amongst the patients' sera positive for AAbs against NSF and DNM1, the number of patients' sera positive for anti-GAD AAbs was 21 and 15, respectively. Remarkably, nine and eight patients' sera that were negative for anti-GAD AAbs were positive for AAbs against NSF and DNM1, respectively. Altogether, patients' positive for anti-GAD AAbs might have a higher prevalence for AAbs against NSF and DNM1 compared those negative for anti-GAD AAbs, whose values were lower but not negative **(Table 19)**. With respect to individual disorders, the prevalence of AAbs against NSF and DNM1 was higher in patients with SPS, PERM, and cerebellitis compared with other associated movement disorders (Table 19).

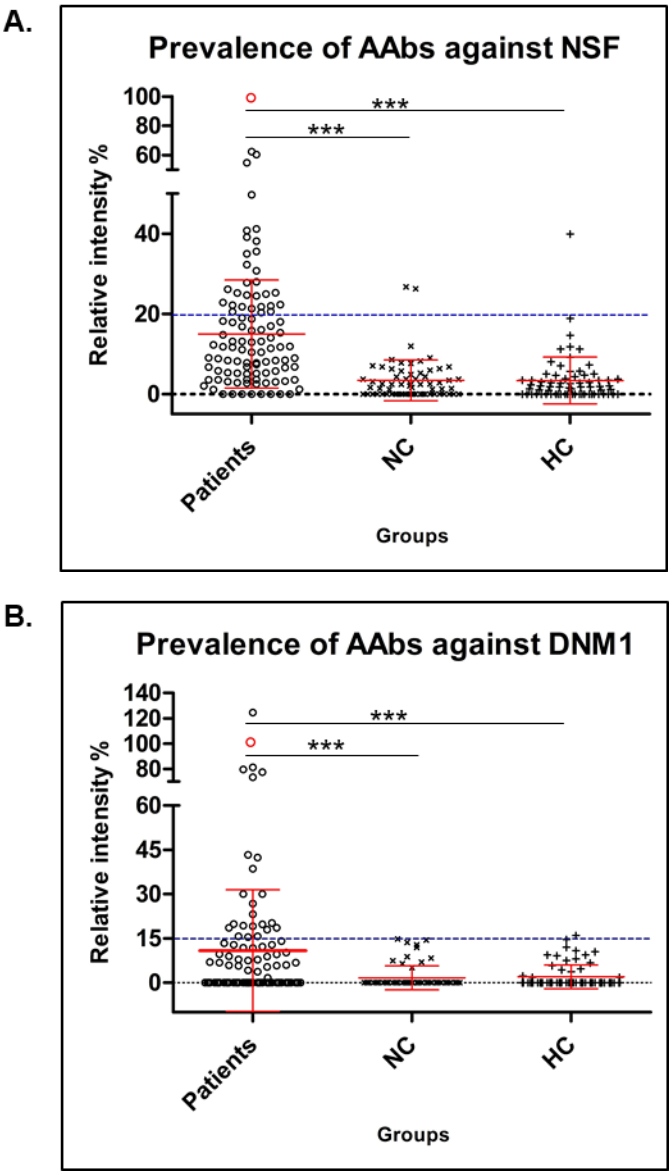

Figure 22: The patient cohort portrayed a significantly higher prevalence of AAbs against NSF and DNM1 compared with the controls

Enriched fractions of NSF and DNM1 were resolved in gels and immunoblotted with patient's sera (n = 100) versus neurological (n = 65) and healthy (n = 70) controls. The relative intensity of each band was normalized against that of a reference serum and was expressed as a percentage of the obtained relative intensity. The values were compared by implementing Kruskal-Wallis test followed by Dunn's multiple comparisons using the Graph Pad prism 5 software. The reference serum **(red dot)** was assigned a value of 100 and a cutoff of 3SD above the mean of healthy controls was calculated **(dashed blue line)** for screening purposes alone. **A and B)** In total, 30 and 23 patients' sera in the patient cohort, 2 and 0 patients' sera in the neurological control (NC), and 1 subject each in the healthy control (HC), exhibited relative intensity values above the cutoff for NSF (20%) and DNM1 (15%), respectively. Therefore, the prevalence of AAbs against NSF and DNM1 were significantly higher in the patient cohort compared with the control groups (***p<0.0001). Graphs represent mean ± SD of each group.

Table 19: Representation of number of patients' sera positive for AAbs against NSF and DNM1 in the entire cohort

	Anti-GAD+		Anti-GAD-	
	Anti-NSF+	**Anti-DNM1+**	**Anti-NSF+**	**Anti-DNM1+**
SPS/SLS (n=54)	14/33	8/33	5/21	3/21
PERM (n=24)	6/18	5/18	1/6	0/6
Hyperekplexia (n=6) (NA: Not applicable)	NA	NA	0/6	1/6
Cerebellitis (n=2)	1/2	2/2	NA	NA
Dystonia (n=5)	NA	NA	2/5	3/5
Anxiety and other associated disorders (n=9)	NA	NA	1/9	1/9
Total	21	15	9	8

3.13. Prevalence of AAbs against NSF using HEK293-NSF[human] in immunoblotting analysis

As a subsequent step, it was important to verify whether patients' AAbs bound to NSF irrespective of its origin in the immunoblotting experiments since patients' sera immunoprecipitated NSF from the cerebellum (Figure 8) as well as from the HEK293-NSF lysates (Figure 19). Approximately 5 µg of IMAC purified NSF from the HEK293-NSF (13 mg/ml) was transferred onto a nitrocellulose membrane **(Figure 23A)**. Subsequently, the membrane was incubated with an antibody against NSF, the internal reference patient serum (PC) that was used in section 3.12 as well as sera from patients (n = 100) versus neurological (n = 65) and healthy controls (n = 70). In addition to the anti-NSF antibody and the reference serum, sera from patients were also immunoreactive against NSF at ≈ 82 kDa **(Figure 23B, arrow)**. Additionally, weak reactivities were observed in some neurological and healthy controls. The relative intensities of all bands were normalized with respect to that of the reference serum and a cut-off of 3SD above the mean of the healthy control was established for screening, comparable to the previous test method (section 3.12). The relative intensities of 29 patients' sera versus one serum each from the control cohort were above the 20% arbitrary cut-off,

revealing that the prevalence of AAbs against NSF was significantly ($p<0.0001$) higher in the patient cohort compared with the controls **(Figure 23C)**.

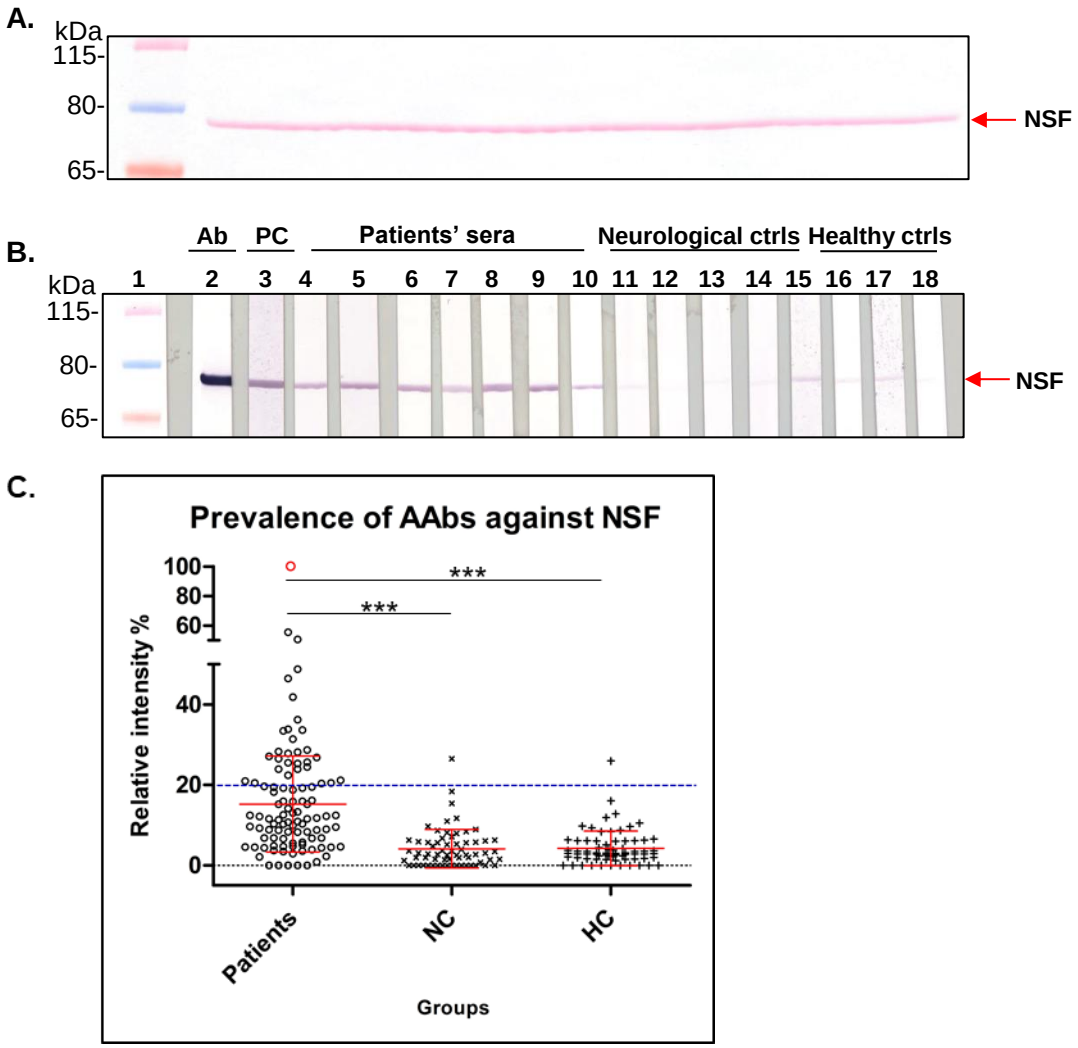

Figure 23: Patients' sera were immunoreactive against NSF purified from His-tagged HEK293-NSF

A) Approximately 5 µg of IMAC purified NSF from HEK293-NSF was transferred on a membrane and stained with Ponceau S to verify the protein transfer **B)** The membrane was cut into strips and incubated with an anti-NSF antibody **(Ab, 1:1000)**, an internal reference serum **(PC, 1:1000)** as well as sera from patients versus neurological and healthy controls (1:1000). In addition to the antibody **(lane 2)** and the reference serum **(lane 3)**, the majority of the patients' sera exhibited reactivities against NSF at ≈ 82 kDa **(lanes: 4-10, arrow)**. Reactivities against NSF in the neurological and healthy controls were negligible **(lanes: 11-18)**. **C)** The relative intensities of all bands were normalized with respect to that of the reference serum **(red dot)**. In total, 29 patients' sera, one serum in the neurological control (NC), and one serum in the healthy control (HC) portrayed a reactivity against NSF above the 20% arbitrary cut-off **(dashed blue line)**. Therefore, the prevalence of AAbs against NSF was significantly higher in the patient cohort compared with the neurological and heathy controls (***$p<0.0001$). Graphs represent mean ± SD of each group (Abbreviations ctrls: controls)

On comparing the reactivity against NSF from the cerebellum tissue, 19 patients' sera were positive in both test methods (Table 21). However, the remaining patients were positive only in either of the test systems. Additionally, the relative intensity values of the majority of patients' sera were slightly higher in the immunoblotting experiments with NSF enriched from the cerebellum tissue compared with the recombinant proteins **(Table 20)**.

In short, patients' sera portrayed a significantly ($p<0.0001$) higher prevalence of AAbs against NSF in both test methods. However, the serum samples were better immunoreactive against NSF from the brain tissue compared with the recombinant proteins.

Table 20: Representation of the percentage Relative Intensity (RI%) values for the prevalence of AAbs against NSF in cerebellum tissue and HEK293 cells and DNM1 in cerebellum tissue alone

(Please find attached table in the following page)

Results

Patient sera	Cerebellum NSF RI%	HEK293-NSF RI%	Cerebellum DNM1 RI%	Healthy controls	Cerebellum NSF RI%	HEK293-NSF RI%	Cerebellum DNM1 RI%	Neurological controls	Cerebellum NSF RI%	HEK293-NSF RI%	Cerebellum DNM1 RI%
PC	100	100	100	PC	100	100	100	PC	100	100	100
M1	14.04	0	11.82	BD1	0	11.88	0	Anti-CASPR2 (1)	11.94	18.4	0
M2	27.77	6.57	0	BD2	0	6.04	4.75	Anti-CASPR2 (2)	3.73	4.72	5.12
M3	0	4.34	79.47	BD3	11.18	6	5.83	Anti-CASPR2 (3)	0	1.97	0
M4	19.01	26.8	18.6	BD4	2.03	2.8	0	Anti-CASPR2 (4)	0	2.7	0
M5	0	10.3	7.8	BD5	0.92	3.49	0	Anti-CASPR2 (5)	7.65	2.7	0
M6	41.2	25.5	19.16	BD6	4.97	6.34	0	Anti-NMDAR (1)	5.22	5.13	0
M7	9	4.79	4.18	BD7	4.64	6.08	8.07	Anti-NMDAR (2)	6.27	6.3	0
M8	8.03	3.7	0	BD8	1.33	0	0	Anti-NMDAR (3)	1.18	5.61	0
M9	2.82	5.17	0	BD9	1.33	1.42	0	Anti-NMDAR (4)	0	1.92	0
M10	1.13	0.86	0	BD10	3.75	2.75	0	Anti-NMDAR (5)	0	0	0
M11	22.33	27.85	0	BD11	0	0	0	Anti-Lgl1 (1)	0	1.16	0
M12	3.19	4.74	0	BD12	0	0	0	Anti-Lgl1 (2)	1.63	1.88	0
M13	20.3	15.84	5.78	BD13	0	0	0	Anti-Lgl1 (3)	1.4	0	0
M14	1.19	4.46	0	BD14	1.57	0	0	Anti-Lgl1 (4)	1.25	1.36	0
M15	21.97	26.5	0	BD15	2.64	9.77	12.02	Anti-Lgl1 (5)	8.6	1.53	0
M16	3.59	4.63	73.53	BD16	0	0	0	Anti-Lgl1 (6)	2.82	3	0
M17	16.04	5.76	81.338	BD17	3.03	0	0	Anti-ARHGAP26 (1)	2.44	1.5	0
M18	25.26	20.5	15.73	BD18	11.81	9.29	9.11	Anti-ARHGAP26 (2)	0	0	0
M19	38.18	28.15	14.13	BD19	4.98	3.52	0	Anti-ARHGAP26 (3)	0	0	0
M20	39.14	23.95	9	BD20	2.67	5.06	0	Anti-ARHGAP26 (4)	2.03	0	0
M21	2	0	0	BD21	1	3.09	6.67	Anti-Hu (1)	2.4	0	6.98
M22	15.29	11.57	8.9	BD22	1.9	2.84	0	Anti-Hu (2)	26.27	6.27	0
M23	5.81	4.47	0	BD23	9.18	3.73	3.75	Anti-Hu (3)	4.27	2.84	0
M24	34.95	18.22	7.5	BD24	2.03	9.61	0	Anti-Hu (4)	2.48	3.04	0
M25	12.9	0	0	BD25	2.78	8.4	0	Anti-Hu (5)	0	5.3	0
M26	6.72	25.31	19.85	BD26	39.9	26	0	Anti-Hu (6)	0	1.48	0
M27	11.8	14.16	0	BD27	5.67	2.58	14.6	Anti-Hu (7)	3.73	8.65	0
M28	7.8	10.7	13.42	BD28	7.27	10.5	4.41	Anti-Ri (1)	1.63	5.66	0
M29	3.54	11.32	0	BD29	3.45	12.82	1.86	Anti-Ri (2)	6.77	3.54	14.44
M30	13.12	8.34	17.93	BD30	1.82	4.25	2.34	Anti-Ri (3)	4.85	15.4	13.64
M31	4.97	12.13	30.05	BD31	3.46	2.83	9.37	Anti-Ri (4)	26.71	26.49	8.8
M32	62.4	46.45	0	BD32	0	1.53	0	Anti-Ri (5)	7.07	2.48	0
M33	27.98	18.78	19.3	BD33	8.01	6.12	0	Anti-Ri (6)	6.32	6.73	0
M34	8.98	13.26	0	BD34	0	2.98	7.5	Anti-Yo (1)	0	3.96	0
M35	40.77	33.64	38.6	BD35	7.04	2.82	0	Anti-Yo (2)	6.77	9.73	12.87
M36	5.7	11.79	9.62	BD36	0	0	9.38	Anti-Yo (3)	5.91	5.58	6.4
M37	22.83	33.84	0	BD37	1.2	1.68	0	Anti-Yo (4)	3.4	2.56	0
M38	30.74	12.45	0	BD38	1.03	1.6	0	Anti-GLRA1 (1)	0	3.45	0
M39	14.8	9.9	0	BD39	1.76	1.91	0	Anti-GLRA1 (2)	2.41	6.05	0
M40	15.83	31.42	12.8	BD40	1.76	0	0	Anti-GABAR-A1 (1)	3.08	0	7.41
M41	11.09	15.22	6.79	BD41	3.49	3.4	0	Anti-GABAR-A1 (2)	5.73	8.37	8.33
M42	11.68	5.48	0	BD42	0	1.15	0	Anti-Titin (1)	0	0	0
M43	7.36	19.2	0	BD43	3.83	3.71	0	Anti-Titin (2)	9	7.93	14.85
M44	8.44	12.22	30.01	BD44	14.64	3.1	0	Anti-Titin (3)	1.36	5.87	0
M45	5.23	8.74	15.44	BD45	2.84	2.16	0	Anti-Titin (4)	0	8.09	0
M46	54.82	50.61	0	BD46	3.5	3.9	0	Anti-Titin (5)	0	0	0
M47	11.77	19.4	43.26	BD47	4.33	2.26	0	Anti-Titin (6)	0	0	0
M48	25.22	8.3	23.24	BD48	4.73	2.38	10.84	Anti-AQPR (1)	0	11.66	0
M49	13.15	8.25	124.51	BD49	1.77	3.44	1.85	Anti-AQPR (2)	4.36	0	0
M50	2.48	8.8	0	BD50	11.24	6.12	0	Anti-AQPR (3)	8.26	0	0
M51	0	11.54	0	BD201	0	2.85	0	Anti-AQPR (4)	3.69	0.73	0
M52	21.8	21.12	6.03	BD202	0	6.28	0	Anti-PCA2 (1)	0	3.61	0
M53	6.8	9.27	0	BD203	2.27	6.54	10.54	Anti-PCA2 (2)	2.43	8.9	0
M54	18.22	6.8	0	BD204	0	4.41	0	Anti-PCA2 (3)	3.66	10.95	0
M55	21.8	15.92	9.7	BD205	0	3.05	0	Anti-PCA2 (4)	0	2.54	0
M56	35.56	22.41	7	BD206	0	2.97	0	Anti-GLUDR2 (1)	7.8	1.36	11.97
M57	8.82	25.63	26.78	BD207	0	1.98	0	Anti-GLUDR2 (2)	1.2	0	0
M58	17.86	27.11	0	BD208	2.91	8.36	15.95	Anti-Flotillin (1)	0	0	0
M59	6.59	10.9	0	BD209	0	1.53	0	Anti-Flotillin (2)	0	1.88	0
M60	26.14	48.8	12.84	BD210	0	2.89	0	Anti-Flotillin (3)	2.57	5.72	0
M61	5.14	12.42	0	BD211	0	16.04	0	Anti-Flotillin (4)	0	0	0
M62	8.38	15.2	0	BD213	18.88	0	0	Anti-SOX1 (1)	0	3.54	0
M63	22.14	15.92	0	BD214	0	3.61	0	Anti-SOX1 (2)	0	0	0
M64	12.28	33.44	0	BD215	0	2.39	0	Anti-SOX1 (3)	0	7.14	0
M65	16.84	13.02	12.25	BD216	0	8.7	0	Anti-SOX1 (4)	0	0	0
M66	16.97	23.89	0	BD217	0	2.55	0				
M67	11.84	19.6	0	BD218	5.76	1.63	0				
M68	18.72	28.66	1.7	BD219	0	6.15	0				
M69	5.31	9.5	77.52	BD220	0	2.09	0				
M70	24.51	41.85	15.74	BD222	0	0	0				
M71	13.11	28.27	10.22								
M72	7.76	19.26	0								
M73	49.69	55.52	0								
M74	20.5	36.21	0								
M75	24.91	20.96	0								
M76	0	2.27	0								
M77	0	24.46	0								
M78	8.37	16.14	0								
M79	0	6.81	0								
M80	2.7	12.54	0								
M81	3.05	9.63	0								
M82	0	0	0								
M83	5.24	0	11.72								
M84	8.2	6.76	3.76								
M85	0	8.85	5.33								
M86	2.73	4.69	7.92								
M87	10.43	10.21	0								
M89	3.1	2.11	0								
M90	20.56	8.98	19.74								
M92	60.4	19.51	6.81								
M93	10.45	3.57	0								
M94	18.02	6.77	5.92								
M95	32.28	20.37	0								
M96	11.4	4.52	0								
M97	3.63	4.38	18.58								
M98	24.66	20.51	5.72								
M99	3.53	3.9	0								
M100	21.3	10.29	42.38								
M101	3.55	3.46	0								
M102	6.78	2.88	20.27								
		NSF positive									
		DNM1 postive									

3.13.1. Neutralization of patients' sera reactivity against NSF using HEK293-NSF[human]

To determine the specificity of reactivity against NSF in the patients' sera, a neutralization experiment was performed using WT HEK293-NSF as depicted in section 2.2.9. Approximately 5 µg of IMAC purified NSF was transferred onto a nitrocellulose membrane **(Figure 24)** and incubated with the anti-NSF antibody (Ab), an internal reference serum that was used as the positive control (PC) in sections 3.12 and 3.13, two patients' sera (P1-P2), and two sera from healthy controls (H1-H2).

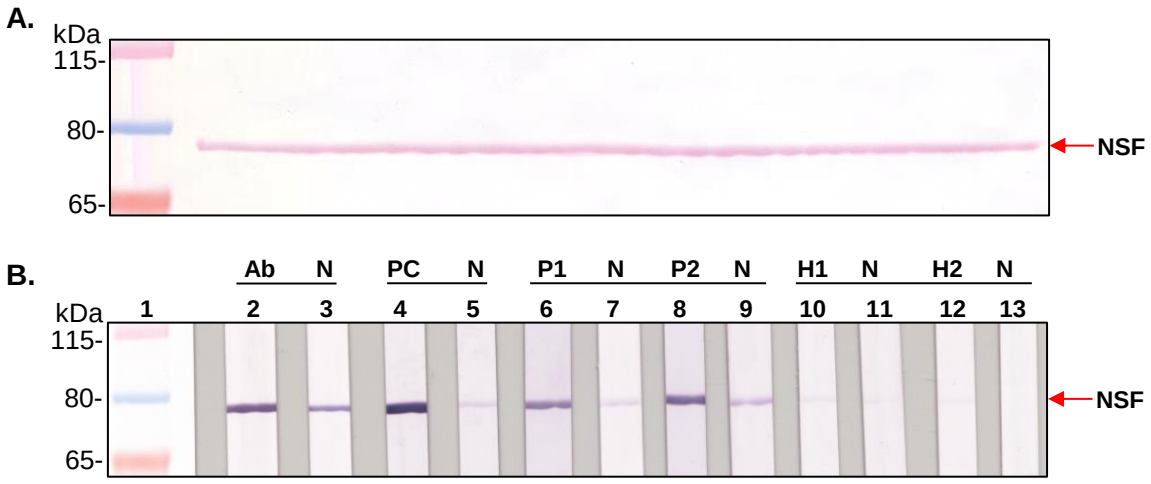

Figure 24: Patients' sera reactivity against NSF was partially neutralized using HEK293-NSF[human]

A) Approximately 5 µg purified NSF from HEK293-NSF was transferred onto a membrane and stained with Ponceau S solution to ensure equal distribution of the protein. The membrane was then incubated with the anti-NSF antibody **(Ab)**, an internal reference serum **(PC)**, and selected sera from patients **(P1-P2)** versus controls **(H1-H2)**. **B)** All samples were pre-incubated for one hour with either the recombinant NSF (Neutralized samples) to nullify the reactivity against NSF or PBS buffer alone (Non-Neutralized samples) as a control. The membrane was then incubated with both the neutralized **(N)** and non-neutralized samples in parallel and the reactivity against NSF was determined using appropriate secondary antibodies **(red arrow)**. The reactivity against NSF (≈ 82 kDa) was partially neutralized with the antibody **(lane 3)**. A moderate reduction in the reactivity against NSF was observed in the reference serum and in all the patients' sera post-neutralization **(lanes: 5, 7, and 9)**. Weak to no reactivity against NSF was observed in the control sera **(lanes: 10-13)**.

The antibody as well as the serum samples were pre-incubated either with the purified NSF (Neutralized samples) or PBS buffer (Non-neutralized samples). Subsequently, the neutralized (N) as well as non-neutralized samples were immunoblotted against the recombinant NSF. The anti-NSF antibody reactivity against NSF (≈ 82 kDa) was only partially neutralized (Figure 24B, lane 3). This could probably be due to a high concentration of the

antibody compared with that of the antigen used for neutralization. Additionally, the reactivity against NSF was only moderately neutralized in the serum samples. A weak reactivity against NSF post-neutralization was observed with the reference serum (Figure 24, lanes: 5) as well as with the patients' sera (Figure 24, lanes: 7 and 9). Almost no reactivity against NSF was detected in the sera from controls (Figure 24, lanes: 10-13).

Therefore, reactivity against NSF in the patients' sera as well as in the antibody was only partially neutralized, but not completely, following incubation with the recombinant antigen.

3.14. Separation of NSF by Isoelectric focusing

In both the immunoprecipitation and immunoblotting tests, there was a difference in the binding of patients' sera to NSF (Figure 8 versus Figure 19). Therefore, an IEF experiment was performed, to separate NSF proteins based on their pI and their molecular weight to investigate any differences in the NSF obtained from the cerebellum tissue compared with that expressed in HEK293 cells. NSF was precipitated by the anti-GRM1 antibody in comparable amounts in the immunoprecipitation tests using both the cerebellum tissue as well as with the HEK293-NSF (Figure 14 and Figure 19). Therefore, these two eluates were processed in IEF (section 2.2.10). The proteins were subsequently transferred onto a nitrocellulose membrane and incubated with anti-NSF and -DNM1 antibodies to detect reactivities against NSF and DNM1 in the cerebellum tissue eluate **(Figure 25A)** and against NSF alone in the HEK293-NSF eluate **(Figure 25B)**. Even though the exact pI could not be determined, a clear difference in the pI of NSF was observed between the two eluates. The pI of NSF was more widespread between the pH 3-7 regions in the eluate obtained from the cerebellum tissue compared with that expressed in HEK293 cells, which was more concentrated around the acidic pH region. These results suggest different populations of NSF between the two sources, which could be attributed due to PTMs, especially differences in phosphorylation of the residues. Figure 25A additionally portrayed the separation of DNM1 in the cerebellum tissue. The identity of the separated proteins was further verified by MS analysis (data not shown) and the spots at ≈ 82 kDa and ≈ 97 kDa regions were identified specifically as NSF and DNM1, respectively, and no additional proteins could be detected in this region.

In short, separation of NSF based on its pI and molecular weight revealed probable presence of mixed populations of NSF between the cerebellum and that expressed in recombinant systems.

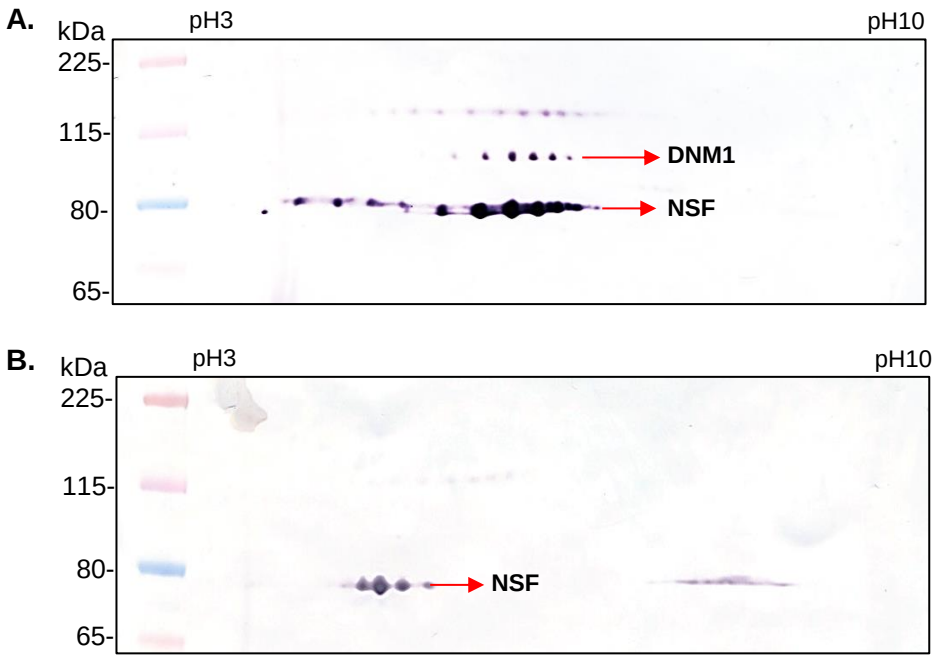

Figure 25: The pI of NSF differed between the cerebellum and that expressed in HEK293 cells

An immunoprecipitation test was performed with human anti-GRM1 IgG antibody plus lysates from the pig cerebellum tissue or HEK293-NSF. Both eluates were subsequently processed by the IEF technique to separate NSF and DNM1 two-dimensionally based on their pI and molecular weight. Following IEF, the proteins from the **A)** cerebellum tissue were analyzed using antibodies against NSF (1:650) and DNM1 (1:1000) and that from the **B)** recombinant proteins were analyzed with anti-NSF antibody alone. The pI of the NSF in the cerebellum tissue was distributed across the pH 3-7 regions **(A, arrow)**, while that in HEK293-NSF was restricted towards the acidic pH alone **(B, arrow)**. Additionally, separation of DNM1 could be identified in the cerebellum tissue **(A, arrow)**. MS analysis verified identity of the proteins at ≈ 82 kDa and ≈ 97 kDa regions as NSF and DNM1, respectively (Data not shown).

3.15. Prevalence of AAbs against STX1B using *E. coli* expressed His-tagged STX1B(ic)

STX1B(ic) was cloned and expressed in a bacterial system, *E. coli*. Approximately 5 µg of IMAC purified protein was transferred onto a nitrocellulose membrane. The membrane was incubated with an antibody against STX1B (Ab), an internal reference serum (Euroimmun AG, Germany) that was positive for STX1B in IFA (data not shown), sera from patients versus controls. The calculation of the relative intensity of the bands was performed as described in section 3.12 and an arbitrary cut-off of 20% relative intensity was implemented for screening purposes alone **(Figure 26A, blue line).** The reactivity against STX1B at ≈ 33 kDa was identified in two patients' sera in addition to the anti-STX1B antibody and the reference serum (Figure 26A, arrow). In total, eight patients' sera, three neurological control sera and one healthy control serum

portrayed values above the cut-off **(Figure 26B)**, without any significant between-group differences. Of the 10 patients' sera positive for AAbs against STX1B in IFA, only two patients were positive in immunoblotting tests, indicating that the sensitivity of the tests might be higher with the IFA compared with immunoblotting tests. A data table summarizing all the tests results for the entire patient cohort is depicted in **Table 21**.

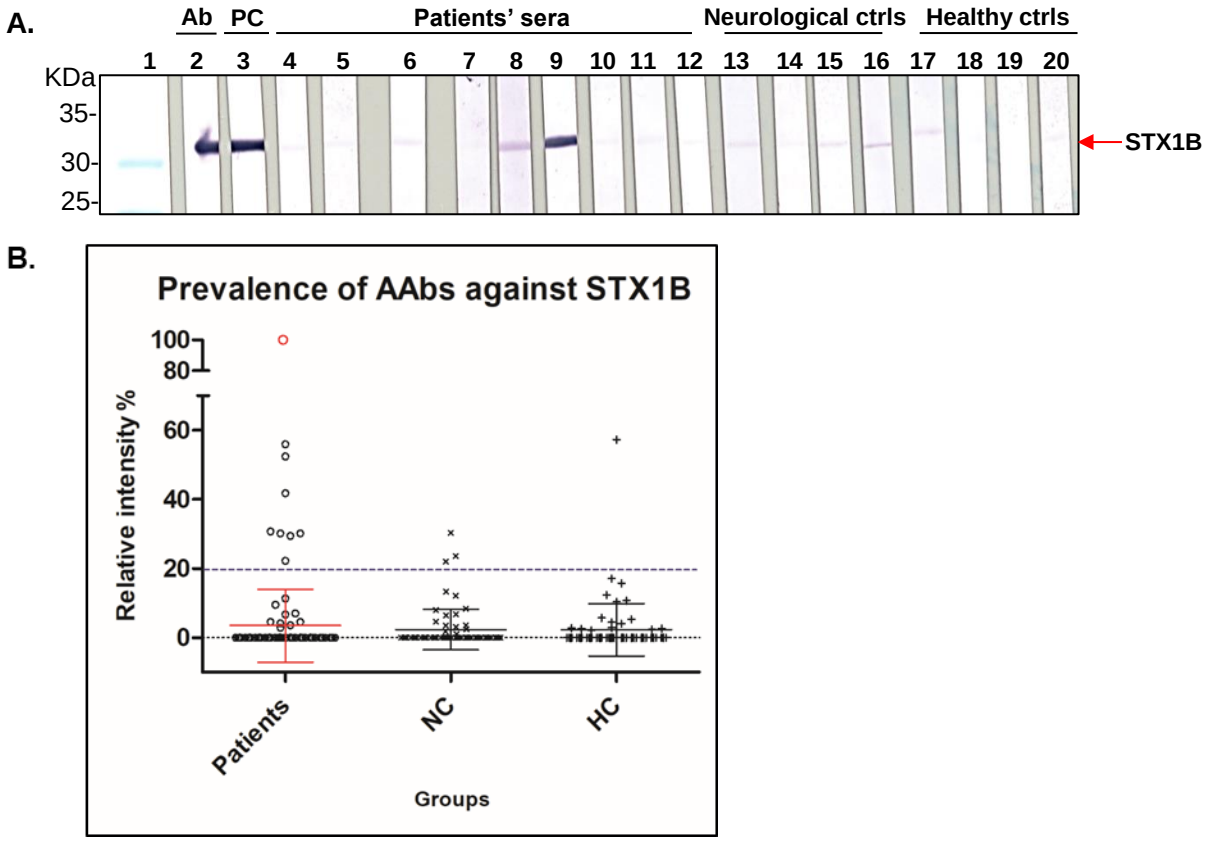

Figure 26: Immunoreactivity against STX1B was minimal in the patients' sera

The intracellular domain (ic) of STX1B was cloned and expressed in *E. coli* **A)** Approximately 5 µg of purified STX1B(ic) were transferred onto nitrocellulose membrane and incubated with anti-STX1B antibody **(Ab, 1:2000)**, an internal reference serum positive for AAbs against STX1B in IFA **(PC, lane 3)**, and nine patients' sera that were positive for anti-STX1B AAbs in the IFA test **(lanes: 4-12)** compared with four healthy **(lanes: 13-16)** and four neurological controls **(lanes: 17-20)**, all diluted 1:350. Reactivity against STX1B was observed in the Ab, PC, and two patients' sera (red arrow). **B)** Positive reactivity against STX1B was determined using an arbitrary cut-off of 20% relative intensity for screening purposes alone. Overall, eight patients' sera, three neurological control (NC), and one healthy control (HC) portrayed a reactivity against STX1B above the cut-off, but without any significant differences between the groups. Graphs represent mean ± SD of each group (Abbreviations ctrls: controls).

Table 21: Data table to represent cumulative test results of the patient cohort in different immunoassays

Cumulative Test Results

Patient Number	Year of Birth	Patient diagnosis	ELISA	IFA	Immunoprecipitation-WB			IFA-SNARE				IMAC-WB (cerebellum tissue)		WB (recombinant proteins)		EUROIMMUN Neuro IFA
			GAD65 450 nm	GAD65&67	GAD65&67	NSF	STX1B	NSF	STX1A	STX1B	Others	DNM1	NSF	HEK-NSF	STX1B (*E.coli*)	Other detected AAbs
Patient 1	1974	Ataxia, Hyperekplexia	1.774	0	0	0	0	0	0	0	0	0	0	0	0	
Patient 2	1949	SPS	>2000	+	+	+	+	0	0	0	0	0	+	0	+	
Patient 3	1934	SPS	1.699	0	0	0	0	0	0	0	0	+	0	0	0	
Patient 4	1942	PERM (SPS + focal Epilepsy)	>2000	+	+	+	+	0	0	0	0	+	0	+	0	
Patient 5	1965	SPS	0.129	0	0	0	0	0	0	0	0	0	0	0	0	
Patient 6	1974	SPS	>2000	+	+	0	0	0	0	0	0	+	+	+	0	
Patient 7	1966	SPS	0.321	0	0	0	+	0	0	0	0	0	0	0	0	GLRA1b
Patient 8	1939	SPS	>2000	+	+	0	+	0	0	0	0	0	0	0	0	Amphiphysin
Patient 9	1964	Psychogenic SPS	1.155	0	0	0	+	0	0	0	0	0	0	0	0	
Patient 10	1950	SPS	>2000	+	65+	0	0	0	0	0	0	0	0	0	0	
Patient 11	1952	SPS	>2000	0	0	0	0	0	0	0	0	0	+	+	0	
Patient 12	1986	Psychogenic SPS	0.204	0	0	0	+	0	0	0	0	0	0	0	0	
Patient 13	1960	SPS	0.161	0	0	0	+	0	+	+	0	0	+	0	0	
Patient 14	1963	PERM (SPS+ oculomotor movement disorder)	>2000	65+	65+	0	0	0	0	0	0	0	0	0	0	
Patient 15	1971	paraspasticism	41.505	0	0	0	0	0	0	0	0	0	+	+	0	
Patient 16	1942	SPS	>2000	+	+	0	+	0	0	borderline	0	+	0	0	0	
Patient 17	1956	SPS	>2000	+	+	+	+	0	0	0	0	+	0	0	+	
Patient 18	1944	SPS	>2000	+	+	+	+	0	0	0	0	+	+	+	0	
Patient 19	1941	Psychogenic SPS	6.299	0	0	0	+	0	0	0	0	0	+	+	0	
Patient 20	1937	SPS	>2000	+	65+	0	+	0	0	0	0	0	+	+	0	
Patient 21	1934	SPS + dysathria + dysphagia	>2000	+	+	+	+	0	0	+	0	0	0	0	0	
Patient 22	1950	SPS	>2000	65+	65+	0	0	0	0	0	0	0	0	0	0	
Patient 23	1956	SPS + dysathria + dysphagia	0.289	0	0	0	0	0	0	0	0	0	0	0	0	
Patient 24	1950	SPS	>2000	+	+	+	+	0	0	+	0	0	+	0	+	
Patient 25	1979	SPS	>2000	+	+	0	0	0	0	0	0	0	0	0	0	
Patient 26	1949	Progressive Hyperekplexia	1.091	0	0	0	+	0	0	0	0	+	0	+	0	
Patient 27	1966	SPS	5.118	0	0	0	0	0	0	0	0	0	0	0	0	
Patient 28	1940	PERM	>2000	65+	65+	0	+	0	0	0	0	0	0	0	0	
Patient 29	1941	PERM (SPS + dysarthria + dysphagia)	0.674	0	0	0	0	0	borderline	0	0	0	0	0	0	
Patient 30	1954	SPS paraneoplastic (breast cancer)	0.514	0	0	+	+	0	0	0	0	+	0	0	0	Amphiphysin
Patient 31	1929	paraneoplastic SPS + dysarthria + dysphagia	0.033	0	0	0	+	0	0	+	0	+	0	0	0	Amphiphysin
Patient 32	2985	SPS + dysathria + dysphagia	0.030	0	0	0	0	0	+	+	0	0	+	+	+	Amphiphysin
Patient 33	1961	SPS	>2000	+	+	+	+	0	0	0	0	+	+	0	0	
Patient 34	1944	SPS	>2000	65+	65+	0	0	0	0	0	0	0	0	0	0	
Patient 35	1968	PERM	>2000	+	+	+	+	+	0	0	0	0	+	+	0	
Patient 36	1935	Cerebellitis	>2000	+	+	0	0	0	+	+	0	+	0	0	0	
Patient 37	1964	PERM	>2000	65+	65+	0	0	0	0	0	0	0	+	+	0	
Patient 38	1940	PERM	3.943	0	0	0	0	0	0	0	0	0	+	0	0	
Patient 39	1986	Dystonia with complex regional pain syndrome	>2000	0	0	0	0	0	0	0	0	0	0	0	0	
Patient 40	nd.	Brother of 45, healthy	1.219	0	0	0	+	borderline	0	0	0	+	0	+	0	
Patient 41	1947	Arteria cerebri media stroke	<0,001	65+	0	0	0	0	0	0	0	0	0	0	0	
Patient 42	1953	SPS	0.175	0	0	0	0	0	0	0	0	0	0	0	0	
Patient 43	1961	SPS	>2000	+	+	+	+	0	0	0	0	0	0	0	0	
Patient 44	1952	Neuromyotonia	0.175	0	0	0	0	0	0	+	VAMP2+	0	0	0	0	
Patient 45	1960	PERM	>2000	0	0	0	0	0	0	0	0	0	0	0	0	
Patient 46	1957	SPS	>2000	+	65+	0	+	0	0	0	0	+	+	+	0	
Patient 47	1987	PERM (SPS + obsessive-compulsive disorder)	>2000	+	65+	0	+	0	0	0	0	+	0	0	0	
Patient 48	1951	SPS	>2000	+	+	+	+	0	0	0	0	0	+	0	0	GLRA1b
Patient 49	1948	Multifocal Motor Neuropathy	0.034	0	0	0	0	0	0	0	0	0	0	0	0	
Patient 50	1944	Dystonia (trunk tremor)	0.167	0	0	0	+	0	0	0	0	+	0	0	0	
Patient 51	1963	PERM paraneoplastic (SPS+Ataxia+Dysarthria) with Pancreatic cancer	>2000	+	+	0	0	0	0	0	0	+	0	0	0	
Patient 52	1963	paroxysmal Dystonia	0.112	0	0	0	+	0	0	0	0	+	+	+	+	
Patient 53	1952	PERM paraneoplastic (breast cancer)	<5	0	0	0	0	0	0	0	0	0	0	0	0	Amphiphysin
Patient 54	1963	PERM	<5	0	0	0	+	0	0	borderline	0	0	0	0	0	GLRA1b
Patient 55	1941	SPS	>2000	65+	+	0	+	0	0	0	0	0	+	0	0	
Patient 56	1949	psychogenic SPS	0.201	0	0	+	+	0	0	0	0	0	+	+	+	
Patient 57	1975	SPS	<5	0	0	0	0	0	0	0	0	0	0	+	0	DPPX
Patient 58	1956	SPS symptomatic?	0.655	0	0	0	+	0	0	0	0	0	0	+	0	
Patient 59	1989	Amyotrophic lateral sclerosis	>2000	0	0	0	+	0	0	0	0	0	0	0	0	
Patient 60	1936	PERM	>2000	+	+	+	+	0	0	0	0	+	+	+	0	
Patient 61	1947	anxiety disorder	<5	0	0	0	+	0	0	0	0	0	0	0	+	
Patient 62	1983	Hyperekplexia (possible graft-vs-host after stem cell transplant)	0.012	0	0	0	0	0	0	0	0	0	0	0	0	
Patient 63	1953	SPS	>2000	+	65+	0	0	0	0	0	0	0	+	0	0	Amphiphysin
Patient 64	1943	SPS	0.023	0	0	0	0	0	0	0	0	0	0	+	0	
Patient 65	1954	Muscle pains without correlation	0.178	0	0	0	0	0	0	0	0	0	0	0	0	SLC6A5
Patient 66	1977	SLS	>2000	+	+	0	+	0	0	0	0	0	0	+	0	
Patient 67	1926	PERM (SPS+Ataxia+Dysarthria)	>2000	65+	65+	0	+	0	0	0	0	0	0	0	0	
Patient 68	1950	SPS + dysathria + dysphagia	>2000	+	+	0	0	0	0	0	0	0	0	+	0	
Patient 69	1929	PERM	>2000	+	+	0	0	0	0	0	0	0	0	0	0	
Patient 70	1979	PERM (SPS+focal Epilepsy)	>2000	+	+	+	+	0	0	0	0	+	+	+	0	Amphiphysin
Patient 71	1946	SPS + dysathria + dysphagia	>2000	+	+	+	+	0	0	0	0	0	0	+	0	
Patient 72	1952	SPS	>2000	+	+	0	0	0	0	0	0	0	0	0	0	
Patient 73	1959	Cerebellitis	>2000	65+	65+	0	+	0	0	0	0	+	+	+	0	
Patient 74	1971	SPS	>2000	+	+	+	+	0	0	0	0	+	+	+	0	
Patient 75	1944	Dystonia (Trunk tremor)	47.017	0	0	+	+	0	0	0	0	0	+	+	0	
Patient 76	1984	SPS	0.378	0	0	+	+	0	0	0	0	0	0	0	0	
Patient 77	1962	SPS	>2000	65+	65+	0	0	0	0	0	0	0	0	+	0	
Patient 78	1943	PERM	>2000	0	0	+	+	0	0	0	0	0	0	0	0	
Patient 79	1945	SLS	>2000	+	+	+	+	0	0	0	0	0	0	0	0	
Patient 80	1933	Hyperekplexia + dysarthria + dysphagia	0.356	0	0	+	+	0	0	0	0	0	0	0	0	
Patient 81	1954	PERM	>2000	+	+	+	+	0	0	0	Munc18+	0	0	0	0	SLC6A5
Patient 82	1950	PERM	>2000	+	+	+	+	0	0	0	0	0	0	0	0	
Patient 83	1974	Hyperekplexia+Ataxia+Downbeat-Nystagmus	0.167	0	0	0	0	0	0	0	0	0	0	0	0	
Patient 84	1966	SPS	>2000	65+	65+	+	+	0	0	0	0	0	0	0	0	
Patient 85	1939	SLS	>2000	0	0	0	0	0	0	0	0	0	0	0	0	
Patient 86	1960	SPS	>2000	+	+	0	0	0	0	0	0	0	0	0	0	
Patient 87	1982	SPS	>2000	+	+	+	+	0	0	0	0	0	0	0	0	
Patient 89	1962	Dyskinesia-paraneoplastic (breast cancer)	1.154	0	0	0	+	0	0	0	0	0	0	0	0	GLRA1b
Patient 90	1965	SPS	>2000	65+	+	+	+	0	0	0	0	0	+	0	0	
Patient 92	1952	PERM (SPS+focal Epilepsy)	>2000	+	+	0	+	0	0	0	0	0	+	0	0	
Patient 93	1949	SPS	>2000	65+	65+	0	+	0	0	0	0	0	0	0	0	
Patient 94	1949	Hyperekplexia + Brainstem encephalitis	0.09	0	0	0	+	0	0	0	0	0	0	0	0	GLRA1b, Gephyrin
Patient 95	1940	SPS	>2000	65+	65+	0	+	0	0	0	0	+	+	+	0	
Patient 96	1948	SPS + dysathria + dysphagia	0.045	0	0	0	0	0	0	0	0	0	0	0	0	DPPX
Patient 97	1940	PERM	>2000	+	+	+	+	0	0	0	0	0	0	0	0	
Patient 98	1969	Psychogenic SPS	7.753	0	0	0	0	0	0	0	0	0	+	+	0	
Patient 99	1955	PERM (SPS+focal Epilepsy)	>2000	+	+	+	+	0	0	0	0	0	0	0	0	
Patient 100	1952	PERM	>2000	+	+	+	+	0	0	0	0	0	+	0	0	
Patient 101	1969	inflammatory motor neuron disease	0.334	0	0	0	0	0	0	0	0	+	0	0	+	
Patient 102	1953	PERM (SPS + sensory disorder + ataxia)	>2000	+	+	0	+	0	0	0	0	0	0	0	0	

Postive result

Postive for GAD65 only

4. Discussion

4.1. The reason behind the incessant research into SPS and associated neurological movement disorders

SPS is a rare, neurological disorder associated with hyperreflexia, extremely painful spasms, and incapacitating muscle rigidity affecting primarily the lumbar, truncal and proximal limb muscles (Ali et al., 2011; Barker et al., 1998). It is an autoimmune disorder with the majority of the patients possessing AAbs against proteins associated with the inhibitory synapses of the CNS including GAD and to a lower extent, antigens like GABARAP, amphiphysin, and gephyrin (Alexopoulos and Dalakas, 2010; Dalakas, 2009). Overall, 80% of patients have AAbs against GAD65 and less than 50% of them target GAD67 (Buddhala et al., 2009). These AAbs might cause a decrease in the synthesis of the inhibitory neurotransmitter, GABA, resulting in an imbalance in neurotransmission due to a dysfunctional GABAergic system (Ali et al., 2011). Anti-GAD AAbs are not restricted to SPS alone, but are observed in a number of other neurological disorders including cerebellar ataxia or cerebellitis (10%), epilepsy (< 10%), limbic encephalitis, T1DM (80%), and PERM (Alexopoulos and Dalakas, 2010; Carvajal-Gonzalez et al., 2014; Hutchinson et al., 2008; Meinck and Thompson, 2002; Solimena and De Camilli, 1991; Vives-Pi and Sabater, 2010; Vulliemoz et al., 2007). Therefore, whether GAD AAbs have a pathogenic significance in these disorders or if they are plain biomarkers for the successful identification of the diseases continues to remain elusive (Fouka et al., 2015). Probably, anti-GAD AAbs targets specific epitopes in different diseases or are not confined to a particular phenotype (Dalakas, 2013). If the anti-GAD AAbs were pathogenic, the primary two ways GABAergic neurotransmission would be impaired are; (1) blocking synthesis of GABA by downregulating the enzymatic activity of GAD or (2) obstruction of proper exocytosis of GABA containing synaptic vesicles (Dinkel et al., 1998; Geis et al., 2010; Ishida et al., 1999; Rakocevic and Floeter, 2012). The majority of the studies support the hypothesis that a functional blockade of the GABAergic inhibitory neurons, rather than a structural damage, results in the continuous firing of the alpha motor neurons causing hyperexcitability and other symptoms associated with patients. This is predominantly because most of the patients portray a normal imaging of the brain and spinal cord. Additionally, the autopsies mostly lack lymphocyte infiltration or atrophic changes within the CNS and there are no of signs of inflammation or cellular destruction. Furthermore, treatment with immunomodulatory agents reverse symptoms in some patients (Ali et al., 2011; Dalakas, 2009; Dalakas, 2013; Holmoy and Geis, 2011; Levy et al., 2005; Rakocevic et al., 2004). Despite decades of research on different GAD-associated syndromes,

the pathogenic significance of anti-GAD AAbs is still debatable. The primary problem is that GAD and other reported antigens are intracellular and the question, how circulating antibodies can reach intracellular targets by crossing the blood-brain barrier and penetrate neurons is controversial. Secondly, there is no correlation between CSF or serum anti-GAD AAb levels and duration and severity of the disease in patients. Lastly, there is no maternal transfer of anti-GAD AAbs and the SPS symptoms have not been successfully transferred into animals using either the purified GAD antigen or GAD-specific IgG from patients (Alexopoulos and Dalakas, 2010; Dalakas, 2009; Dalakas, 2013; Dalakas et al., 2001; Gresa-Arribas et al., 2015; Holmoy and Geis, 2011; Levy et al., 1999; Vincent, 2008). Joseph Dalmau's group specifically demonstrated that anti-GAD65 AAbs interacted with GAD65 only when the membrane was permeabilized, but not in live primary neuronal cultures, suggesting no direct pathogenic significance of the anti-GAD65 AAbs (Gresa-Arribas et al., 2015). Therefore, it was speculated that anti-GAD AAbs might be associated with additional AAbs targeting other synaptic proteins involved in the GABAergic transmission. Furthermore, the diversity of the neurological symptoms between patients and recovery of only some patients upon immunotherapy point towards the presence of other associated AAbs, targeting preferably cell-surface or intracellular proteins (Alexopoulos and Dalakas, 2010; Ali et al., 2011; Butler et al., 2000; Dalakas, 2013; Fouka et al., 2015; Haselmann et al., 2015; Holmoy and Geis, 2011; Irani et al., 2014; Lancaster and Dalmau, 2012; Werner et al., 2015). Therefore, my doctoral thesis focused on identifying other unknown target antigens in SPS, PERM and other neurology-related hyperexcitability disorders.

4.2. Characterization of the patients included in the study

In this study, clinically characterized patients having SPS (n = 51), SLS (n = 3), PERM (n = 24), cerebellitis (n = 2), hyperekplexia (n = 6), dystonia (n = 5), and anxiety associated movement disorders (n = 9) were included with an aim to recognize novel auto-antigens across a diverse spectrum of diseases. Anti-GAD AAbs are also found in a majority of patients with T1DM (80%), but with 50-100 times lower titers compared with SPS. Patients with T1DM rarely develop SPS, suggesting that the systemic synthesis of anti-GAD65 AAbs is not adequate to mediate neurological symptoms, which could be caused by the intrathecal synthesis of GAD65-specific antibodies, as observed in SPS (Baekkeskov et al., 2000; Dalakas et al., 2000; Manto et al., 2007). Therefore, patients with T1DM were not included in this study due to lack of any neurological symptoms.

Approximately 20-30% of the SPS patients negative for anti-GAD AAbs also portrayed all the classical symptoms of SPS, probably indicating the presence of additional AAbs in these

patients (Ali et al., 2011). Furthermore, most of the studies conducted to identify novel AAbs or to determine the effect of GAD AAbs, primarily included patients positive for anti-GAD65 AAbs (Carvajal-Gonzalez et al., 2014; Fouka et al., 2015; Geis et al., 2011; Haselmann et al., 2015; Levy et al., 2005; Raju et al., 2006; Werner et al., 2015). However, this study included patients both positive and negative for anti-GAD65/67 AAbs, with an aim to identify a common, yet individual biomarker across the patient cohort, irrespective of the presence of anti-GAD AAbs. In the current study, characterization of the patients using the anti-GAD ELISA resulted in 63 patients' sera positive and 37 patients' sera negative for anti-GAD65 AAbs **(Table 21)**. Antibodies against GAD65 and GAD67 are observed in 80% and less than 50% of SPS patients, respectively (Alexopoulos and Dalakas, 2010; Ali et al., 2011; Meinck et al., 2001; Rakocevic and Floeter, 2012). Results from the IFA revealed that 39 patients' sera were positive for anti-GAD65/67 AAbs and 14 patients' sera were positive only for anti-GAD65 AAbs. Altogether, the rate of patients' sera positive for anti-GAD65 and -GAD67 AAbs were 53% and 39%, respectively and the remaining 47% of patients' sera were negative for anti-GAD AAbs **(Table 15)**. Despite, a slight variation from literature data, this study managed to incorporate a balanced number of anti-GAD AAb positive and negative patients for a comparative analysis. In general, anti-GAD AAbs are measured both in the CSF and the serum of the patients. Nevertheless, the CSF levels are 50-times lower than the serum, but with 10-times higher rate of synthesis suspected due to the intrathecal synthesis of GAD-specific IgG within the CNS (Alexopoulos and Dalakas, 2010; Rakocevic et al., 2004; Saiz et al., 2008). In diagnostics, an ideal sample for biomarker investigations would be the patients' serum compared with their CSF. Various reasons contribute to such a preference: primarily, the ease of sample collection with the serum compared with an invasive, potentially painful lumbar puncture procedure for the CSF. Additionally, the complicated protocols involved with the CSF handling, transportation, storage, cost-factors etc. increases the advantages for performing analysis with serum over CSF samples. Therefore, the present study characterized only serum samples from all patients in different test methods and no paired CSF/serum study was performed.

4.3. No novel AAb patterns were detected in the GAD65ko substrate with the patient cohort

In the GAD65ko BIOCHIP Mosaic™, the majority of patients' sera positive for anti-GAD AAbs produced a GAD65-specific pattern on all wild-type tissue substrates **(Figure 5B-E)**. Additionally, the immunofluorescence signal observed in the pig cerebellum cryosection was slightly higher compared to the other tissue substrates **(Figure 5E)**. The GAD65-specific pattern

is very dominant and it is difficult to identify any underlying or other unrevealed AAb patterns in the wild-type tissue substrates. Therefore, a GAD65ko substrate was included to identify unknown or underlying AAb patterns. However, no specific or unique pattern was observed in the GAD65ko substrate with the patient cohort **(Figure 5A)**. Additionally, no patients' sera were positive for anti-GAD67 AAbs alone and no specific pattern was observed for anti-GAD67 AAbs in the GAD65ko substrate, suggesting that these AAbs might not produce a specific pattern on the tissue substrates and require alternate techniques to identify them. Furthermore, the ELISA test reported 63 patients' sera positive for anti-GAD65 AAbs, but only 53 patients' sera were identified by IFA **(Table 15)**. These results revealed that the (1) detection of anti-GAD65 AAbs could be more sensitive with the gold standard anti-GAD ELISA compared with the IFA analysis, (2) some epitopes could be masked or inaccessible to AAbs in IFA resulting in false negatives, and (3) ELISA being a quantitative test method for the measurement of anti-GAD65 AAbs could be preferred over IFA, which is semi-quantitative. Although IFA is a very sensitive technique, it could be possible that some AAbs do not produce a very specific pattern on the tissue substrates or that it cannot be distinctly identified from dominant patterns such as the GAD65-specific pattern. Additionally, the target proteins could be partially folded or some epitopes could be masked preventing these AAbs from producing an appropriate florescence signal in IFA. Taking these rationales into consideration for other unknown AAbs, the search for additional autoantigens continued using further immuno-biochemical assays.

4.4. Proteins associated with synaptic vesicular trafficking were immunoprecipitated by the patients' sera

The prevailing hypothesis explaining the pathogenicity of anti-GAD AAbs includes the inhibition of the GABAergic neuronal circuits resulting in the involuntary firing of the alpha-motor neurons and impeding function of the voluntary muscles (Alexopoulos and Dalakas, 2010). Searching for novel AAbs independent or associated with the anti-GAD AAbs till date resulted in identification of mostly synaptic proteins associated with the regulation of neurotransmission in the inhibitory synapses (Holmoy and Geis, 2011). These proteins either regulated the GABA receptor signaling or the synthesis of GABA in the post-synaptic or pre-synaptic regions, respectively. Amphiphysin was identified as the main target antigen in the paraneoplastic variant of SPS in patients diagnosed with breast cancer. Amphiphysin is a pre-synaptic cytosolic protein and plays an important role in vesicular endocytosis by interacting with dynamin (Camilli et al., 1993). Compared with the anti-GAD AAbs, the pathogenic significance of anti-amphiphysin AAbs is well documented in the paraneoplastic SPS. Classical symptoms of SPS were

observed in an animal model after systemic passive transfer of high titer amphiphysin-specific IgG from an SPS patient. Furthermore, both AAb titers and disease symptoms could be reduced following immunotherapy, pointing towards a direct pathogenic role of anti-amphiphysin antibodies (Geis et al., 2010; Sommer et al., 2005; Wessig et al., 2003). In the current study, seven patient's sera were positive for anti-amphiphysin AAbs and of them, three were also positive for anti-GAD AAbs **(Table 21)**, despite anti-GAD AAbs being rarely observed in paraneoplastic SPS (Rakocevic and Floeter, 2012).

Antibodies against gephyrin and glycine receptors are often observed in a subset of SPS patients. Gephyrin is a post-synaptic cytosolic protein, involved in the clustering of the glycine receptors and GABA-A receptors in the brain and spine. Similar to anti-amphiphysin AAbs, they are associated with the paraneoplastic variant of SPS (Butler et al., 2000). In 10-12% of SPS patients (Alexopoulos and Dalakas, 2010; McKeon et al., 2013) and in some PERM patients (Carvajal-Gonzalez et al., 2014) antibodies against the glycine receptors are also observed. In the present study, five patients with AAbs against GLRA1 and one with co-existing gephyrin were included **(Table 14)**. Another post-synaptic target antigen is GABARAP in SPS, which is vital for appropriate surface expression of GABA-A receptors in the post-synaptic membranes (Raju et al., 2006). Most of the identified candidate antigens including gephyrin, GABARAP, GLRA1 are all residents of the post-synaptic terminus. However, patch-clamp recordings of GABAergic synaptic transmission in murine granule cells following incubation with IgG from a SPS patient portrayed differences in the frequency of spontaneous quantal release in the pre-synaptic region of hippocampal slices, hinting that the antigens belonging to the pre-synaptic region would be preferentially targeted by unknown AAbs in SPS in comparison with the post-synaptic region (Werner et al., 2015).

In the present study, no novel AAb pattern was detected with the patients' sera in IFA. Therefore, a cumulative search for other unknown target antigens was performed using immunoprecipitation analysis. Two different types of immunoprecipitation methods were conducted in this study, one using pig cerebellum tissue lysate and the other using cerebellum cryosections. The pig cerebellum tissue was chosen as the standard tissue for immunoprecipitation since the immunostaining of the pig cerebellum was higher compared with other wild-type animal cerebellar cryosections in IFA. Additionally, cerebellum is one of the GABA rich regions in the brain apart from the thalamus, hippocampus, temporal cortex etc. A reduction in GABA levels was observed in these regions following infusion with SPS patient IgG in vivo (Dalakas, 2013; Levy et al., 2005). A comparable result was observed in both immunoprecipitation tests, wherein the majority of the patients' sera immunoprecipitated

synaptic vesicular associated proteins such as NSF and DNM1, in addition to the known target antigens GAD65 and GAD67. Additionally, the pull-down of NSF and DNM1 was not restricted to just anti-GAD AAb positive patients' sera, but was also observed in anti-GAD AAb negative patients' sera **(Figure 7)**. Furthermore, not all patients' sera positive for anti-GAD AAbs immunoprecipitated the above-mentioned proteins **(Figure 6)**. Therefore, NSF and DNM1 were precipitated independently of the GAD antigens and could be possible additional candidate antigens in patients with SPS, PERM and associated movement disorders. The pull-down of the said proteins was specific to the patient cohort since it was not detected in any of the sera from controls, indicating precipitation of these proteins explicitly in patients with specific neurological disorders. NSF is an enzyme that catalyzes the dephosphorylation of adenosine triphosphate (ATP) and plays an important role in vesicular fusion since in its absence the internal-cisternae transport of proteins in the Golgi stacks were blocked (Block et al., 1988). In yeast and Drosophila, NSF is encoded by the Sec18 gene and comatose gene (neuron specific), respectively. When these genes were conditionally disabled, termination of membrane transport and buildup of the SNARE complexes was observed (Littleton et al., 1998). NSF is associated with the superfamily of SNARE proteins and mediates the disassembly of the 7s supercomplex, formed by interaction between syntaxins, SNAP25, and VAMP, by triggering ATP hydrolysis (Bonifacino and Glick, 2004; Whiteheart et al., 1994; Whiteheart et al., 2001; Zhao et al., 2015). DNM1 is the neuronal-isoform of dynamin, present abundantly in the synapses. Mutations in dynamin resulted in the blocking of endocytosis and accumulation of long tubules bound to the plasma membrane. Therefore, dynamin with functional guanosine-5'-triphosphate (GTP) hydrolysis is required for precise receptor-mediated endocytosis and synaptic vesicle recycling (Damke et al., 1994). These pre-synaptic proteins play an important role in vesicular trafficking and AAbs to such proteins might impede exocytosis/endocytosis of synaptic vesicles carrying GABA in the inhibitory neuronal circuits. Such an effect could cause continuous firing of the motor neurons resulting in stiffness and rigidity as observed in these patients.

As a subsequent step, the pull-down of different SNARE proteins was verified in the entire cohort using commercial antibodies against the SNARE proteins.

4.4.1. Immunoprecipitation of NSF, STX1B, and DNM1 by the patient cohort

The immunoprecipitation of various synaptic proteins was verified in the patient cohort by IP-WB analysis using polyclonal animal antibodies **(Figure 8)**. In addition to NSF and DNM1, the reactivity against another SNARE protein, STX1B, was also verified in the immunoblotting tests. Syntaxins are a group of membrane-inserted receptors and are important members of the

SNARE proteins. STX1A and STX1B are the neuronal isoforms of syntaxin, which are 84% homologous and bind to the calcium-sensor synaptotagmin. STX1A is mainly concentrated in the autonomic and sensory nervous system, while STX1B is located in the motor neurons. Such a diverse distribution results in the variations in synaptic structure and functions of syntaxins (Aguado et al., 1999). Deletion of STX1B in mice reduced the number of docked vesicles in the pre-synaptic terminus and decreased the frequency of vesicle release, resulting in an accumulation of vesicle pools in the glutamatergic and GABAergic synapses (Mishima et al., 2014).

In the present study, 52 patients' sera were positive for AAbs against GAD65/67 as identified by the IP-WB analysis, which was one less compared with the IFA. This was because one sample had extremely low titers of anti-GAD65 AAbs, which could not be verified in the WB test. Additionally, patients' sera that were borderline positive for anti-GAD67 AAbs in the IFA were negative in the WB tests, suggesting that the sensitivity of the detection of AAbs against the GAD antigens was higher in the ELISA, followed by the IFA and IP-WB analysis **(Table 15 and Table 16)**. Overall, 23 and 37 patients' sera positive for anti-GAD AAbs and six and 22 patients' sera negative for anti-GAD AAbs immunoprecipitated NSF and STX1B, respectively. Despite a higher rate of pull-down of STX1B, the intensity of reactivity against STX1B was lower in comparison with other proteins, even though the lysate portrayed sufficient concentrations of STX1B **(Figure 8, Lys)**. This could probably be due to a low concentration of anti-STX1B AAbs in patients' sera or decreased affinity of the AAbs against STX1B or that STX1B was immunoprecipitated together with NSF and other SNARE proteins. Furthermore, the pull-down of NSF, DNM1, and STX1B was specific to the patient cohort and was not observed in the controls including both neurological and healthy subjects **(Figure 11)**.

Reactivity against DNM1 was not measured for the entire cohort since the protein was identified much later in the project, but the pull-down of DNM1 was observed to be close to that of NSF in a subset of patients, indicating similar immunoprecipitation results for NSF and DNM1 **(Figure 8)**. During vesicular endocytosis, amphiphysin binds to dynamin and assembles into ring-like structures around the neck of the clathrin-coated pits to mediate membrane invagination and subsequent endocytosis (Takei et al., 1999). However, the pull-down of amphiphysin was not observed in patients' sera that immunoprecipitated DNM1, revealing that DNM1 was not co-immunoprecipitated with amphiphysin. These results indicate that DNM1 could be an additional, yet independent target antigen in this patient cohort. Therefore, patients with SPS and associated movement disorders might have additional AAbs, apart from amphiphysin, against other proteins involved in vesicular endocytosis such as DNM1.

Raju et al identified GABARAP as an additional candidate antigen in 70% of anti-GAD65 positive SPS patients using immunoprecipitation and immunoblotting tests. Additionally, the group observed that incubation of patient IgG on rat hippocampal neurons reduced GABA-A receptor expression on the axonal processes and therefore, a pathogenic significance of anti-GABARAP AAbs was proposed (Raju et al., 2006). Furthermore, studies have reported a direct interaction between GABARAP and NSF and their relationship is important for trafficking of GABA-A receptors to the post synaptic cell-surface (Chen et al., 2007; Kittler et al., 2001). However, in the current study, no patients' sera immunoprecipitated GABARAP and hence, it could not be a common target antigen in this patient cohort **(Figure 10)**. Furthermore, the pull-down of NSF was not associated with that of GABARAP and hence, NSF could be an independent candidate antigen in the patient cohort. Another study reported comparable results, wherein patients diagnosed with SPS, epilepsy, limbic encephalitis, or cerebellar ataxia were not immunoreactive against recombinant GABARAP in IFA and immunoblotting tests (Gresa-Arribas et al., 2015).

4.4.2. Immunoprecipitation of mostly t-SNARE proteins by the patient cohort

Synaptic vesicles are considered a classical model to represent vesicular membrane trafficking. There are more than 80 different integral membrane proteins involved in membrane trafficking and approximately 20 different SNARE proteins participate in exocytosis as well as early and late endosome fusion steps (Takamori et al., 2006). SNARE proteins are categorized based on their location as vesicle (v-SNARE) or target membrane (t-SNARE) SNAREs. V-SNAREs mainly include the VAMPs and t-SNAREs consist of the syntaxins and SNAP25. During synaptic vesicular fusion, members of the SNARE proteins, primarily STX1, SNAP25, and VAMP interact with one another and mediate the fusion of the vesicles with the plasma membrane (Söllner et al., 1993). The SNARE assembly mainly involves the cytoplasmic domains of the SNARE proteins consisting of several heptad repeats of 60-70 amino acid residues called the SNARE motifs that assemble into four parallel, twisted, alpha-helices forming the core-complex (Jahn and Scheller, 2006; Südhof and Rothman, 2009). There are additional regulatory proteins which prevent the assembly of SNARE complex until a fusion signal arrives. For example STXBP1 (or Munc18) retains STX1 in a closed conformation until the right signal arrives and therefore, is an inhibitory regulator of the SNARE complex assembly in the pre-synaptic nerve terminals (Dulubova et al., 2007; Pérez-Brangulí et al., 2002).

There are two major functions of the SNARE proteins: firstly, they aid in vesicular fusion reactions. Secondly, they warrant only specific membrane fusions. Even though several

isoforms of SNAREs could facilitate fusion reactions at lower rates, the most effective fusion reactions are mediated by the cognate SNAREs including STX1, VAMP2, and SNAP25 (Bonifacino and Glick, 2004; Hussain and Davanger, 2011).

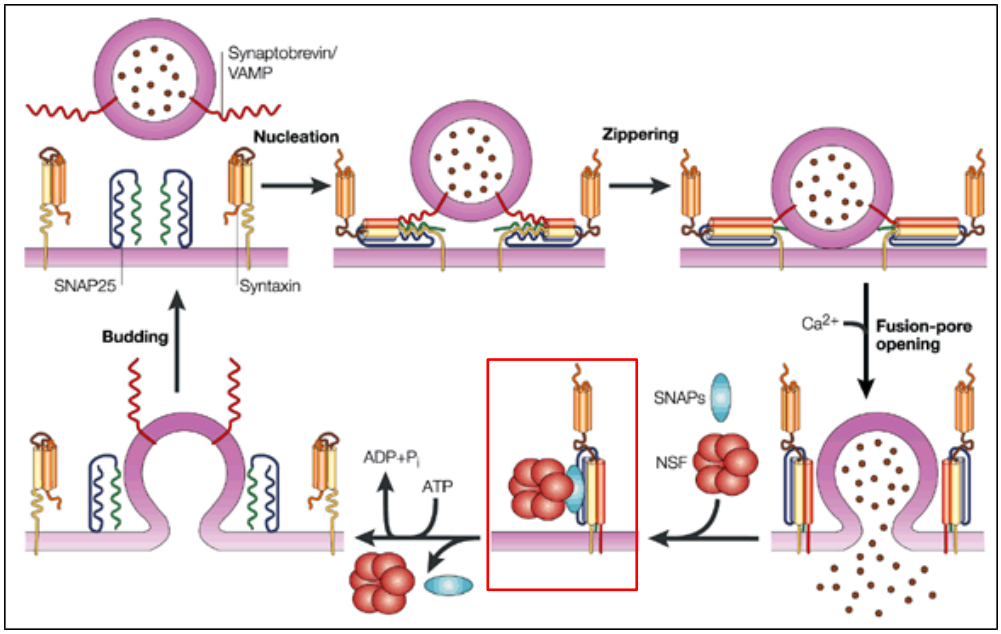

Figure 27: Representation of the SNARE complex assembly and disassembly

Adapted from (Rizo and Sudhof, 2002)

Nucleation begins with the opening of the closed conformation of syntaxin, mediated by detachment of STXBP1, to allow heterodimerization with SNAP25 and subsequent binding of VAMP. The SNARE motifs assemble into a twisted, parallel, four alpha-helix bundles by binding of the syntaxin and SNAP25 (t-SNARE) together with VAMP (v-SNARE). The complex then begins to zipper-up from the N- to the C-terminus, ultimately fusing the membranes together. The energy generated during the SNARE complex assembly drives the fusion of the lipid bilayers, either by direct or indirect methods. Exocytosis is initiated by binding of Ca^{2+} to synaptotagmin, which is bound to the core complex, and ultimately creation of a fusion pore. Following fusion, all SNARE proteins remain on one membrane in a cis-configuration, which is disassembled by binding of NSF to its adaptor soluble NSF attachment protein and by triggering ATP hydrolysis. The resulting multi-protein complex is called the 20s supercomplex **(red box)**, which is vital for releasing the SNARE proteins. Consequently, the SNARE proteins are recycled and prepared for next round of vesicular exocytosis.

The assembly of the core complex begins with the opening of the closed conformation of STX1, which is the nucleation step **(Figure 27)**. Subsequently, the SNARE motifs arrange into a coiled-coil, parallel, twisted, four-helix bundle, with the hydrophobic core buried inside. The loosely arranged trans-SNARE complex begins to zipper-up from the N-terminus to the C-terminus to form a stable cis-SNARE complex **(Figure 27)**. Specifically, calcium ions regulate

the synaptic vesicular exocytosis and therefore, binding of Ca^{2+} to synaptotagmin initiates the process of exocytosis by altering the conformations of the SNARE proteins. The cis-SNARE complex is disassembled by the binding of NSF to its adaptor protein called soluble NSF attachment protein and thereby triggers ATP hydrolysis. The resulting multi-subunit protein complex formed between NSF and the cis-SNARE complex is termed the 20s supercomplex and is vital for the disassembly of SNARE proteins **(Figure 27, box)**. Therefore, NSF provides energy for the fusion reaction and also recycles the SNARE proteins for subsequent fusion cycles (Bonifacino and Glick, 2004; Hanson et al., 1997; Hussain and Davanger, 2011; Rizo and Sudhof, 2002; Südhof and Rothman, 2009; Sutton et al., 1998; Teng et al., 2001; Woodman, 1997; Zhao et al., 2007; Zhao et al., 2015).

In the current study, patients' sera were additionally screened for the pull-down of seven other proteins associated with synaptic vesicular trafficking including EXOC4, Rab3A, SNAP25, STXBP1, synaptotagmin 1, synaptophysin 1, and VAMP2 based on information obtained from literature and "The Human Protein Atlas" (www.proteinatlas.org),. The majority of the patients' sera immunoprecipated SNARE proteins such as: NSF, STX1B, and SNAP25 as well as an associated regulatory protein, STXBP1 **(Figure 16)**. The proteins that were immunoprecipated chiefly belonged to the t-SNAREs or were associated with the plasma membrane, suggesting that these membrane associated proteins could be easily targeted by patients' AAbs resulting in their pull-down. Additonally, it can be speculated that the SNARE proteins were immunoprecipitated in the form of a complex, particulary the 20s supercomplex, whilst one or more of the proteins were directly targeted by the patients' AAbs.

Conversely, immunoprecipiation of v-SNAREs such as VAMP2 or synpatotagmin were not detected with the patients' sera **(Figure 16)**, despite VAMP2 being an intergral member of the supercomplex. It could be possible that other isoforms of VAMP were involved in this process, which were not screened in this study. Although syntaxins and synaptobrevins might be present in similar areas of the nervous system, only a particular combination of the protein isoforms plus SNAP25 result in formation of a stable 7s core complex mediating vesicular exocytosis (Pérez-Brangulí et al., 1999). Additionally, the interaction between the v-SNAREs and t-SNARE might be weak *in vitro* in the absence of a fusion signal and therefore, VAMP2 could not be immunoprecipitated in sufficient amounts.

NSF binds to the SNAP-SNARE complex in the presence of non-hydrolysable ATP e.g. in the presence of ATP/EDTA, resulting in the formation of the stable 20s multi-subunit protein supercomplex that can be purified. Pull-down assays cannot purify these complexes in conditions favoring ATP hydrolysis e.g. in the presence of ATP/Mg^{2+} due to only unstable and

transient binding (Whiteheart and Matveeva, 2004). Additionally, NSF is not detectable in the presence of adenosine diphosphate or adenosine monophosphate and therefore, NSF should be preferably in the ATP-bound state for detection in vitro (Whiteheart and Matveeva, 2004; Zhao et al., 2007). In the present study, immunoprecipitation analyses were also performed under conditions preventing ATP hydrolysis since the solubilization buffer contained EDTA, which is a chelator of metal ions such as Mg^{2+}. Additionally, based on literature it is presumed that NSF probably exists in the ATP-bound conformation, which in-turn binds to the SNARE proteins resulting in the immunoprecipitation of above-mentioned proteins.

Therefore, results from the IP-WB analysis revealed that patient's sera, but not controls, immunoprecipitated SNARE proteins such as NSF, STX1, SNAP25, and STXBP1, probably in the form of a complex. Additionally, DNM1 is closely associated with the plasma membrane during vesicular endocytosis and could be immunoprecipitated together or independent of the SNARE proteins. Consequently, it was important to determine which of these proteins associated with vesicular trafficking were directly targeted by patient AAbs.

4.5. IFA with recombinant SNAREs failed to detect immunoreactivity in the patients' sera

SNARE proteins such as NSF, STX1B, SNAP25, STXBP1, were primarily suspected as possible direct target antigens in the patient cohort. A multi-parametric testing was performed to simultaneously detect AAbs against various recombinant SNARE proteins **(Figure 4B)**. The SNARE slides also included a substrate with co-expressed cognate SNARE proteins (STX1B + SNAP25 + VAMP2) to detect plausible AAbs against this complex, since it was suspected that the patients' sera immunoprecipitated SNARE proteins as a complex. DNM1 was excluded from the cell-based assay since it was not categorized as a SNARE protein. Following screening of the cohort, the rate of immunoreactivity against NSF, STX1A/B, VAMP2, and STXBP1 was 2%, 10%, 1%, and 1%, respectively **(Table 17)**. Despite the immunoreactivity against the SNARE proteins being minimal in the patient cohort, these results were comparable with the IFA results with the GAD65ko substrate, wherein no novel AAb patterns were detected or could be matched to the patterns observed with the anti-SNARE antibodies **(Figure 5A and Figure 13)**. Therefore, it could be possible that additional AAbs against the SNARE proteins were present in very low concentrations, which was comparable with the immunoprecipitation test result with the HEK293-NSF, wherein only a minimal amount of NSF was pulled down by the patient cohort **(Figure 19)**. Additionally, the AAbs probably could not bind to their target antigens in IFA conditions, wherein the right epitopes could be masked / hidden as observed with the detection

of anti-GAD65 AAbs. In the ELISA test, 63 patients' sera were positive for anti-GAD65 AAbs, while only 53 patients' sera were positive by IFA **(Table 15)**, suggesting that some epitopes were probably masked in IFA. Furthermore, NSF exists in 2 different nucleotide states; ATP-bound and ADP-bound, possessing large conformational differences between them (Zhao et al., 2015). It was predicted that NSF could be present in the ATP-bound conformation, which bound to other SNARE proteins and resulted in the immunoprecipitation of the 20s supercomplex in the IP-WB analysis **(Figure 16)**. Therefore, whether NSF was expressed in the right conformation in IFA was unclear. All SNARE proteins undergo various PTMs including S-nitrosylation and phosphorylation which play an important role in the SNARE complex assembly/disassembly (Bradley and Steinert, 2016; Morgan and Burgoyne, 2004). Probably, the recombinant proteins were not expressed with the right PTMs. Additionally, SNARE antibodies against STXBP1, Rab3A, and synaptophysin 1 that did not portray any specific pattern in the tissue substrates in IFA, but were reactive against their target antigens in the WB analysis **(Figure 12)**. Therefore, it could be possible that the patient AAbs were better reactive to their target antigens in the immunoblotting technique compared with IFA. Keeping these hypotheses in mind, it was realized that IFA might be not be a suitable method to detect AAbs against SNARE proteins and therefore, immunoblotting tests were performed to screen for AAbs against the SNARE proteins.

VAMP proteins are specifically targeted by the tetanus toxin and patients infected with tetanus portray a phenotype similar to SPS. The toxin tends to specifically target the inhibitory nerve terminals and cleaves the VAMP proteins. Consequently, the release of inhibitory neurotransmitters is blocked causing rigidity and spasms in the affected patients (Hassel, 2013). Although AAbs against VAMP2 could rationalize the pathophysiology in patients with hyperexcitability disorders, their prevalence was very low in the current study. However, a study reported VAMP2 as an additional minor target antigen in T1DM patients. Overall, 21% patients had significantly higher prevalence of AAbs against VAMP2 compared with non-diabetic controls (Hirai et al., 2008). Therefore, detection of VAMP2 might aid in the differential diagnosis of patients with T1DM from SPS and associated neurological movement disorders. Furthermore, AAbs against Munc18 were reported in 20% of patients with Rasmussen encephalitis. Brain biopsies of these patients showed B- and plasma cell infiltration of the perivascular region. Coincidently, in the current study, one of the PERM patients were autoreactive against Munc18 (patient number: 81, Table 21), indicating Munc18 could be an additional target antigen in a sub-group of patients with encephalitis associated with lymphocyte infiltration.

4.6. Immunoreactivity observed against synaptic proteins in immunoblotting tests with the patients' sera

4.6.1. Immunoreactivity detected against NSF and DNM1 enriched from the cerebellum

Patients' sera immunoprecipitated NSF and DNM1 in higher amounts compared with other SNARE proteins from the cerebellum tissue **(Figure 8)**. Additionally, patients' sera bound weakly to the recombinant NSF **(Figure 19)** compared with NSF from the cerebellum. To determine if patients' sera were better immunoreactive against the original brain proteins, SNARE proteins were enriched by an IMAC technique using the pig cerebellum lysate plus a mouse anti-GRM1-IgG antibody, which simultaneously precipitated different SNARE proteins without any interference by the GAD antigens **(Figure 20)**. There was a difference in the mobility of the proteins observed between the tissue lysate and the immunoprecipitated eluates, which could be attributed to the differences in overall protein concentration between the two protein sources. Additionally, the antibody perhaps bound to specifically modified proteins during immunoprecipitation, which could cause a differential binding of SDS to the protein resulting in a slower mobility of these proteins as observed in the immunoprecipitates **(Figure 20B)**. In the IMAC protocol, the elution was modified to obtain only enriched fractions of SNARE proteins, while the elution of the bound antibody was minimal **(Figure 20A)**. Cognate SNARE proteins including syntaxins, VAMP, and SNAP25 form a stable, 7s core complex, which is resistant to SDS, unless heated at high temperatures and could be isolated from animal brains (Littleton et al., 1998). Therefore, it could be possible that the SNARE proteins were immunoprecipitated as a complex with the GRM1 antibody, in a direct or indirect manner during immunoprecipitation. The SNARE proteins were then dissociated when the eluted proteins were heated and separated by SDS-PAGE as performed in the immunoprecipitation analysis (section 2.2.4.1). In this study, the anti-GRM1 antibody was used as a model substance or a purification tool for the isolation of SNARE proteins from the cerebellum tissue. However, the reasons behind the interaction between the anti-GRM1 antibody and the SNARE proteins are cryptic and were not analyzed.

Immunoblotting of the sera of the patient cohort against enriched fractions of SNARE proteins allowed simultaneous screening of all suspected AAb targets including NSF, STX1B, and SNAP25 in addition to DNM1. An arbitrary cut-off of 3SD above the mean relative intensity of healthy controls was selected, for screening purposes alone, to identify positive samples (section 3.12). Overall, the prevalence of AAbs against NSF was 30%, 3%, and 1% and against

DNM1 was 23%, 0, and 1% in sera from patients, neurological, and healthy controls, respectively **(Figure 22)**. SPS and related disorders including cerebellitis affect mostly women (Alexopoulos and Dalakas, 2010; Vives-Pi and Sabater, 2010) and similarly, the prevalence of AAbs against NSF, but not DNM1, was observed to be higher in females compared with males in the current study (NSF: 33% versus 24% and DNM1: 20% versus 27%). Furthermore, not just patients' sera positive for anti-GAD AAbs, but also those negative for these AAbs revealed AAbs against NSF and DNM1 **(Table 19)**, confirming that the prevalence of AAbs against SNARE proteins was independent of the GAD and amphiphysin antigens. AAbs against amphiphysin are paraneoplastic markers of underlying cancers in patients due to the expression of the target antigen in the neurons as well as by the cancer cells (Lancaster and Dalmau, 2012). However, AAbs against DNM1 were not restricted to patients with underlying tumors and were distributed across the patient cohort, signifying that AAbs against DNM1 might not be a paraneoplastic marker.

In short, even though SNARE proteins could be immunoprecipitated in form of a supercomplex, individual AAbs against NSF and DNM1 do exist in the patient cohort. On comparing the individual disorders, patients with SPS, PERM, and cerebellitis might have a higher prevalence of AAbs against NSF and DNM1 compared with those diagnosed with dystonia, hyperekplexia, and anxiety related disorders **(Table 19)**.

4.6.2. Immunoreactivity observed against recombinant NSF

The majority of the patients' sera were not immunoreactive against the SNARE proteins in the cell-based assays **(Figure 18)** and this could probably be due to partial folding of the proteins resulting in masked/hidden epitopes in IFA. However, the immunoprecipitation analysis revealed that patients' sera pulled down SNARE proteins, specifically NSF, from the cerebellum tissue and from HEK293-NSF lysate, with a difference in the amount of NSF that was precipitated between the two sources **(Figure 8 versus Figure 19)**. Immunoblotting against enriched fractions of SNARE proteins revealed that the immunoreactivity against NSF was significantly higher in 30% of the patients' sera compared with the controls. Therefore, it was speculated that patient's AAbs were probably better reactive to SNAREs isolated from original brain proteins compared with those expressed in the recombinant systems. To verify this hypothesis, patients' sera were immunoblotted against recombinant NSF and it was observed that 29% of patients' sera had significantly higher reactivity against NSF compared with the controls **(Figure 23)**. Therefore, the patient's AAbs were probably better immunoreactive against linear epitopes of

NSF in comparison with conformational epitopes. This is further corroborated by the results from the ELISA test, wherein patients' sera were not immunoreactive against NSF (data not shown). Overall, 19 patients' sera portrayed a conclusive immunoreactivity against NSF in both test methods. However, the remaining patients' sera were positive only in either of the test methods, suggesting that the patients' AAbs probably targeted a mixed population of NSF, depending on whether it was obtained from the cerebellum or the recombinant proteins. Additionally, most of the patients' sera demonstrated a higher immunoreactivity against the NSF obtained from the cerebellum tissue compared with the recombinant protein in immunoblotting tests **(Table 20)**. In the neutralization test, the recombinant NSF could only partially neutralize the reactivity against NSF in the patients' sera **(Figure 24)**, indicating the patient AAbs probably targeted additional epitopes of NSF which was perhaps folded and inaccessible in the recombinant proteins or that the recombinant systems displayed an altered or imperfect epitope expression. Altogether, results from the immunoprecipitation and immunoblotting tests indicated a possible difference between the NSF expressed in the cerebellum in comparison with the recombinant protein. Therefore, NSF from both the sources was separated two-dimensionally based on their pI and molecular weight in an IEF experiment. Two different isoelectric points was observed for NSF depending on whether it was obtained from the cerebellum tissue or expressed in the HEK293 cells. NSF has at least 75 different isoelectric points ranging from 3.96-6.37, depending on the number of residues that are phosphorylated, with 6.52 being the pI of the unphosphorylated NSF (https://www.phosphosite.org). In the IEF test, the pI of NSF from the cerebellum tissue was distributed across the pH 3-7 regions, indicating differently phosphorylated residues compared with NSF expressed in HEK293 cells, wherein the pI was concentrated more towards the acidic region **(Figure 25)**. These results indicate that NSF could be differentially modified in the cerebellum compared with when expressed recombinantly. The patients' AAbs probably interacted with specifically modified NSF, which could attribute to the increased pull-down of NSF from the cerebellum tissue compared with the recombinant source and also rationalize the differences in the patients' sera reactivity against NSF in the immunoblotting tests.

In short, synaptic proteins such as NSF (ATPase) and DNM1 (GTPase) might be difficult to mimic in the recombinant systems in terms of appropriate PTMs, conformation, and structure in comparison with the original brain proteins. Therefore, AAbs against NSF and DNM1 could be better identified using immunoprecipitation followed by immunoblotting tests with the patient cohort compared with methodologies such as IFA and ELISA.

4.7. Detection of AAbs against STX1B was preferable in IFA compared with immunoblot

AAbs against STX1A/B were detected in 10 patients' sera in IFA **(Table 17)**. However, immunoblotting of patient versus control cohort against recombinant STX1B(ic) revealed a positive immunoreactivity against STX1B in eight patients' sera **(Figure 26)**. Of them, only two patients' sera were positive in both the tests systems. Additionally, there were no significant between-group differences in the immunoblotting tests. These results indicate that AAbs against STX1B might bind both linear and conformational epitopes. Patients' sera probably portrayed a difference in reactivity against STX1B, depending on the availability of epitopes, in the different test systems. In comparison with the immunoblotting tests, the specificity and sensitivity for the detection of AAbs against STX1 was higher in the IFA, wherein no controls were immunoreactive against STX1A/B. Moreover, the expression system in the two methods was different; STX1A/B was expressed in HEK293 cells in IFA, whereas only the intracellular domain of STX1B was expressed in *E. coli* for the immunoblotting tests. Therefore, it might be difficult to compare the different expression systems in terms of protein folding, modifications, structure etc. NSF and DNM1 are enzymes, which undergo a conformation change by triggering ATP or GTP hydrolysis, respectively, to alter the structure and function of the protein they are bound to. Therefore, a stable conformation of such proteins with accessibility of all epitopes might be difficult to achieve in IFA. On the contrary, syntaxins are not enzymes and could be stably expressed in IFA. Therefore, detection of AAbs against syntaxins could be preferable in IFA tests compared with immunoblotting tests.

In short, patients with SPS, PERM and associated movement disorders might have additional AAbs against the SNARE proteins, primarily NSF followed by DNM1 and STX1B. However, precise identification of such AAbs might encompass different test systems. Even though the pathogenic significance of the AAbs against the SNARE proteins was not determined in this study, possible mechanisms how these AAbs might target synaptic proteins and the probable association between dysfunctional SNARE proteins and the impairment of inhibitory neuronal circuits has been described.

4.8. Possible mechanisms how AAbs could target synaptic proteins

Although AAbs against NSF and DNM1 were observed in the patient cohort independent of the GAD antigens, its prevalence was higher in patients' sera positive for anti-GAD AAbs compared with those that were negative **(Table 19)**, suggesting a common etiology between these two

AAbs. It is hypothesized that peptide fragments or epitopes of intracellular candidate antigens, such as GAD65 and amphiphysin, might be exposed transiently to the extracellular environment during synaptic vesicular exocytosis or endocytosis and are subsequently spotted by the immune system (Alexopoulos and Dalakas, 2010; Fouka et al., 2015; Holmoy and Geis, 2011; Irani, 2016; Lancaster and Dalmau, 2012; Rakocevic and Floeter, 2012). However, this theory could be more plausible for the SNARE proteins and other synaptic vesicle-associated proteins such as DNM1, which play a primary role in regulating synaptic vesicular exocytosis and endocytosis. Particularly, during vesicular fusion, SNARE proteins assume a cis-configuration and following binding of NSF, a very stable 20s multiprotein supercomplex is assembled **(Figure 27)**. It is plausible that fragments of this complex could be transiently exposed to the extracellular surface during vesicular release or reuptake mechanisms, providing the AAbs the brief opportunity to interact with them. Furthermore, certain endocytosis mechanisms could transport antibodies to the neurons (Ali et al., 2011) and it has been shown that amphiphysin-specific IgG recognized their target antigen during vesicular endocytosis in the spinal cord pre-synapses (Geis et al., 2010). It could be possible that T-cells recognize these antigens during an infection in the periphery or an alteration with the antigen presenting cells, which then presents self-antigens to auto-aggressive T-cells under special circumstances (Holmoy and Geis, 2011). Although there are limitations to the molecules crossing the CNS parenchyma, activated T-cells, but not resting T-cells have the ability to cross the blood brain barrier, irrespective of the antigen specificity (Larochelle et al., 2011). Therefore, vesicular proteins like NSF and DNM1 could be primarily recognized by the immune system and targeted by the AAbs. Subsequently, GAD antigens could be targeted by the immune system as a repercussion of the primary immune response against the SNARE proteins. AAbs against NSF and DNM1 might affect the function of these synaptic proteins destabilizing the synaptic vesicle release and reuptake mechanisms, thereby impairing neurotransmitter release. A mutation in NSF prevented SNARE complex disintegration in drosophila synapses and resulted in an increase in number of docked vesicles impairing subsequent fusion cycles (Littleton et al., 1998). An impairment in the trafficking of GABA containing vesicles might cause a deficit of functional GABA available to the neurons resulting in the continuous firing of alpha-motor neurons leading to various clinical symptoms as observed in patients with SPS and associated hyperexcitability disorders.

4.9. Probable relationship between dysfunctional SNARE proteins and its effect on the inhibitory neuronal circuits

In the majority of the anti-GAD AAb disorders such as SPS, PERM, cerebellar ataxia, limbic encephalitis etc. it is hypothesized that a dysfunction of the CNS inhibitory neuronal circuit might cause hyperexcitability of the motor cortex and in turn hyperactivity of the muscles (Dalakas, 2013). With GABA being the predominant inhibitory neurotransmitter in the brain, a dysfunction in its production, release, or reuptake pathways could explain the continuous firing of motor neurons, despite relaxation, as observed in patients (Meinck et al., 1984; Sandbrink et al., 2000). Many studies have reported that an obstruction in the release of GABA containing vesicles could contribute to a suppressed GABAergic neurotransmission resulting in various clinical symptoms (Dinkel et al., 1998; Geis et al., 2010; Levy et al., 2005; Rakocevic and Floeter, 2012; Werner et al., 2015). Furthermore, the lack of lymphocyte infiltration, inflammation or cellular destruction within the CNS and normal brain imaging of patients lead to the conclusion that SPS and other associated movement disorders could be caused due to a functional impairment of the GABAergic circuits rather than a structural damage (Ali et al., 2011; Dalakas, 2009; Dalakas, 2013; Holmoy and Geis, 2011; Levy et al., 2005; Rakocevic et al., 2004). The present study has provided evidence that patients with SPS, PERM and associated movement disorders might have additional AAbs against proteins closely associated with trafficking of synaptic vesicles such as NSF, STX1B, and DNM1, apart from GAD and amphiphysin. It could be possible that AAbs against these proteins might cause a dysfunctional GABAergic neuronal circuit by impeding recycling, replenishment, or reuptake of GABA containing vesicles resulting in the hyperexcitability of the motor cortex.

AAbs against different SNARE proteins could specifically affect GABAergic neuronal circuits because the SNARE proteins mainly play an important role in rapid renewal of synaptic vesicles and aid in fast neurotransmitter release, which is a prerequisite in inhibitory compared to excitatory neuronal circuits during elevated neuronal activity (Geis et al., 2010; Irani, 2016; Rakocevic and Floeter, 2012). In addition, the function of some vesicles-associated proteins depends on the neuronal cell-type and these proteins specifically regulate the number of vesicles present at the reserve and ready releasable pools in the inhibitory circuits, which could be disturbed by dysfunctional SNARE proteins (Matteoli et al., 2009; Teng et al., 2001). In a mouse model lacking DNM1, accumulation of tube-like invaginations of the plasma membrane surrounded by clathrin-coated pits were observed during spontaneous exogenous stimulation, indicating the importance of DNM1 during elevated neuronal activity (Ferguson et al., 2007).

A study revealed that there was a significant increase in the frequency of spontaneous vesicle fusions in rat hippocampal slices following incubation of IgG from a SPS patient compared with controls. It was hypothesized that unknown antigens belonging to the pre-synaptic regions, might be reason for increased spontaneous quantal releases, which could homeostatically decrease the expression of GABA-A receptors and desensitize them. Furthermore, the study reported no change in the vesicle pool size or GABA content in individual vesicles, indicating that there was no hindrance in GABA production in these patients (Werner et al., 2015). In the neuronal synapses, the release of neurotransmitters could be either calcium dependent (evoked) or calcium-independent (spontaneous). Evoked release occurs in the presence of an action potential and exerts very rapid post-synaptic response, whereas spontaneous quantal currents occur randomly at very slow rates and are associated with neurotransmitter release from single vesicles. It was shown that these two release mechanisms use different set of vesicle pools. The evoked fusions utilized vesicles from the readily releasable and reserve pool, while the spontaneous fusions used the vesicles from the resting pool (Fredj and Burrone, 2009). Werner et al. revealed that there was no change in vesicle pool size (Werner et al., 2015), but it was not mentioned which vesicle pool size was specifically affected as the two pools have different molecular identity attributed by different SNARE proteins. Deletion of the calcium-sensor, synaptotagmin I or SNAP25 dramatically reduced evoked neurotransmitter release, without any change in spontaneous release frequency (Fredj and Burrone, 2009). Therefore, based on the results from Werner et al., impairment of synaptotagmin I or SNAP25 proteins could not have caused the increase in spontaneous release frequencies, corroborating to the results from the current study, wherein no AAbs against synaptotagmin I or SNAP25 were observed in the patient cohort. Furthermore, a temperature-sensitive mutation in dynamin caused blockade of endocytosis and resulted in the utilization and release of synaptic vesicles from the resting pool (Poskanzer and Davis, 2004). Therefore, a probable inhibition in the function of DNM1 due to the anti-DNM1 AAbs, could cause an increased frequency of spontaneous quantal releases as observed in the study by Werner et al. However, the impact of AAbs against the SNARE proteins on the quantal release mechanisms must be tested to validate these hypotheses.

In a subsequent study by Werner et al. it was revealed that anti-amphiphysin AAbs targeted the GABAergic pre-synaptic vesicle pool and affected its molecular composition (Werner et al., 2016). A reduction in the GABAergic vesicle pool size and depletion of the clathrin coated vesicles was observed following intrathecal administration of anti-amphiphysin AAbs in the spinal cord of rats during sustained high frequency stimulation. Additionally, under unstimulated

(resting) conditions, the density of the vesicles and endocytic intermediates was significantly increased in rats treated with anti-amphiphysin AAbs compared with rats treated with control IgG, suggesting complementary mechanisms for vesicle recruitment (Werner et al., 2016). Exhaustion of synaptic vesicles in the reserve pool and arrest of the readily releasable pool at the pre-synaptic terminus could be also caused due to dysfunctional synaptic proteins like; NSF and DNM1. Temperature-sensitive paralytic mutations of NSF in Drosophila failed to dissociate SNARE complexes, which accumulated on endocytosed vesicles preventing subsequent fusion cycles. Additionally, effective pairing between v-SNAREs and t-SNAREs is important to mediate vesicular fusions. Mutations in syntaxin affected the formation of an effective SNARE core complex by reducing the binding affinity of syntaxin to VAMP in drosophila (Littleton et al., 1998). Therefore, defective NSF or syntaxins might arrest vesicles at the pre-synaptic terminus during basal synaptic activity, which might get extinguished during high-frequency stimulation. Furthermore, a reduction in clathrin coated vesicles resulting in sluggish endocytosis observed in the study by Werner et al. could be also due to faulty DNM1, which is required to mediate effective endocytosis of synaptic vesicles necessary for subsequent fusion cycles.

Cumulatively, AAbs against SNARE proteins or DNM1 could cause a malfunction in GABAergic synapses by affecting efficient maintenance and recycling of vesicle pools and in turn reducing synaptic transmission. Subsequently, to compensate for the rapid depletion of synaptic vesicles from the readily releasable pools, alternative mechanism could be activated such as recruitment of vesicles from the resting pool and increasing spontaneous vesicle releases. Specifically, GABAergic circuits could be targeted since these inhibitory circuits are associated with a higher vesicle turnover and fast synaptic transmission during high neuronal activity compared with excitatory synapses (Geis et al., 2010; Werner et al., 2015).

4.10. An overview of the current study

A comprehensive outline of the all test methods conducted in this study with their respective outcomes and analysis is summarized in the next page.

Discussion

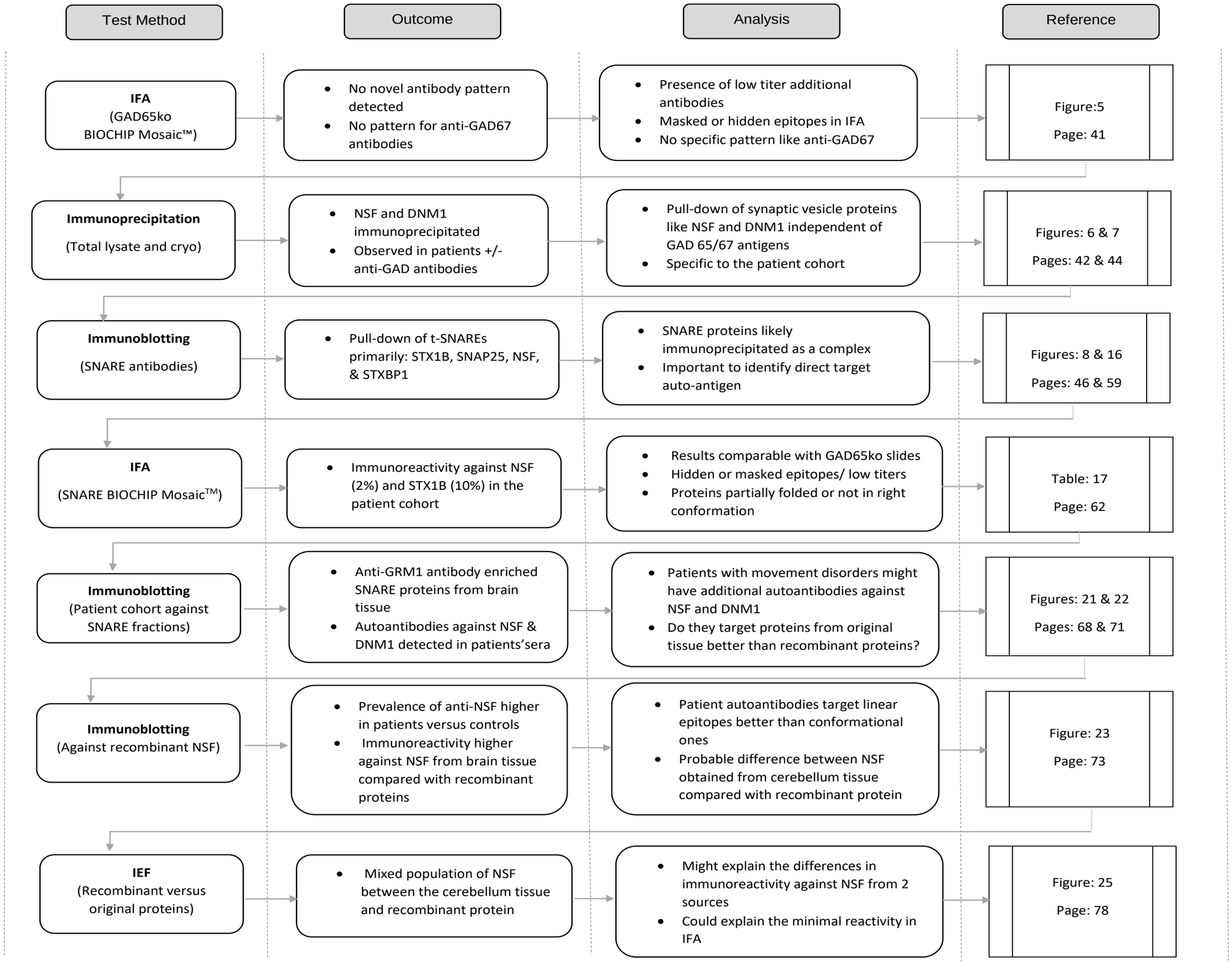
Test Method
Outcome
Analysis
Reference
IFA
(GAD65ko
BIOCHIP Mosaic™)
No novel antibody pattern detected
No pattern for anti-GAD67 antibodies
Presence of low titer additional antibodies
Masked or hidden epitopes in IFA
No specific pattern like anti-GAD67
Figure:5
Page: 41
Immunoprecipitation
(Total lysate and cryo)
NSF and DNM1 immunoprecipitated
Observed in patients +/- anti-GAD antibodies
Pull-down of synaptic vesicle proteins like NSF and DNM1 independent of GAD 65/67 antigens
Specific to the patient cohort
Figures: 6 & 7
Pages: 42 & 44
Immunoblotting
(SNARE antibodies)
Pull-down of t-SNAREs primarily: STX1B, SNAP25, NSF, & STXBP1
SNARE proteins likely immunoprecipitated as a complex
Important to identify direct target auto-antigen
Figures: 8 & 16
Pages: 46 & 59
IFA
(SNARE BIOCHIP Mosaic™)
Immunoreactivity against NSF (2%) and STX1B (10%) in the patient cohort
Results comparable with GAD65ko slides
Hidden or masked epitopes/ low titers
Proteins partially folded or not in right conformation
Table: 17
Page: 62
Immunoblotting
(Patient cohort against SNARE fractions)
Anti-GRM1 antibody enriched SNARE proteins from brain tissue
Autoantibodies against NSF & DNM1 detected in patients'sera
Patients with movement disorders might have additional autoantibodies against NSF and DNM1
Do they target proteins from original tissue better than recombinant proteins?
Figures: 21 & 22
Pages: 68 & 71
Immunoblotting
(Against recombinant NSF)
Prevalence of anti-NSF higher in patients versus controls
Immunoreactivity higher against NSF from brain tissue compared with recombinant proteins
Patient autoantibodies target linear epitopes better than conformational ones
Probable difference between NSF obtained from cerebellum tissue compared with recombinant protein
Figure: 23
Page: 73
IEF
(Recombinant versus original proteins)
Mixed population of NSF between the cerebellum tissue and recombinant protein
Might explain the differences in immunoreactivity against NSF from 2 sources
Could explain the minimal reactivity in IFA
Figure: 25
Page: 78

5. Conclusions and future perspectives

In conclusion, disorders such as SPS continue to remain rare and mystifying, having a paraneoplastic or idiopathic origin. SPS is often misdiagnosed, mandating the need for an early diagnostic biomarker and interpretation of the pathogenic significance of these targets in SPS (Alexopoulos and Dalakas, 2010). In the present study, it was observed that patients with SPS, PERM and associated movement disorders might have additional AAbs targeting synaptic proteins such as NSF, STX1B and DNM1, which are associated with vesicular trafficking including release and reuptake of synaptic vesicles carrying neurotransmitters. These AAbs were independent of the already detected well-known neuronal target antigens such as GAD and amphiphysin. However, the prevalence of the anti-GAD AAbs was higher compared with AAbs against NSF or DNM1 (80% versus ≈ 30% each) and therefore, detection of anti-GAD AAbs would continue be the primary diagnostic biomarker for successful identification these patients. Nevertheless, considering synaptic proteins, primarily the SNARE proteins, as possible antibody targets in patients with neurological disorders, suspected due to dysfunctional neuronal circuits, might shed more light in explaining the etiology of the disease. AAbs targeting this machinery could cause dysfunction of synaptic neurotransmission by preventing appropriate release of neurotransmitters. It could be possible that a multifaceted immune response is initiated in such patients involving spreading of humoral autoimmunity against synaptic proteins from both sides of the synapse, which in turn mediates the effective course of the disease.

As a subsequent step, it is vital to determine the pathogenic relevance of AAbs against NSF and DNM1 in SPS. In the present study, it was revealed that there could be a difference between the NSF expressed in the brain in comparison to that expressed in recombinant systems. Therefore, it might be preferable to analyse the effect of these AAbs on the neuronal synapses *in vivo*. Understanding the role of these AAbs at the molecular or ultrastructural level, particularly if they lead to a defective GABAergic synaptic transmission, might aid exploring the key pathophysiologic mechanism in SPS. Whole-cell patch clamp analysis of rat/mice hippocampal granule cells following incubation with patient- versus control-IgG could be performed to demonstrate any differences in spontaneous or evoked inhibitory post synaptic currents in the GABAergic synapses under resting and stimulated conditions (Geis et al., 2010). Additionally, intrathecal delivery of patient versus control IgG into animals followed by prolonged high-frequency stimulation would be useful to evaluate the structural changes in the neuronal pre-synaptic vesicles (Werner et al., 2016). Such an experiment will shed some light on the vesicle cycle, with an emphasis on the effect of the AAbs on the readily releasable pool vesicle

size and endocytic intermediates. It would be also interesting to address the AAb-mediated effects on the expression levels of cognate SNARE proteins such as STX1, VAMP2, and SNAP25 since they are functionally co-dependent.

Altogether, the current study hypothesizes that AAbs against the NSF and DNM1 might affect efficient vesicle preparation for subsequent neurotransmitter release in GABAergic neuronal circuits especially during high tonic activity. A reduction in the GABAergic functional inhibition might result in the involuntary and excessive firing of the motor neurons leading to stiffness, rigidity and other clinical symptoms as observed in patients with hyperexcitability disorders.

6. References

Aguado, F., G. Majo, B. Ruiz-Montasell, J. Llorens, J. Marsal, and J. Blasi. 1999. Syntaxin 1A and 1B display distinct distribution patterns in the rat peripheral nervous system. *Neuroscience*. 88:437–446.

Alberca, R., M. Romero, and J. Chaparro. 1982. Jerking stiff-man syndrome. *Journal of Neurology, Neurosurgery & Psychiatry*. 45:1159-1160.

Alexopoulos, H., and M.C. Dalakas. 2010. A critical update on the immunopathogenesis of Stiff Person Syndrome. *European Journal of Clinical Investigation*. 40:1018-1025.

Ali, F., M. Rowley, B. Jayakrishnan, S. Teuber, M.E. Gershwin, and I.R. Mackay. 2011. Stiff-person syndrome (SPS) and anti-GAD-related CNS degenerations: protean additions to the autoimmune central neuropathies. *Journal of autoimmunity*. 37:79-87.

Atassi, M.Z., P. Casali, M.Z. Atassi, and P. Casali. 2008. Molecular mechanisms of autoimmunity. *Autoimmunity*. 41:123-132.

Baekkeskov, S., H.-J. Aanstoot, S. Christgau, A. Reetz, M. Solimena, M. Cascalho, F. Folli, H. Richter-Olesen, and D.P. Camilli. 1990. Identification of 64K as autoantigen in insulin-dependent diabetes as the GABA-synthesizing enzyme glutamic acid decarboxylase. *Nature*. 347:151-156.

Baekkeskov, S., J. Kanaani, J.C. Jaume, and S. Kash. 2000. Does GAD have a unique role in triggering IDDM? *Journal of autoimmunity*. 15:279-286.

Barker, R.A., T. Revesz, M. Thom, C.D. Marsden, and P. Brown. 1998. Review of 23 patients affected by the stiff man syndrome: clinical subdivision into stiff trunk (man) syndrome, stiff limb syndrome, and progressive encephalomyelitis with rigidity. *Journal of neurology, neurosurgery, and psychiatry*. 65:633-640.

Bayreuther, C., S. Hieronimus, P. Ferrari, P. Thomas, and C. Lebrun. 2008. Auto-immune cerebellar ataxia with anti-GAD antibodies accompanied by de novo late-onset type 1 diabetes mellitus. *Diabetes & metabolism*. 34:386-388.

Bennett, M.K., N. Calakos, and R.H. Scheller. 1992. Syntaxin: A Synaptic Protein Implicated in Docking of Synaptic Vesicles at Presynaptic Active Zones. *Science*. 257:255-259.

Bhatti, A.B., and Z.A. Gazali. 2015. Recent Advances and Review on Treatment of Stiff Person Syndrome in Adults and Pediatric Patients. *Cureus*. 7:e427.

Bidwell, D.E., A.A. Buck, h.J. Diesfeld, B. Enders, J. Haworth, G. Huldt, N.H. Kent, C. Kirsten, P. Mattern, E.J. Ruitenberg, and A. Voller. 1976. The enzyme-linked immunosorbent assay (ELISA). *Bulletin of the World Health Organization*. 54:129-139.

Block, M.R., B.S. Glick, C.A. Wilcox, F.T. Wieland, and J.E. Rothman. 1988. Purification of an N-ethylmaleimide-sensitive protein catalyzing vesicular transport. *Proceedings of the National Academy of Sciences of the United States of America*. 85:7852-7856.

Bonifacino, J.S., and B.S. Glick. 2004. The Mechanisms of Vesicle Budding and Fusion. *Cell*. 116:153-166.

Bradley, S.A., and J.R. Steinert. 2016. Nitric Oxide-Mediated Posttranslational Modifications: Impacts at the Synapse. *Oxid Med Cell Longev*. 2016:5681036.

Brown, P., and C.D. Marsden. 1999. The stiff man and stiff man plus syndromes. *Journal of neurology, neurosurgery, and psychiatry*. 246:648-652.

Bruckner, W.J. 1957. "Stiff-Man" Syndrome Progressive Fluctuating Muscular Rigidity and Spasm. *California medicine*. 87:336-338.

Buddhala, C., C.-C. Hsu, and J.-Y. Wu. 2009. A novel mechanism for GABA synthesis and packaging into synaptic vesicles. *Neurochemistry international*. 55:9-12.

Burbelo, P.D., S. Groot, M.C. Dalakas, and M.J. Iadarola. 2008. High Definition Profiling of Autoantibodies to Glutamic Acid Decarboxylases GAD65/GAD67 in Stiff-Person Syndrome. *Biochemical and biophysical research communications*. 366:1-7.

References

Butler, M.H., A. Hayashi, N. Ohkoshi, C. Villmann, C.M. Becker, G. Feng, D.P. Camilli, and M. Solimena. 2000. Autoimmunity to Gephyrin in Stiff-Man Syndrome. *Neuron*. 26:307-312.

Butler, M.H., M. Solimena, R. Dirkx, A. Hayday, and D.P. Camilli. 1993. Identification of a Dominant Epitope of Glutamic Acid Decarboxylase (GAD-65) Recognized by Autoantibodies in Stiff Man Syndrome. *The Journal of experimental medicine*. 178:2097-2106.

Camilli, D.P., A. Thomas, R. Cofiell, F. Folli, B. Lichte, G. Piccolo, H.M. Meinck, M. Austoni, G. Fassetta, G. Bottazzo, D. Bates, N. Cartlidge, M. Solimena, and M.W. Kilimann. 1993. The Synaptic Vesicle-associated Protein Amphiphysin Is the 128-kD Autoantigen of StiffMan Syndrome with Breast Cancer. *The Journal of experimental medicine*. 178:2219-2223.

Carvajal-Gonzalez, A., M.L. Isabel, P. Waters, M. Woodhall, E. Coutinho, B. Balint, B. Lang, P. Pettingill, A. Carr, U.-M. Sheerin, R. Press, M.P. Lunn, M. Lim, P. Maddison, H.M. Meinck, W. Vandenberghe, and A. Vincent. 2014. Glycine receptor antibodies in PERM and related syndromes: characteristics, clinical features and outcomes. *Brian*. 137:2178-2192.

Chang, C.C., S.D. Eggers, J.K. Johnson, A. Haman, B.L. Miller, and M.D. Geschwind. 2007. Anti-GAD antibody cerebellar ataxia mimicking Creutzfeldt-Jakob disease. *Clinical neurology and neurosurgery*. 109:54-57.

Chaplin, D.D. 2010. Overview of the immune response. *Journal of Allergy and Clinical Immunology*. 125:S3-S23.

Chen, Z.W., C.S. Chang, T.A. Leil, and R.W. Olsen. 2007. C-terminal modification is required for GABARAP-mediated GABA(A) receptor trafficking. *The Journal of neuroscience : the official journal of the Society for Neuroscience*. 27:6655-6663.

Dalakas, M.C. 2009. Stiff person syndrome: advances in pathogenesis and therapeutic interventions. *Curr Treat Options Neurol.* 11:102-110.

Dalakas, M.C. 2013. Progress and stiff challenges in understanding the role of GAD-antibodies in stiff-person syndrome. *Experimental neurology*. 247:303-307.

Dalakas, M.C., M. Fujii, M. Li, B. Lutfi, J. Kyhos, and B. McElroy. 2001. High-dose of intravenouse immune globulin for stiff-person syndrome. *The New England journal of medicine*. 345:1870-1876.

Dalakas, M.C., M. Fujii, M. Li, and B. McElroy. 2000. The clinical spectrum of anti-GAD antibody-positive patients with stiff-person syndrome. *Neurology*. 55:1531–1535.

Damke, H., T. Baba, D.E. Warnock, and S.L. Schmid. 1994. Induction of mutant dynamin specifically blocks endocytic coated vesicle formation. *The Journal of cell biology*. 127:915-934.

De Jong, A.S.H., M. Van Kessel-Van Vark, and A.K. Raap. 1985. Sensitivity of various visualization methods for peroxidase and alkaline phosphatase activity in immunoenzyme histochemistry. *The Histochemical Journal*. 17:1119-1130.

Dinkel, K., H.M. Meinck, K.M. Jury, W. Karges, and W. Richter. 1998. Inhibition of gamma-aminobutyric acid synthesis by glutamic acid decarboxylase autoantibodies in stiff-man syndrome. *Annals of neurology*. 44:194–201.

Dulubova, I., M. Khvotchev, S. Liu, I. Huryeva, T.C. Sudhof, and J. Rizo. 2007. Munc18-1 binds directly to the neuronal SNARE complex. *Proceedings of the National Academy of Sciences of the United States of America*. 104:2697-2702.

Ellis, T.M., and M.A. Atkinson. 1996. The clinical significance of an autoimmune response against glutamic acid decarboxylase. *Nature medicine*. 2:148–153.

EUROIMMUN, A. The indirect immunofluorescence test performed using the TITERPLANE Technique.

Fenalti, G., and A.M. Buckle. 2010. Structural biology of the GAD autoantigen. *Autoimmunity reviews*. 9:148-152.

Ferguson, S.M., G. Brasnjo, M. Hayashi, M. Wölfel, C. Collesi, S. Giovedi, A. Raimondi, L.-W. Gong, P. Ariel, S. Paradise, E. Toole, R. Flavell, O. Cremona, G. Miesenböck, T.A. Ryan, and P. De Camilli.

2007. A Selective Activity-Dependent Requirement for Dynamin 1 in Synaptic Vesicle Endocytosis. *Science*. 316:570.

Folli, F., M. Solimena, R. Cofiell, M. Austoni, G. Tallini, G. Fassetta, D. Bates, N. Cartlidge, G.F. Bottazzo, G. Piccolo, and D.P. Camilli. 1993. Autoantibodies to 128 Kda protein in three women with the Stiff-Man Syndrome and Breast cancer. *The New England journal of medicine*. 328:546-551.

Fouka, P., H. Alexopoulos, S. Akrivou, O. Trohatou, P.K. Politis, and M.C. Dalakas. 2015. GAD65 epitope mapping and search for novel autoantibodies in GAD-associated neurological disorders. *Journal of neuroimmunology*. 281:73-77.

Fredj, N.B., and J. Burrone. 2009. A resting pool of vesicles is responsible for spontaneous vesicle fusion at the synapse. *Nature neuroscience*. 12:751-758.

Garfin, D.E. 2003. Gel electrophoresis of proteins *Essential Cell Biology*. 1:197-268.

Geis, C., A. Weishaupt, B. Grunewald, T. Wultsch, A. Reif, M. Gerlach, R. Jr Dirkx, M. Solimena, D. Perani, M. Heckmann, K.V. Toyka, F. Folli, and C. Sommer. 2011. Human Stiff-Person Syndrome IgG Induces Anxious Behavior in Rats. *PloS one*. 6:1-9.

Geis, C., A. Weishaupt, S. Hallermann, B. Grunewald, C. Wessig, T. Wultsch, A. Reif, N. Byts, M. Beck, S. Jablonka, M.K. Boettger, N. Uceyler, W. Fouquet, M. Gerlach, H.M. Meinck, A.L. Siren, S.J. Sigrist, K.V. Toyka, M. Heckmann, and C. Sommer. 2010. Stiff person syndrome-associated autoantibodies to amphiphysin mediate reduced GABAergic inhibition. *Brain : a journal of neurology*. 133:3166-3180.

Gresa-Arribas, N., K. Ruprecht, H. Ariño, E. Martínez-Hernández, M. Petit-Pedrol, L. Sabater, A. Saiz, J. Dalmau, and F. Graus. 2015. Antibodies to Inhibitory Synaptic Proteins in Neurological Syndromes Associated with Glutamic Acid Decarboxylase Autoimmunity. *PloS one*. 10:e0121364.

Hagopian, H.A., B. Michelsen, A.E. Karlsen, F. Larsen, A. Moody, C.E. Grubin, R. Rowe, J. Petersen, R. Mcevoy, and A. Lernmark. 1993. Autoantibodies in IDDM primarily recognize the 65,000-Mr isoform of glutamic acid decarboxylase. *Diabetes*. 42:631-636.

Hajjioui, A., K. Benbouazza, A. Faris Mel, A. Missaoui, and N.H. Hassouni. 2010. Stiff limb syndrome: a case report. *Cases journal*. 3:60.

Hansen, N., B. Grünewald, A. Weishaupt, M.N. Colaço, K.V. Toyka, C. Sommer, and C. Geis. 2013. Human Stiff person syndrome IgG-containing high-titer anti-GAD65 autoantibodies induce motor dysfunction in rats. *Experimental neurology*. 239:202-209.

Hanson, P.I., J.E. Heuser, and R. Jahn. 1997. Neurotransmitter release — four years of SNARE complexes. *Current Opinion in Neurobiology*. 7:310-315.

Haselmann, H., L. Röpke, C. Werner, A. Kunze, and C. Geis. 2015. Interactions of Human Autoantibodies with Hippocampal GABAergic Synaptic Transmission – Analyzing Antibody-Induced Effects ex vivo. *Frontiers in neurology*. 6:136.

Hassel, B. 2013. Tetanus: Pathophysiology, Treatment, and the Possibility of Using Botulinum Toxin against Tetanus-Induced Rigidity and Spasms. *Toxins*. 5:73-83.

He, F. 2011. BCA (Bicinchoninic Acid) Protein Assay. *Bio protocol*. 101.

Hirai, H., J. Miura, Y. Hu, H. Larsson, K. Larsson, A. Lernmark, S.A. Ivarsson, T. Wu, A. Kingman, A.G. Tzioufas, and A.L. Notkins. 2008. Selective Screening of Secretory Vesicle-Associated Proteins for Autoantigens in Type 1 Diabetes: VAMP2 and NPY are New Minor Autoantigens. *Clinical Immunology (Orlando, Fla.)*. 127:366-374.

Holmoy, T., and C. Geis. 2011. The immunological basis for treatment of stiff person syndrome. *Journal of neuroimmunology*. 231:55-60.

Holt, M., D. Riedel, A. Stein, C. Schuette, and R. Jahn. 2008. Synaptic Vesicles Are Constitutively Active Fusion Machines, Which Function Independently of Ca(2+). *Current biology : CB*. 18:715-722.

Hughes, E.G., X. Peng, A.J. Gleichman, M. Lai, L. Zhou, R. Tsou, T.D. Parsons, D.R. Lynch, J. Dalmau, and R.J. Balice-Gordon. 2010. Cellular and Synaptic Mechanisms of Anti-NMDA Receptor Encephalitis. *Journal of Neuroscience*. 30:5866-5875.

Hussain, S., and S. Davanger. 2011. The discovery of the soluble N-ethylmaleimide-sensitive factor attachment protein receptor complex and the molecular regulation of synaptic vesicle transmitter release: the 2010 Kavli Prize in neuroscience. *Neuroscience*. 190:12-20.

Hutchinson, M., P. Waters, J. McHugh, G. Gorman, S. O'Riordan, S. Connolly, H. Hager, P. Yu, C.M. Becker, and A. Vincent. 2008. Progressive encephalomyelitis, rigidity, and myoclonus: A novel glycine receptor antibody. *Neurology*. 71:1291-1292.

Irani, S.R. 2016. 'Moonlighting' surface antigens: a paradigm for autoantibody pathogenicity in neurology? *Brain : a journal of neurology*. 139:304-306.

Irani, S.R., J.M. Gelfand, A. Al-Diwani, and A. Vincent. 2014. Cell-surface central nervous system autoantibodies: Clinical relevance and emerging paradigms. *Annals of neurology*. 76:168-184.

Ishida, K., H. Mitoma, S.-Y. Song, T. Uchihara, A. Inaba, S. Eguchi, T. Kobayashi, and H. Mizusawa. 1999. Selective suppression of cerebellar GABAergic transmission by an autoantibody to glutamic acid decarboxylase. *Annals of neurology*. 46:263–267.

Ishida, K., H. Mitoma, Y. Wada, T. Oka, J. Shibahara, Y. Saito, S. Murayama, and H. Mizusawa. 2007. Selective loss of Purkinje cells in a patient with anti-glutamic acid decarboxylase antibody-associated cerebellar ataxia. *Journal of Neurology, Neurosurgery & Psychiatry*. 78:190-192.

Jahn, R., and R.H. Scheller. 2006. SNAREs [mdash] engines for membrane fusion. *Nat Rev Mol Cell Biol*. 7:631-643.

Jarius, S., M. Scharf, N. Begemann, W. Stocker, C. Probst, Serysheva, II, S. Nagel, F. Graus, D. Psimaras, B. Wildemann, and L. Komorowski. 2014. Antibodies to the inositol 1,4,5-trisphosphate receptor type 1 (ITPR1) in cerebellar ataxia. *Journal of neuroinflammation*. 11:206.

Kim, J., M. Namchuk, T. Bugawan, Q. Fu, M. Jaffe, Y. Shi, H.J. Aanstoot, C.W. Turck, H. Erlich, V. Lennon, and B. S. 1994. Higher autoantibody levels and recognition of a linear NH2-terminal epitope in the autoantigen GAD65, distinguish stiff-man syndrome from insulin-dependent diabetes mellitus. *180*. 2.

Kittler, J.T., P. Rostaing, G. Schiavo, J.M. Fritschy, R. Olsen, A. Triller, and S.J. Moss. 2001. The subcellular distribution of GABARAP and its ability to interact with NSF suggest a role for this protein in the intracellular transport of GABA(A) receptors. *Molecular and cellular neurosciences*. 18:13-25.

Koy, C., S. Mikkat, E. Raptakis, C. Sutton, M. Resch, K. Tanaka, and M.O. Glocker. 2003. Matrix-assisted laser desorption/ionization- quadrupole ion trap-time of flight mass spectrometry sequencing resolves structures of unidentified peptides obtained by in-gel tryptic digestion of haptoglobin derivatives from human plasma proteomes. *Proteomics*. 3:851-858.

Lamigeon, C., J.P. Bellier, S. Sacchettoni, M. Rujano, and B. Jacquemont. 2001. Enhanced neuronal protection from oxidative stress by coculture with glutamic acid decarboxylase-expressing astrocytes. *Journal of neurochemistry*. 77:598-606.

Lancaster, E., and J. Dalmau. 2012. Neuronal autoantigens--pathogenesis, associated disorders and antibody testing. *Nature reviews. Neurology*. 8:380-390.

Larochelle, C., J.I. Alvarez, and A. Prat. 2011. How do immune cells overcome the blood–brain barrier in multiple sclerosis? *FEBS letters*. 585:3770-3780.

Levy, L.M., M.C. Dalakas, and M.K. Floeter. 1999. The Stiff-Person Syndrome: An autoimmune disorder affecting neurotransmission of gamma-aminobutyric acid *Annals of Internal Medicine*. 131:523-530.

Levy, L.M., I. Levy-Reis, M. Fujii, and M.C. Dalakas. 2005. Brain gamma-aminobutyric acid changes in Stiff-Person Syndrome. *Archives of neurology*. 62:970-974.

Lilleker, J.B., V. Biswas, and R. Mohanraj. 2014. Glutamic acid decarboxylase (GAD) antibodies in epilepsy: diagnostic yield and therapeutic implications. *Seizure : the journal of the British Epilepsy Association*. 23:598-602.

Littleton, J.T., E.R. Chapman, R. Kreber, M.B. Garment, S.D. Carlson, and B. Ganetzky. 1998. Temperature-Sensitive Paralytic Mutations Demonstrate that Synaptic Exocytosis Requires SNARE Complex Assembly and Disassembly. *Neuron*. 21:401-413.

Lleo, A., P. Invernizzi, B. Gao, M. Podda, and M.E. Gershwin. 2010. Definition of human autoimmunity — autoantibodies versus autoimmune disease. *Autoimmunity reviews*. 9:A259-A266.

Lobo, M.E., M.L.B. Araújo, C.A.B. Tomaz, and N. Allam. 2010. Stiff-person syndrome treated with rituximab. *BMJ case reports*. 2010:bcr0520103021.

Mackay, I.R. 2010. Travels and travails of autoimmunity: A historical journey from discovery to rediscovery. *Autoimmunity reviews*. 9:A251-A258.

Manto, M.U., M.A. Laute, M. Aguera, V. Rogemond, M. Pandolfo, and J. Honnorat. 2007. Effects of anti-glutamic acid decarboxylase antibodies associated with neurological diseases. *Annals of neurology*. 61:544-551.

Martin, D.L., and K. Rimvall. 1993. Regulation of gamma-Aminobutyric Acid Synthesis in the Brain. *Journal of neurochemistry*. 60:395-407.

Martinez-Martinez, P., P.C. Molenaar, M. Losen, and M.H. de Baets. 2014. Glycine receptor antibodies in PERM: a new channelopathy. *Brain : a journal of neurology*. 127:2110-2118.

Matteoli, M., D. Pozzi, C. Grumelli, S.B. Condliffe, C. Frassoni, T. Harkany, and C. Verderio. 2009. The synaptic split of SNAP-25: Different roles in glutamatergic and GABAergic neurons? *Neuroscience*. 158:223-230.

McKeon, A. 2013. Paraneoplastic and other autoimmune disorders of the central nervous system. *The Neurohospitalist*. 3:53-64.

McKeon, A., E. Martinez-Hernandez, E. Lancaster, J.Y. Matsumoto, R.J. Harvey, K.M. McEvoy, S.J. Pittock, V.A. Lennon, and J. Dalmau. 2013. Glycine Receptor Autoimmune Spectrum With Stiff-Man Syndrome Phenotype. *JAMA neurology*. 70:44.

McLeod, B.C., I. Sniecinski, D. Ciavarella, H. Owen, T.H. Price, M.J. Randels, and J.W. Smith. 1999. Frequency of immediate adverse effects associated with therapeutic apheresis. *Transfusion*. 39:282-288.

Meinck, H.M., L. Faber, N. Morgenthaler, J. Seissler, S. Maile, M. Butler, M. Solimena, D.P. Camilli, and W.A. Scherbaum. 2001. Antibodies against glutamic acid decarboxylase : prevalence in neurological diseases. *Journal of neurology, neurosurgery, and psychiatry*. 71:100-103.

Meinck, H.M., K. Ricker, and B. Conrad. 1984. The stiff-man syndrome: new pathophysiological aspects from abnormal exteroceptive reflexes and the response to clomipramine, clonidine, and tizanidine. *Journal of Neurology, Neurosurgery & Psychiatry*. 47:280-287.

Meinck, H.M., and P.D. Thompson. 2002. Stiff man syndrome and related conditions. *Movement disorders : official journal of the Movement Disorder Society*. 17:853–866.

Mishima, T., T. Fujiwara, M. Sanada, T. Kofuji, M. Kanai-Azuma, and K. Akagawa. 2014. Syntaxin 1B, but Not Syntaxin 1A, Is Necessary for the Regulation of Synaptic Vesicle Exocytosis and of the Readily Releasable Pool at Central Synapses. *PloS one*. 9:e90004.

Miske, R., C.C. Gross, M. Scharf, K.S. Golombeck, M. Hartwig, U. Bhatia, A. Schulte-Mecklenbeck, K. Bonte, C. Strippel, L. Schols, M. Synofzik, H. Lohmann, I.M. Dettmann, M. Deppe, S. Mindorf, T. Warnecke, Y. Denno, B. Teegen, C. Probst, S. Brakopp, K.P. Wandinger, H. Wiendl, W. Stocker, S.G. Meuth, L. Komorowski, and N. Melzer. 2017. Neurochondrin is a neuronal target antigen in autoimmune cerebellar degeneration. *Neurology(R) neuroimmunology & neuroinflammation*. 4:e307.

References

Morgan, A., and R.D. Burgoyne. 2004. Membrane traffic: controlling membrane fusion by modifying NSF. *Current biology : CB*. 14:R968-970.

Murinson, B.B., M. Butler, K. Marfurt, S. Gleason, D.P. Camilli, and M. Solimena. 2004. Markedly elevated GAD antibodies in SPS: effects of age and illness duration. *Neurology*. 63:2146-2148.

Nemni, R., S. Braghi, M.G. Natali-Sora, V. Lampasona, E. Bonifacio, G. Comi, and N. Canal. 1994. Autoantibodies to glutamic acid decarboxylase in palatal myoclonus and epilepsy. *Annals of neurology*. 36:665–667.

Nemni, R., L.M. Caniatti, M. Gironi, E. Bazzigaluppi, and D. De Grandis. 2004. Stiff person syndrome does not always occur with maternal passive transfer of GAD65 antibodies. *Neurology*. 62:101-102.

Nicholls, J.G., A.R. Martin, and B.G. Wallace. 1992. From neuron to brain : a cellular and molecular approach to the function of the nervous system. *Sinauer Associates, Inc, Sunderland, Massachusetts*.

Patel, A.B., R.A. de Graaf, D.L. Martin, G. Battaglioli, and K.L. Behar. 2006. Evidence that GAD65 mediates increased GABA synthesis during intense neuronal activity in vivo. *Journal of neurochemistry*. 97:385-396.

Pérez-Brangulí, F., A. Muhaisen, and J. Blasi. 2002. Munc 18a Binding to Syntaxin 1A and 1B Isoforms Defines Its Localization at the Plasma Membrane and Blocks SNARE Assembly in a Three-Hybrid System Assay. *Molecular and Cellular Neuroscience*. 20:169-180.

Pérez-Brangulí, F., B. Ruiz-Montasell, and J. Blasi. 1999. Differential interaction patterns in binding assays between recombinant syntaxin 1 and synaptobrevin isoforms. *FEBS letters*. 458:60-64.

Poletaev, A., and P. Boura. 2011. The immune system, natural autoantibodies and general homeostasis in health and disease. *Hippokratia*. 15:295-298.

Porath, J., and B. Olin. 1983. Immobilized metal ion affinity adsorption and immobilized metal ion affinity chromatography of biomaterials. Serum protein affinities for gel-immobilized iron and nickel ions. *Biochemistry*. 22:1621-1630.

Poskanzer, K.E., and G.W. Davis. 2004. Mobilization and fusion of a non-recycling pool of synaptic vesicles under conditions of endocytic blockade. *Neuropharmacology*. 47:714-723.

Probst, C., L. Komorowski, E. de Graaff, M. van Coevorden-Hameete, V. Rogemond, J. Honnorat, L. Sabeter, F. Graus, S. Jarius, R. Voltz, B. Wildemann, D. Franciotta, I.M. Blocker, W. Schlumberger, W. Stocker, and P.A. Sillevis Smitt. 2015. Standardized test for anti-Tr/DNER in patients with paraneoplastic cerebellar degeneration. *Neurology(R) neuroimmunology & neuroinflammation*. 2:e68.

Pugliese, A., M. Solimena, Z.L. Awdeh, C.A. Alper, T. Bugawan, H.A. Erlich, D.P. camilli, and G.S. Eisenbarth. 1993. Association of HLA-DQB1*0201 with stiff-man syndrome. . *The Journal of clinical endocrinology and metabolism*. 77:1550-1553.

Radzimski, C., C. Probst, B. Teegen, K. Rentzsch, I.M. Blocker, C. Dahnrich, W. Schlumberger, W. Stocker, D.P. Bogdanos, and L. Komorowski. 2013. Development of a recombinant cell-based indirect immunofluorescence assay for the determination of autoantibodies against soluble liver antigen in autoimmune hepatitis. *Clinical & developmental immunology*. 2013:572815.

Raju, R., G. Rakocevic, Z. Chen, G. Hoehn, C. Semino-Mora, W. Shi, R. Olsen, and M.C. Dalakas. 2006. Autoimmunity to GABAA-receptor-associated protein in stiff-person syndrome. *Brain : a journal of neurology*. 129:3270-3276.

Rakocevic, G., and M.K. Floeter. 2012. Autoimmune stiff person syndrome and related myelopathies: understanding of electrophysiological and immunological processes. *Muscle & nerve*. 45:623-634.

Rakocevic, G., R. Raju, and M.C. Dalakas. 2004. Anti–Glutamic Acid Decarboxylase Antibodies in the Serum and Cerebrospinal Fluid of Patients With Stiff-Person Syndrome. *Archives of neurology*. 61:902-904.

Reetz, A., M. Solimena, M. Matteoli, F. Folli, K. Takei, and D.P. Camilli. 1991. GABA and pancreatic beta-cells: colocalization of glutamic acid decarboxylase (GAD) and GABA with synaptic-like microvesicles suggests their role in GABA storage and secretion. *The EMBO journal*. 10:1275-1284.

Righetti, P.G. 1983 Isoelectric Focusing: Theory, Methodology and Application, Volume 11 385.

Rizo, J., and T.C. Sudhof. 2002. Snares and munc18 in synaptic vesicle fusion. *Nature reviews. Neuroscience*. 3:641-653.

Saiz, A., Y. Blanco, L. Sabater, F. Gonzalez, L. Bataller, R. Casamitjana, L. Ramió-Torrentà, and F. Graus. 2008. Spectrum of neurological syndromes associated with glutamic acid decarboxylase antibodies: diagnostic clues for this association. *Brain : a journal of neurology*. 131:2553–2563.

Saiz, A., F. Graus, F. Valldeoriola, J. Valls-Sole, and E. Tolosa. 1998. Stiff-leg syndrome: a focal form of stiff-man syndrome. *Annals of neurology*. 43:400-403.

Sandbrink, F., N.A. Syed, D.M. Fujii, M.C. Dalakas, and M.K. Floeter. 2000. Motor cortex hyper excitability in stiff-person syndrome. *Brain : a journal of neurology*. 123:2231-2239.

Scharf, M., R. Miske, F. Heidenreich, R. Giess, P. Landwehr, I.M. Blocker, N. Begemann, Y. Denno, S. Tiede, C. Dahnrich, W. Schlumberger, M. Unger, B. Teegen, W. Stocker, C. Probst, and L. Komorowski. 2015. Neuronal Na+/K+ ATPase is an autoantibody target in paraneoplastic neurologic syndrome. *Neurology*. 84:1673-1679.

Scofield, R.H. 2004. Autoantibodies as predictors of disease. *The Lancet*. 363:1544-1546.

Smith, P.K., R.I. Krohn, G.T. Hermanson, A.K. Mallia, F.H. Gartner, M.D. Provenzano, E.K. Fujimoto, N.M. Goeke, B.J. Olson, and D.C. Klenk. 1985. Measurement of protein using bicinchoninic acid. *Analytical biochemistry*. 150:76-85.

Solimena, M., and P. De Camilli. 1991. Autoimmunity to glutamic acid decarboxylase (GAD) in Stiff-Man syndrome and insulin-dependent diabetes mellitus. *Trends in Neurosciences*. 14:452-457.

Solimena, M., F. Folli, R. Aparisi, G. Pozza, and P. De Camilli. 1990. Autoantibodies to GABAergic neurons and pancreatic beta cells in stiff-man syndrome. *The New England journal of medicine*. 322:1555–1560.

Söllner, T., M.K. Bennett, S.W. Whiteheart, R.H. Scheller, and J.E. Rothman. 1993. A protein assembly-disassembly pathway in vitro that may correspond to sequential steps of synaptic vesicle docking, activation, and fusion. *Cell*. 75:409-418.

Sommer, C., A. Weishaupt, J. Brinkhoff, L. Biko, C. Wessig, R. Gold, and K.V. Toyka. 2005. Paraneoplastic stiff-person syndrome: passive transfer to rats by means of IgG antibodies to amphiphysin. *Lancet*. 365:1406–1411.

Steffen, H., N. Menger, R. W., B. Nolle, H. Krastel, C. Stayer, G.H. Kolling, H. Wassle, and H.M. Meinck. 1999. Immune-mediated retinopathy in a patient with stiff-man syndrome. *Ophthamol*. 237:212–219.

Stern, W.M., R. Howard, R.M. Chalmers, M.R. Woodhall, P. Waters, A. Vincent, and M.M. Wickremaratchi. 2014. Glycine receptor antibody mediated Progressive Encephalomyelitis with Rigidity and Myoclonus (PERM): a rare but treatable neurological syndrome. *Practical Neurology*. 14:123-127.

Stöcker, W. 1987. Processes and devices for examinations on immobilised biological material; European Patent No. 0117262.

Südhof, T.C., and J.E. Rothman. 2009. Membrane Fusion: Grappling with SNARE and SM Proteins. *Science (New York, N.Y.)*. 323:474-477.

Sutton, R.B., D. Fasshauer, R. Jahn, and A.T. Brunger. 1998. Crystal structure of a SNARE complex involved in synaptic exocytosis at 2.4[thinsp]A resolution. *Nature*. 395:347-353.

Takamori, S., M. Holt, K. Stenius, E.A. Lemke, M. Gronborg, D. Riedel, H. Urlaub, S. Schenck, B. Brugger, P. Ringler, S.A. Muller, B. Rammner, F. Grater, J.S. Hub, B.L. De Groot, G. Mieskes, Y. Moriyama,

J. Klingauf, H. Grubmuller, J. Heuser, F. Wieland, and R. Jahn. 2006. Molecular anatomy of a trafficking organelle. *Cell*. 127:831-846.

Takei, K., V.I. Slepnev, V. Haucke, and D.P. Camilli. 1999. Functional partnership between amphiphysin and dynamin in clathrin-mediated endocytosis. *Nature cell biology*. 1:33-39.

Teng, F.Y.H., Y. Wang, and B.L. Tang. 2001. The syntaxins. *Genome biology*. 2:3012.3011–3012.3017.

Todd, J.A. 1995. Genetic analysis of type 1 diabetes using whole genome approaches. *Proceedings of the National Academy of Sciences of the United States of America*. 92:8650-8655.

Vincent, A. 2008. Stiff, twitchy or wobbly--are GAD antibodies pathogenic? *Brain : a journal of neurology*. 131:2536-2537.

Vives-Pi, M., and L. Sabater. 2010. Stiff person syndrome and cerebellar ataxia associated with glutamic acid decarboxylase antibodies and type 1 diabetes: What is the link between neurological diseases and autoimmunity to the beta cell? *Inmunología*. 29:119-124.

Vulliemoz, S., G. Vanini, A. Truffert, C. Chizzolini, and M. Seeck. 2007. Epilepsy and cerebellar ataxia associated with anti-glutamic acid decarboxylase antibodies. *Journal of Neurology, Neurosurgery & Psychiatry*. 78:187-189.

Waagepetersen, H.S., U. Sonnewald, and A. Schousboe. 1999. The GABA Paradox: Multiple Roles as Metabolite, Neurotransmitter, and Neurodifferentiative Agent. *Journal of neurochemistry*. 73:1335-1342.

Walker, J.M. 1994. The Bicinchoninic Acid (BCA) Assay for Protein Quantitation. *In* Basic Protein and Peptide Protocols. J.M. Walker, editor. Humana Press, Totowa, NJ. 5-8.

Wegner, S.V., and J.P. Spatz. 2013. Cobalt(III) as a Stable and Inert Mediator Ion between NTA and His6-Tagged Proteins. *Angewandte Chemie International Edition*. 52:7593-7596.

Werner, C., H. Haselmann, A. Weishaupt, K.V. Toyka, C. Sommer, and C. Geis. 2015. Stiff person-syndrome IgG affects presynaptic GABAergic release mechanisms. *Journal of neural transmission*. 122:357-362.

Werner, C., M. Pauli, S. Doose, A. Weishaupt, H. Haselmann, B. Grünewald, M. Sauer, M. Heckmann, K.V. Toyka, E. Asan, C. Sommer, and C. Geis. 2016. Human autoantibodies to amphiphysin induce defective presynaptic vesicle dynamics and composition. *Brain : a journal of neurology*. 139:365-379.

Wessig, C., R. Klein, M.F. Schneider, K.V. Toyka, M. Naumann, and C. Sommer. 2003. Neuropathology and binding studies in anti-amphiphysin-associated stiff-person syndrome. *Neurology*. 61:195-198.

Whiteheart, S.W., and E.A. Matveeva. 2004. Multiple binding proteins suggest diverse functions for the N-ethylmaleimide sensitive factor. *Journal of structural biology*. 146:32-43.

Whiteheart, S.W., K. Rossnagel, S.A. Buhrow, M. Brunner, R. Jaenicke, and J.E. Rothman. 1994. N-ethylmaleimide-sensitive fusion protein: a trimeric ATPase whose hydrolysis of ATP is required for membrane fusion. *The Journal of cell biology*. 126:945-954.

Whiteheart, S.W., T. Schraw, and E.A. Matveeva. 2001. N-Ethylmaleimide Sensitive Factor (NSF) Structure and Function. *International Review Of Cytology*. 207:71-112.

Wiechelman, K.J., R.D. Braun, and J.D. Fitzpatrick. 1988. Investigation of the bicinchoninic acid protein assay: Identification of the groups responsible for color formation. *Analytical biochemistry*. 175:231-237.

Woodman, P.G. 1997. The roles of NSF, SNAPs and SNAREs during membrane fusion. *Biochimica et biophysica acta*. 1357:155-172.

Wu, H., Y. Jin, C. Buddhala, G. Osterhaus, E. Cohen, H. Jin, J. Wei, K. Davis, K. Obata, and J.-Y. Wu. 2007. Role of glutamate decarboxylase (GAD) isoform, GAD65, in GABA synthesis and transport into synaptic vesicles—Evidence from GAD65-knockout mice studies. *Brain research*. 1154:80-83.

References

Zaenker, P., E.S. Gray, and M.R. Ziman. 2016. Autoantibody Production in Cancer—The Humoral Immune Response toward Autologous Antigens in Cancer Patients. *Autoimmunity reviews*. 15:477-483.

Zhao, C., J.T. Slevin, and S.W. Whiteheart. 2007. Cellular functions of NSF: not just SNAPs and SNAREs. *FEBS letters*. 581:2140-2149.

Zhao, M., S. Wu, Q. Zhou, S. Vivona, D.J. Cipriano, Y. Cheng, and A.T. Brunger. 2015. Mechanistic insights into the recycling machine of the SNARE complex. *Nature*. 518:61-67.

List of Figures

List of Figures

List of Tables

List of Abbreviations

AAbs	Autoantibodies
AMPAR	α-amino-3-hydroxy-5-methyl-4-isoxazolepropionic acid receptor
ARHGAP26	Rho GTPase-activating protein 26
ARHGEF9	Rho guanine nucleotide exchange factor 9
ATP	Adenosine Tri-Phosphate
AQP4	Aquaporin-4
BCA	Bicinchoninic acid Solution
BSA	Bovine serum albumin
CASPR2	Contactin-associated protein-like 2
CNS	central nervous system
CSF	Cerebrospinal fluid
DMEM	Dulbecco's Modified Eagle Medium
DNM1	Dynamin 1
DPPX	Dipeptidyl aminopeptidase-like protein 6
DRD2	D(2) dopamine receptor
DTT	Dithiothreitol
E. coli	Escherichia coli
EDTA	Ethylenediamine tetra acetic acid
ELISA	Enzyme linked immunosorbent assay
EXOC4 or Sec8	Exocyst Complex Component 4
GABA	γ-aminobutyric acid
GABA-A receptor	GABA receptor-A (ionotropic receptor)
GABAR-A1	GABA-A receptor subunit α1
GABAR-A1+B3	GABA-A receptor subunit α1 + β3
GABA-B receptor	GABA receptor-B (metabotropic receptor)
GABARB1_2	GABA-B receptor subunit B1/2
GABARAP	GABA receptor associated protein
GAD	Glutamic acid decarboxylase
GL	Granular layer of cerebellum
GLRA1	Glycine receptor subunit α-1
GLRB	Glycine receptor subunit β
GLUDR2	Glutamate receptor ionotropic delta-2
GRM1	Metabotropic glutamate receptor 1
GTP	Guanosine-5'-triphosphate

List of Abbreviations

HEK293 cells	Human embryonic kidney cells 293
HEK293-GAD65/GAD67	HEK293 cells transfected with plasmids coding for GAD65/GAD67
His-tag	Histidine-tag
HLA	Human leukocyte antigen
IEF	Isoelectric focusing
IFA	Indirect Immunofluorescence Assay
Ig	Immunoglobulins
IMAC	Immobilized Metal Ion Affinity Chromatography
IP-WB	Immunoprecipitation followed by western blot analysis
IU	International units
IVIG	Intravenous immunoglobulins
ko	knock-out
LGI1	Leucine-rich glioma-inactivated protein 1
MALDI	Matrix Assisted Laser Desorption/Ionization
MALDI-TOF-MS	MALDI - Time of Flight Mass Spectrometry
MHC	Major Histocompatibility Complex
ML	Molecular layer of cerebellum
MS	Mass Spectrometry
NBT/BCIP	Nitro-blue tetrazolium and 5-bromo-4-chloro-3'-indolyphosphate
NMDAR	N-methyl-D-aspartate receptor
NR1a	NMDAR subtype 1a
NSF	N-ethylmaleimide-sensitive factor
PBS	Phosphate buffered saline
PCA-2	Purkinje cell cytoplasmic antibody type 2
PERM	Progressive encephalomyelitis with rigidity and myoclonus
pI	Isoelectric point
PLP	Pyridoxal phosphate
PMSF	Phenylmethylsulphonyl fluoride
PTMs	Post-translational modifications
RI%	Relative intensity in percentage
ROI	Region of interest
SD	Standard deviation
SDS	Sodium dodecyl sulfate
SDS-PAGE	Sodium dodecyl sulfate polyacrylamide gel electrophoresis
SLC6A5	Sodium-and chloride-dependent glycine transporter 2
SLS	Stiff-limb-syndrome

List of Abbreviations

SNAP25	Synaptosomal-associated protein 25
SNARE	Soluble NSF Attachment Protein Receptor
SOX-1	Transcription factor SRY-Box 1
SPS	Stiff-Person-Syndrome
STX	Syntaxin
STX1B(ic)	Intracellular domain of STX1B
STXBP1	Syntaxin-binding protein 1
T1DM	Type 1 diabetes mellitus
t-SNARE	Target membrane-SNARE proteins
VAMP	Vesicle associated membrane protein
v-SNARE	Vesicle-SNARE proteins
WB	Western blot
WT NSF	Wild-type NSF

Acknowledgements

I would like to sincerely thank Prof. Dr. med. Winfried Stöcker for giving me the opportunity to perform my doctoral studies at EUROIMMUN AG, Germany. Thank you for providing me with all the necessary support and resources as well as helping me gain an insight into the industrial field work. My sincere gratitude to Prof. Dr. med. Detlef Zillikens for accommodating me as a graduate student in the RTG1727 network and Prof. Dr. med. Ralf Ludwig for accepting to be my principal investigator (*Doktorvater*) and providing me with all the necessary academic assistance during my PhD tenure.

I am forever indebted to my supervisor and mentor Dr. Lars Komorowski, without whom this study would not have been possible. I am grateful for your support, guidance, and scientific wisdom, which has made me scientifically competent and independent. I would like to also thank Dr. Christian Probst for his valuable inputs, suggestions, and his benevolence. I would like to express my gratitude to PD Dr. med. vet. Jennifer Hundt for being a terrific mentor and providing me with all the needed support and counsel. My sincere gratitude to Susann Satow and Laura Olejko for teaching me the different techniques implemented in the department and for always being patient with me. My heartfelt thanks to Dr. Ramona Miske and Dr. Madeleine Scharf, who always lend me an ear and bounced back scientific ideas and expertise. I am grateful to Swantje Mindorf and Dr. Inga Dettmann for evaluating my IFT slides as well as educating me on how to read them accurately. I would like to extend my appreciation and gratitude to all my colleagues including Dr. Christiane Burkhardt, Dr. Stefanie Hahn, Melanie König, Cindy Thomas, Donatella, Maxi, Herdis, Dr. Britta Brix, Dr. Nora Begemann, Thomas Nitzsche, Kristin Gand, and Zitao Zeng for their constant encouragement and friendly support. My special thanks to Yvonne Denno for being the expert in Mass spectrometry and helping me analyze and recognize novel proteins in my study and to Jonas Joneleit for being the best and effective lab partner during the final year of my PhD. A big shout-out to Rittika Chunder for being more than just a friend and a fellow PhD student. Words cannot describe all the mental and physical support and guidance she has provided these past 4 years. I am forever grateful to Jana for answering all my queries and supporting me during my dissertation writing phase.

My PhD would not have been possible without the constant backing and encouragement from my parents. I am grateful to have such a loving husband, Sriram, who has endured all my outbursts and tantrums, been a problem solver, and is the backbone of my survival. I am fortunate to have such a dexterous and proficient programmer as a brother, Ashwin, without whom my computer skillset would have hit rock bottom.